LAND AND WATER FLAGSHIP
www.csiro.au

Geochemical Baseline Monitoring

Axel Suckow, Andrew Taylor, Phil Davies, Fred Leaney
February 2016

GISERA Gas Industry Social & Environmental Research Alliance

ISBN (online) 978-1-4863-0584-1

Citation

Suckow, Axel, Taylor, Andrew, Davies, Phil, Leaney, Fred (2016) Geochemical baseline monitoring. Final Report. CSIRO, Australia.

Copyright and disclaimer

Important disclaimer

Content

Acknowledgments vi

Executive summary vii

Background vii

Key results vii

Conclusion and Recommendations viii

1 Introduction 1

2 Methods 3

2.1 Study area 3

2.2 Experimental design for the field study 6

2.3 Field sampling methods 7

2.4 Analytical methods 8

2.5 Lumped Parameter Models 9

2.6 Interpretation of tracer data by particle tracking 10

3 Results 11

3.1 Cross plots 11

3.2 General flow direction in the Hutton inferred from ^{14}C and ^{36}Cl 14

3.3 Horizontal and vertical flow velocities in the Hutton 16

3.4 Geochemical influences on ^{14}C and ^{36}Cl 20

3.5 Influence of double porosity on ^{14}C and ^{36}Cl in the Hutton 27

3.6 Support of the double porosity model by other tracers 29

3.7 Particle tracking 33

3.8 Precipice Sandstone 35

4 Discussion 37

4.1 Hutton flow system 37

4.2 Other tracers 39

4.3 Tracers and numerical models 40

4.4 Conclusions and Recommendations 41

References 42

Appendix A Using environmental tracers to quantify groundwater time scales 47

Figures

Figure 2.1: Conceptual model of the groundwater systems in the Surat Cumulative Management Area (QWC 2012) 4

Figure 2.2: Potentiometric surface for the Hutton Sandstone inferred by geophysical methods (Hodgkinson et al. 2010) 5

Figure 2.3: Potentiometric surface for the Hutton Sandstone in the vicinity of the Dawson River catchment inferred using geophysical techniques (Ransley and Smerdon 2012) 5

Figure 2.4: Position of the two north-south transects sampled east and west of the Mimosa Syncline with focus on the Hutton Sandstone. 7

Figure 3.1: Plot of ^{3}H versus ^{14}C for all samples from the area, from the GISERA, OGIA, GA and GABWRA datasets. The right figure is an inset of the left, showing details for small values of ^{3}H and ^{14}C. 12

Figure 3.2: Plot of ^{3}H versus SF_6 (left) and SF_6 versus ^{14}C for all samples from the GISERA Baseline project. Model curves are for a recharge altitude of 250 m AHD, a temperature of 15°C, and freshwater recharge without excess air (see Appendix A for a discussion on SF_6 dating) 13

Figure 3.3: Plot of ^{14}C versus ^{36}Cl for all samples from the GABWRA, GA, OGIA and GISERA datasets in the Hutton Sandstone 14

Figure 3.4: All result for ^{14}C and $^{36}Cl/Cl$ from earlier datasets (GA, GABWRA, OGIA) and acquired during this project. 15

Figure 3.5: All values for ^{14}C and $^{36}Cl/Cl$ in the Hutton Sandstone versus latitude 16

Figure 3.6: Depth profiles for all values of ^{14}C and $^{36}Cl/Cl$ and comparison with vertical model velocities 17

Figure 3.7: North-South transects for all values of ^{14}C in the Hutton Sandstone on the western (top left) and eastern (top right) transect and for $^{36}Cl/Cl$ on the western (bottom left) and eastern (bottom right) transect 18

Figure 3.8: Illustration how the flow distances were calculated for the two transects (left) and for different flow lines on the shortest connection from the outcrop (right) 19

Figure 3.9: Plot of *all* samples from the Hutton Sandstone for ^{14}C (top) and $^{36}Cl/Cl$ (bottom) between longitudes 149E and 150.5E versus the distance to the closest point of the outcrop of Hutton Sandstone ..20

Figure 3.10: Increase of total dissolved inorganic carbon (TDIC) in the Hutton with depth and with distance to outcrop. 21

Figure 3.11: Absolute ^{14}C concentration in atoms/L (bottom) and geochemically corrected $^{14}C/C$ values (top) versus distance to outcrop. Phillips model lines assume a rate of TDIC increase along the flow path of 0.4 mMol/(L km). 22

Figure 3.12: Depth profile and transect of chloride concentration in groundwater (samples from this study only). 23

Figure 3.13: Cl concentration in the Hutton Sandstone in the vicinity of the Mimosa Syncline. 24

Figure 3.14: Geochemical cross-plots of the ^{36}Cl-Cl system: $^{36}Cl/Cl$ versus Cl (top) and ^{36}Cl versus Cl (bottom). The mass-balance was evaluated using the Phillips model for an initial Cl concentration of 120 mg/L, a $^{36}Cl/Cl$ ratio of $1.3 \cdot 10^{-13}$ and for a diffusive chloride increase flux of 0.04 µg/(L·year). Arrows indicate how different components of the mass-balance for ^{36}Cl and Cl could impact on observed concentrations. 25

Figure 3.15: Absolute ^{36}Cl concentration (bottom) and geochemically corrected $^{36}Cl/C$ values (top) versus distance to outcrop. For the Philips model, the initial Cl concentration was 120 mg/L, the $^{36}Cl/Cl$ ratio $1.3 \cdot 10^{-13}$ and the diffusive chloride flux 0.04 µg/(L·year) 26

Figure 3.16: Flow-velocities as described by the Sudicky and Frind (1981) model. This model assumes *the same* flow velocity of 1 m/year for both tracers (^{14}C and ^{36}Cl). The displayed brown curve is for an aquifer thickness of 10 m, a dispersivity α_L of 10 m, and porosities of aquifer and aquitard of 20% and 30%, respectively.....28

Figure 3.17: Stable isotope results plotted versus the distance from Hutton outcrop. Indicated are model results for a palaeoclimatic shift of 2.5‰ and 20‰ in ^{18}O and ^{2}H respectively and 1.2m/year distance velocity.....29

Figure 3.18: Map of ^{18}O values in groundwater in the Hutton Sandstone.....30

Figure 3.19: Map of helium concentrations in groundwater of the Hutton Sandstone. 31

Figure 3.20: Depth profile (left) and transect of helium concentration versus distance to Hutton outcrop (right).....32

Figure 3.21: Cross plots for ^{4}He with ^{14}C (left) and $^{36}Cl/Cl$ (right) with their best matching piston flow, exponential and binary mixing models. The PM and EM models used a helium production rate of 10^{-11} cc(STP)/(g·year). 33

Figure 3.22: Visualisation of MODFLOW-ADV2 generated particle tracks for a sample well (Sreekanth and Moore 2015).....34

Figure 3.23: Comparison of particle-tracking derived ^{14}C (left) and $^{36}Cl/Cl$ (right) values with the actually measured tracer concentrations.....34

Figure 3.24: Map of ^{14}C (top) and $^{36}Cl/Cl$ (bottom) for all samples from the GABWRA, GA, OGIA and GISERA datasets in the Precipice Sandstone 36

Figure 4.1: Length of recharge segment of Hutton Sandstone between the two dominant fault systems and recharge values according to the Chloride Mass Balance approach (Smerdon and Ransley 2012).....39

Figure A.1: Principle of the application of environmental tracers to deduce groundwater age (Suckow 2014).....47

Figure A.2: Input function of tritium in Kaitoke and several Australian stations (IAEA/WMO 2015).....50

Figure A.3: The principle how CFCs and SF_6 are used to deduce time, SH and NH being 'southern' and 'northern' hemisphere respectively.....51

Figure A.4: Decay chain of ^{238}U (Suckow 2009), providing a total of 8 helium atoms per decaying ^{238}U (yellow arrows) 54

Figure A.5: Spreading of age distributions due to different processes relevant in groundwater (Torgersen et al. 2013).....56

Figure A.6: Tracer retardation by matrix diffusive loss into stagnant zones (Purtschert *et al.* 2013).....57

Acknowledgments

This report was funded by the Gas Industry Social and Environmental Research Alliance (GISERA). GISERA is a collaborative vehicle established to undertake publicly-reported independent research addressing the socio-economic and environmental impacts of Australia's natural gas industries. The governance structure for GISERA is designed to provide for and protect research independence and transparency of funded research. See www.gisera.org.au for more information about GISERA's governance structure, funded projects, and research findings.

This report would not have been possible without the continuous support of a number of individuals and organisations. Special thanks to our colleagues at CSIRO, including Megan Lefournour (field work and sample custody), Michelle Caputo (SF_6 & CFC analyses), Stan Smith (helium measurements and tracer interpretation), Matthias Raiber (aquifer geometry and geochemistry), and Catherine Moore and Sreekanth Janardhanan (interpretation of tracer data using particle-tracking modelling). This work was also greatly facilitated by contributions from several staff from the Office of Groundwater Impact Assessment (OGIA), including Steve Flook, Michael Jamieson, Sanjeev Pandey and Steve Clohessy. The project obtained substantial scientific support from Origin, mainly from Kathryn Harris, Ryan Morris and Andrew Moser during planning of the field trip, Jason MacCartie and Marcus Horgan during sampling, and from Peter Evans for his insight into the structural geology of the study area. Andrew Feitz (Geoscience Australia) allowed us to use his geochemical and isotope dataset for the Surat Basin before it was officially published and citeable.

Besides all these scientific and organisational contributions, this project would not have been possible without the support of the farmers and landowners who welcomed us warmly, provided free access to their bores, local knowledge and field support. Special thanks to the people at Alkoomie, Amusen, Barton Spring, Caenby, Cattle Downs, Dangarfield, Hillside, Juandah, Killara, Loch Lamond, Moorabinda, Pine Hills, Pony Hills, Robinson Flat, Rochdale, The Peaks, Utopia Downs, Wallumbilla, Weemala, Wongalea, and Woodvale.

This report was subject to an intense CSIRO-internal review, and special thanks is due to Sebastien Lamontagne, Dirk Mallants and Stan Smith.

Executive summary

Background

The degree to which Coal Seam Gas (CSG)-driven depressurisation in coal seams is propagated into adjacent aquifers and, potentially, surface water features such as wetlands and springs can only be assessed with thorough understanding of these adjacent aquifers and their degree of connectivity with the gas reservoir. The natural water balance for potentially impacted aquifers is often poorly known, but important for quantifying the impacts of depressurisation. One of the tools available to assess the water balance of deep aquifers is environmental tracers – substances either dissolved in groundwater or part of the water molecule that provide information about its origin, transport pathways and flow velocity. The GISERA Baseline project used available and new tracer information in the Mimosa Syncline and sought to improve the water balance in the Hutton Sandstone, the first major aquifer below the Walloon Coal Measures of the Surat Basin. The Walloon Coal Measures is undergoing development for CSG, whilst the Hutton Sandstone is a key regional aquifer supplying farm wells and a recharge component of the Great Artesian Basin. In this study, groundwater velocity and flow direction in the Hutton Sandstone were evaluated using environmental tracers. In a second component to the Baseline project, Smith (2015) evaluated the permeability of the aquitards between the Walloon Coal Measures and underlying aquifers (that is, evaluated connectivity between gas reservoirs and aquifer).

- New environmental tracer data were obtained and existing data re-evaluated.
- Consistent flow velocities could only be derived using a double-porosity conceptualization of the Hutton Sandstone and then were in good agreement for ^{14}C, ^{36}Cl, ^{18}O, ^{2}H.
- Flow in the Hutton Sandstone happens only in a small part (<50m) of the total formation thickness (≈200m).
- Flow velocities in the Hutton Sandstone in the Mimosa Syncline are on the order of 1m/year
- Effective recharge to the deeper Hutton is much smaller than earlier estimates. This is probably due to 'rejected recharge' discharging in the spring complexes.

Current potentiometric surfaces for the Hutton Sandstone have incongruities, such as an apparent groundwater flow towards the hypothesised recharge areas for the aquifer (Hodgkinson *et al.* 2010). Groundwater flow velocity and direction were re-evaluated by sampling for environmental tracers in 23 wells along two north-south transects – which was the hypothesised direction for groundwater flow in the Hutton – combined with a re-interpretation of past tracer data collected for this system. The tracers considered included major ions, stable isotopes of the water molecule ($^{18}O/^{2}H$), ^{14}C, ^{36}Cl, noble gases, SF_6, and tritium. However, ^{36}Cl and ^{14}C were analysed in more detail because these can estimate groundwater flow velocities at a suitable scale for the Hutton Sandstone (>10,000 years). Tracer distribution along the two transects was interpreted using several conceptualizations of the geochemical and hydrogeological environment, such as the input of 'dead' Cl from neighbouring aquitards, dead carbon from oxidation of organic carbon, a single versus double porosity aquifer, etc. Limited sampling for environmental tracers was also undertaken in the underlying Precipice Formation to evaluate potential vertical exchanges between the Hutton and Precipice aquifers.

Key results

HUTTON SANDSTONE

Both ^{14}C and ^{36}Cl in groundwater decreased from north to south along the East and West transects and with depth, consistent with a downward and north to south groundwater flow. However, when using a simple piston flow model approximation of groundwater flow, both horizontal and vertical groundwater velocities were ten times larger when using ^{14}C relative to ^{36}Cl. For example, when using all data available, the

groundwater velocity was ~0.5 m/year and ~0.05 m/year for ^{14}C and ^{36}Cl, respectively. Flow velocity estimates were further refined by including potential geochemical effects on the tracers such as input of 'dead' carbon or chloride and subsurface production of ^{36}Cl, and by assuming that the Hutton is a double porosity aquifer. Under the double porosity assumption, most of the groundwater flow in the Hutton occurs over a small thickness of the aquifer (possibly as low as 5-10% based on previous studies on the transmissivity of this aquifer) with the other areas representing more or less stagnant zones. This double porosity assumption could best describe the discrepancies between groundwater velocities derived from ^{14}C and ^{36}Cl. As the radioactive tracers diffuse from the main flow path to the stagnant zones, older apparent ages (i.e. lower apparent velocities) are observed. Because of its longer half-life, this effect is stronger for ^{36}Cl than for ^{14}C, resulting in apparent retardation factors on the order of 4 for ^{14}C and 40 for ^{36}Cl. When assuming a double porosity aquifer, horizontal velocities are in the range of 1 m/year for both ^{14}C and ^{36}Cl (instead of <1 m/year) and are similar to an independent estimate (~1 m/year) obtained using a palaeoclimate signal in the stable isotopes of water (^{18}O, ^{2}H). This tracer-constrained double porosity model allows estimating the total groundwater flux at depth in the Hutton. This derived value is 452 ML/y, or 2.7% of the recharge rate estimated using chloride mass balance (CMB). Thus, most of the recharge to the Hutton Sandstone is probably diverted to shallower flow paths discharging close to the recharge areas. This process ('rejected recharge') is a common feature of GAB aquifers.

The study design with two north-south sampling transects excludes a natural flow direction northward, but not an eastward or westward one. The maps of ^{36}Cl distribution do not exclude flow towards the southeast or east (e.g. towards the Dawson River). Thus, the Hutton Sandstone north of the Great Dividing Range may not represent one large flow system contributing recharge to the Great Artesian Basin but instead would decompose into several regional flow systems, each discharging into the tributaries of the Dawson River. A more detailed study would be needed to study each of these local flow systems and to quantify each local groundwater flow system towards the Dawson River. In the companion study, Smith (2015) could not determine the level of connectivity between the Walloon Coal Measures and the Hutton Sandstone using environmental tracers because of limited available information.

PRECIPICE FORMATION

Despite its increasing significance as a regional aquifer supplying farm water, there is limited existing environmental tracer information for the Precipice. Due to a number of factors (low ^{14}C, uncertain initial $^{36}Cl/Cl$ at recharge, scarcity of data), groundwater velocity in the Precipice Formation could not be evaluated with the available information. In the companion study, Smith (2015) determined that the Hutton and the Precipice are poorly or not connected.

REPRESENTATION OF TRACER DISTRIBUTION BY PARTICLE TRACKING

A three-dimensional groundwater flow model (QWC 2012) was used to evaluate travel times in the Hutton Sandstone using particle tracking. While not an ideal representation of tracer movement, particle tracking has the advantage to be computationally relatively simple and efficient. The approach appeared useful for visualizing the origin of groundwater pumped at individual wells, but less so for the interpretation of the Hutton tracer data. The primary reason for the poor fit was that the effects of the double porosity nature of the aquifer on tracer distribution cannot be captured by particle tracking. A more advanced numerical interpretation of the Hutton tracer data will require the use of a more complex solute transport model taking into account dispersion and diffusion into stagnant zones. An important benefit of such a more detailed model would be a deeper insight into the flow system and a spatially better resolved water balance and flow velocity.

Conclusion and recommendations

The differences in the inferred groundwater flow direction in the Hutton Sandstone between the contemporary potentiometric surface and environmental tracers suggest that this system may be in a

transition phase. The contemporary piezometric surface may reflect ongoing changes driven by climate or extraction whilst tracers would reflect the natural flow system prior to development. The trends in the environmental tracers support the concept of the low effective transmissivity of the Hutton and much smaller recharge than previously assumed, making this system more vulnerable to groundwater extraction or to depressurisation in neighbouring geological formations than anticipated. In other words, as only a small proportion of the aquifer effectively transmits water, the sustainable yield for this aquifer is probably low. Determining the connectivity of the Walloon Coal Measures to the Hutton Sandstone should still be considered a key knowledge gap.

The study highlighted other knowledge gaps, including:

1. The initial tracer values at the northern and eastern recharge areas for the Hutton Sandstone are not known (and are required to properly set the 'groundwater clock')
2. The magnitude of groundwater flow from the south-eastern recharge area towards the centre of the Mimosa Syncline is not known
3. The initial tracer values in recharge areas for the Precipice Sandstone are unknown and tracer data in general is lacking for this aquifer
4. The water balances for the Hutton and the Precipice sandstones remain sketchy, complicating the assessment of the potential impacts of depressurisation in the Walloon Formation or of groundwater extraction from these aquifers.

Key recommendations from the study include to:

1. Strategically sample additional wells in the Hutton and Precipice aquifers to improve the spatial coverage for tracer distribution, especially in recharge areas of both aquifers
2. Strategically sample for ^{39}Ar in recharge areas and ^{81}Kr farther along flow paths to help constrain the more numerous ^{14}C and ^{36}Cl data. Whilst more complicated to sample in the field, ^{39}Ar and ^{81}Kr can quantify groundwater flow velocity at the right timescales (intermediate for ^{39}Ar and very old for ^{81}Kr) and are relatively easy to interpret
3. Evaluate groundwater velocity and recharge rates for the Precipice Formation
4. Use the tracer distribution in the Hutton as calibration target for a numerical groundwater flow and solute transport model
5. Continue efforts to quantify the connectivity between the Walloon Coal Measures and neighbouring geological formations.

1 Introduction

The degree to which Coal Seam Gas (CSG)-driven depressurisation in coal seams is propagated into adjacent aquifers and, potentially, surface water features such as wetlands and springs will depend to a large degree on how well adjacent aquifers are connected or disconnected from coal seams. Measuring this connectivity is not a simple task because of the complexity of coal-bearing subsurface environments, including the presence of multiple aquifers and aquitards, faults and fractures. Even when a connection exists, quantifying impacts can be difficult because the water balance for most deep aquifers is poorly known. Only if this water balance and detailed baseline knowledge on geochemical and environmental tracer concentrations is established, CSG impact can be detected as changes of this baseline. The GISERA Baseline project has evaluated the connectivity and the water balance for key geological formations of the Surat Basin. In this report, groundwater flow direction and velocity were evaluated in the Hutton Sandstone, the first major aquifer below the Walloon Coal Measures of the Surat Basin. The Walloon Coal Measures is undergoing development for CSG, whilst the Hutton Sandstone is a key regional aquifer used for farm water supply and a component of the Great Artesian Basin (GAB), a nationally significant hydrogeological system (Smerdon et al. 2012). The study aimed to answer a paradox for the Hutton, where current potentiometric surfaces suggest groundwater flow is towards its hypothesised recharge area to the north. In a second component to the Baseline project, Smith (2015) evaluated the permeability of the aquitards between the Walloon Coal Measures and over- or underlying aquifers – in other words, determined the connectivity between some of these geological formations at specific locations.

- This study focused on the Hutton Sandstone and used environmental tracers to derive groundwater flow velocities *within* this aquifer.
- Connectivity *between* different aquifers was addressed in a companion study using helium in quartz as proxy to derive vertical pore water velocities in aquitards.

The assessment of the water balance for the Hutton Sandstone was largely made using environmental tracers – natural or anthropogenic trace substances in groundwater that provide clues as to its origin and movement. The tracers considered included major ions, stable isotopes of the water molecule ($^{18}O/^{2}H$), ^{14}C, ^{36}Cl, noble gases, SF_6, and tritium (^{3}H). However, ^{36}Cl and ^{14}C were analysed in more detail because these can quantify groundwater flow velocity at a suitable scale for the Hutton Sandstone (>1000 years). Existing environmental tracer data was first obtained from a literature study for the Hutton Sandstone and then the data was supplemented by targeted sampling of 23 wells along two north-south transects in the study area. These transects extended from hypothesised recharge areas to deeper sections of the aquifer further south, with the southmost samples taken north of the Roma – Miles line (see Figure 2.4 on page 7). Some additional sampling was undertaken in the underlying Precipice Formation, another GAB aquifer, because of its increasing importance as water supply source and target of reinjection of CSG process water.

In the following, a review of the hydrogeological environment and of the current potentiometric surface in the Hutton is provided, along with a summary of previous tracer measurements in this system. The historical and new tracer data collected were interpreted to evaluate both groundwater flow direction and velocity in the Hutton. The interpretation of environmental tracers to evaluate groundwater flow processes can be quite complex (IAEA 2013; Suckow 2014) and is covered in several scientific text books. Since it cannot be reviewed in detail here, the interested reader is provided with a very short summary on environmental tracers and the processes important for this report in Appendix A following page 47. The implications of the study for evaluating the impact of groundwater extraction on the Hutton aquifer or depressurisation in nearby formations are discussed.

2 Methods

2.1 Study area

The Surat Basin is a 440,000 km^2 intracratonic basin of south-central Queensland and north-central New South Wales. It consists of up to 2500 m of layered sediments of Jurassic-Cretaceous age. The Surat Basin overlies the Permo-Triassic Bowen Basin, which extends farther to the north up to the latitude of Rockhampton (-23.4°N, see inset in Figure 2.4 where the blue area is the Bowen Basin), whereas the northern margin of the Surat basin is defined by the northern outcrop of the Jurassic formations (Precipice Sandstone at the latitude of Bundaberg, -24°N). Both basins were formed by sedimentation of a trough extending from north to south, the Mimosa Syncline. Changes in the sedimentary environment over time resulted in the formation of several aquifers, intercalated aquitards and coal bearing formations in the Surat and the Bowen basins. Key hydrostratigraphical units in the Mimosa Syncline include (from top to bottom, see also Figure 2.1): the Mooga Sandstone (aquifer), Orallo formation (aquitard), Gubberamunda Sandstone (aquifer), Walloon Coal Measures (coal bearing formation, containing aquifer & aquitard layers), Hutton Sandstone (aquifer), Evergreen Formation (aquitard) and the Precipice Sandstone (aquifer) (Hodgkinson *et al.* 2010). The underlying Moolayember formation (aquitard) and Clematis Sandstone (aquifer) are part of the Bowen Basin.

- The study area can be described as a layered cake of aquifer-aquitard systems in a natural depression.
- New groundwater samples were obtained along two north-south transects for 23 wells and combined with existing data.
- To ensure robust analysis necessary in old groundwater systems, a multi-tracer approach was adopted to obtain multiple lines of evidence for interpretation.
- Simple zero- and one-dimensional models were used to check data for consistency and to describe the governing factors of groundwater flow

The Surat Basin is regarded as part of the Great Artesian Basin (GAB). The western margin of both the Surat and the Bowen Basin is defined by the Nebine Ridge, where the aquifers of the Surat and Bowen basins thin out but are assumed to be connected to the aquifers of the Eromanga Basin of the GAB further to the west (Habermehl 1980; Radke *et al.* 2000). The eastern margin of Surat and Bowen basins is defined by the Kumbarilla Ridge, where both are connected to the Clarence Moreton Basin. In the south, the Surat Basin extends far into New South Wales and includes the Coonamble Embayment and the Oxley Basin, both overlying the Gunnedah Basin (Habermehl 1980). The deepest formation in the Surat Basin is the Jurassic Precipice Sandstone, which unconformably overlies the Triassic formations of the Bowen Basin (Figure 2.1). The Precipice Sandstone is isolated from the overlying Hutton Sandstone by a shale-rich horizon at the top of the formation and by the Evergreen Formation aquitard (Hodgkinson *et al.* 2010). The Walloon Coal Measures have variable hydraulic properties. Whereas the upper and lower parts of the Walloon Coal Measures form aquitards, the hydraulic transmissivity of the inner section is significantly larger. Further to the south and centre of the Mimosa Syncline, the Walloon Coal Measures are overlain by the Springbok Sandstone, which is considered an aquifer and equivalent to the Adori Sandstone in other parts of the GAB. It is overlain by the Westbourne Formation (aquitard), Gubberamunda Sandstone (aquifer) Orallo formation (aquitard) and Mooga Sandstone aquifer (Hodgkinson *et al.* 2010). The Mooga and Gubberamunda Sandstones together are considered equivalent to the Cadna-owie Hooray Aquifer of the Eromanga Basin (Radke *et al.* 2000; Smerdon and Ransley 2012). Two structural faults exist at the margins of the Mimosa Syncline, which created only minor deformations and displacements in the Jurassic-Cretaceous sequence. Both run north-south and are reactivated Permo-Triassic fault systems. They are described as the Hutton-Wallumbilla fault in the west and the Moonie-Goondiwindi and Burunga-Leichhardt fault system in the east (hereafter referred to as the Burunga-Leichhardt fault).

The best quality groundwater in the Mimosa Syncline is found in the Gubberamunda and Precipice aquifers. However, the Gubberamunda can only be found south of Wandoan (see Figure 2.4 and all following maps) and the Precipice can be only assessed at greater depth. Water from the Hutton Sandstone generally has a

higher salinity and the formation has a lower yield. Extensive sediment core testing for hydraulic conductivity by the enterprises engaged in CSG exploration (mainly lab triaxial permeability) generally gave a wide range of values for the Hutton Sandstone of roughly six orders of magnitude of ($1{\cdot}10^{-5}$–1) m/day in both vertical and horizontal direction. Values for the Precipice were generally higher and less variable (0.001–10) m/day; (APLNG 2014). There are also lateral differences in the hydrochemistry of groundwater, with generally fresher water in the Hutton Sandstone close to the northern and western outcrops and much higher salinities towards the south and east, especially east of the Burunga-Leichhardt fault and south of Wandoan (APLNG 2014).

2.1.1 RECHARGE AREAS

The sedimentation history into the basement trough and the later erosion of the sediment layers explains the shape of the outcrop areas, which resembles an upside-down 'U' around Taroom and Injune for the Hutton Sandstone and Precipice Sandstone (see Figure 2.4 and all following maps). The later deposited Springbok, Gubberamunda and Mooga Sandstones, which outcrop north of the Roma-Wallumbilla-Miles line but south of the Injune-Wandoan line, show this 'U' shape to a much lesser extent. In this report the outcrop areas are functionally all regarded as recharge areas for the respective aquifers and the terms 'outcrop area' and 'recharge area' are used interchangeably.

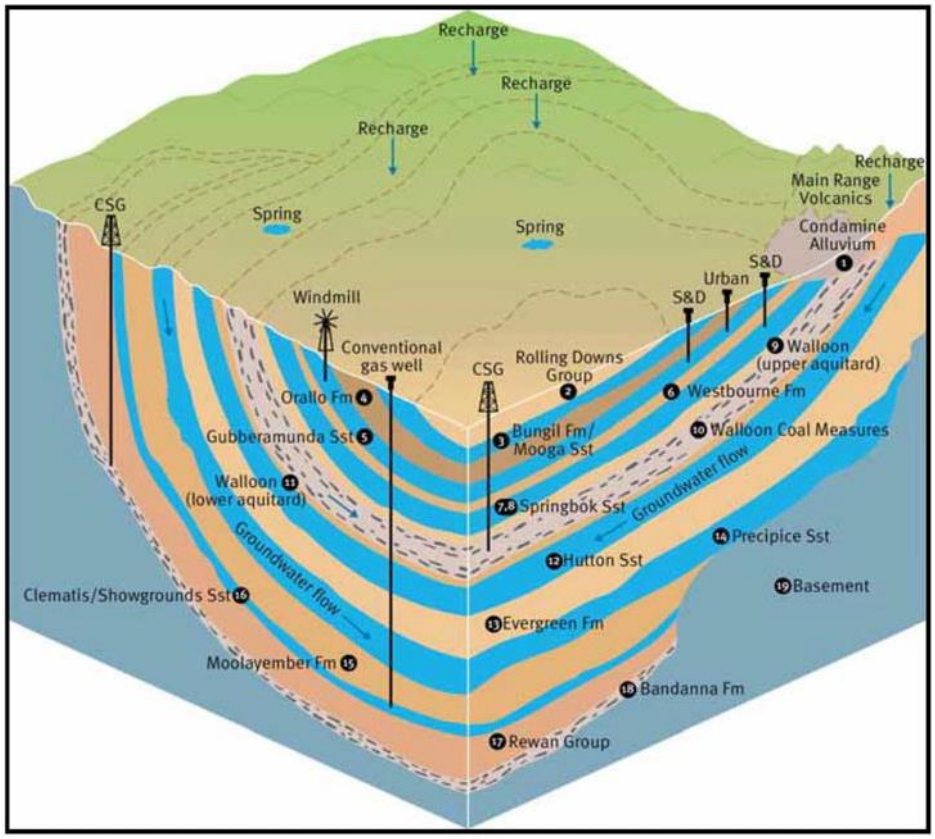

Figure 2.1: Conceptual model of the groundwater systems in the Surat Cumulative Management Area (QWC2012)

2.1.2 POTENTIOMETRIC SURFACE IN THE HUTTON SANDSTONE

The potentiometric surface for the Hutton Sandstone was recently evaluated by Hodgkinson et al. (2010) (Figure 2.2). Major recharge areas would occur to the north and east and the inferred groundwater flow would fan in several directions from there, including to the south, north-east and east. Groundwater flow to the north-east appears focussed around Dawson River tributaries (Figure 2.3).

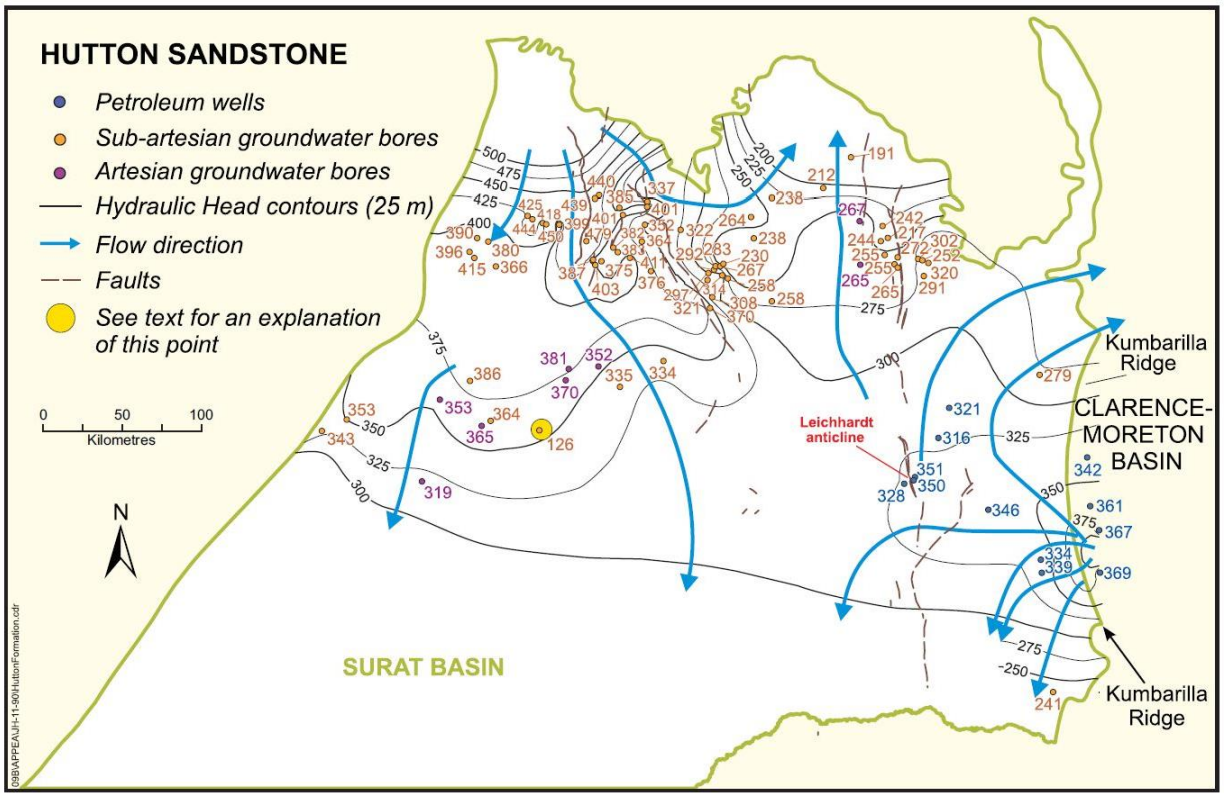

Figure 2.2: Potentiometric surface for the Hutton Sandstone inferred by geophysical methods (Hodgkinson et al. 2010)

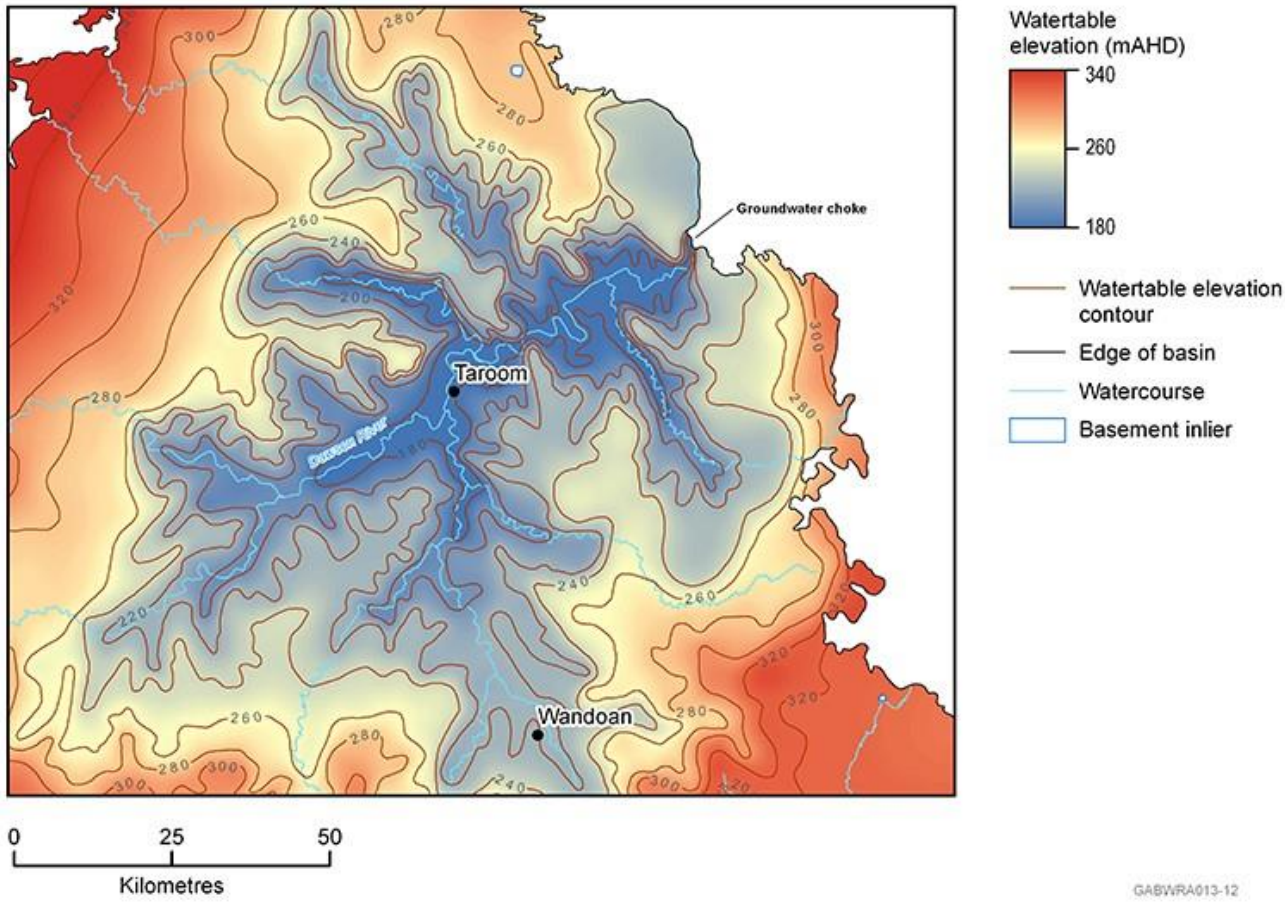

Figure 2.3: Potentiometric surface for the Hutton Sandstone in the vicinity of the Dawson River catchment inferred using geophysical techniques (Ransley and Smerdon 2012)

At the Mimosa Syncline, the Hutton outcrops towards Taroom and, farther south, towards Wallumbilla. Using water level measurements in bores (corrected for salinity and temperature), the potentiometric surface for the Hutton shows a depression centred around Taroom. This implies groundwater is flowing towards the outcrop, which is counterintuitive. Hodgkinson *et al*. (2010) recently found similar results for the Evergreen Formation and Precipice Sandstone.

2.2 Experimental design for the field study

Using environmental tracers, a field study was designed to determine whether or not groundwater flow is principally from north to south in the Mimosa Syncline. In a first step, the available environmental tracer database for the Hutton Sandstone was reviewed. Two databases were combined, one from Geoscience Australia ('GA database'; Feitz *et al*. 2014) and another from the GABWRA project ('GABWRA database'; Ransley and Smerdon 2012). In general, ^{14}C and ^{36}Cl was higher in recharge areas, consistent with a north to south flow direction (that is, the concentration for both tracers will tend to decrease in a downstream direction because of radioactive decay). These findings were used to identify 23 wells along two transects in the Mimosa Syncline (Figure 2.4). The western transect started close to the south-eastern corner of the Hutton outcrop and led to the south via Reedy Creek to Wallumbilla. The eastern transect started close to the northern corner of the Hutton outcrop and followed the road from Taroom to Miles. Suitable wells for the Hutton Sandstone were not found south of Wallumbilla. The municipal water supply well at Wallumbilla pumps groundwater from both the Hutton and the Gubberamunda sandstones, but was included here nevertheless.

The wells selected for the field study aimed to best fill the gap in space for ^{14}C and ^{36}Cl measurements and thus provide a more rigorous evaluation of groundwater flow direction and velocity for this section of the Hutton. The identification of appropriate groundwater bores for environmental tracer sampling was conducted using the Queensland Digital Groundwater Database (QDGWD) provided by the State Of Queensland (DNRM 2013). The two overarching requirements for identifying a bore as appropriate were: 1) the aquifer/hydrostratigraphic formation the bore was open or screened to was known and 2) the geographic location of a given bore in relation to the Hutton recharge area, as well as being situated on flow lines towards the Reedy Creek and Condabri industrial sites. In addition, information relating to the operational status of the facility (such as recent hydraulic head data) and the presence or absence of on-ground or down-hole equipment (such as headworks or windmills) was considered to ensure a bore was practical for sampling. Once a suitable spatial distribution and a practical number of bores were identified and plotted, property information specific to each bore was used to acquire contact details of landholders and industry representatives. Through contact with landholders and industry, basic information specific to individual bores sites were confirmed and the provision of site access was established in a verbal and written format. This resulted in the sampling locations shown in Figure 2.4.

Despite the anticipated relatively old age for groundwater along the transects (>10,000 years) both 'young' (^{3}H, CFCs and SF_6) and 'old' (^{14}C, ^{36}Cl and ^{4}He) groundwater tracers were sampled in order to evaluate potential mixing between young and old groundwater sources, as recommended in text books for dating old groundwater (IAEA 2013). The presence of 'young' tracers in the Hutton could either reflect a natural or artificial (i.e. bore leakage) connectivity with a shallower aquifer. This needs to be assessed and if necessary corrected for before using a tracer like ^{14}C and ^{36}Cl to derive flow velocities. Major ions, noble gases and $\delta^{18}O/\delta^{2}H$ of water were also measured to either help calibrate other tracers (i.e. Cl for $^{36}Cl/Cl$ dating) or provide an additional dating tool in the form of an anticipated palaeoclimate signal preserved in the Hutton ($\delta^{18}O/\delta^{2}H$). Additional bores were sampled in the Precipice and Gubberamunda sandstones (usually in the vicinity of bores sampled in the Hutton) to collect vertical tracer profiles across key hydrostratigraphical units, such as at the Reedy Creek injection site.

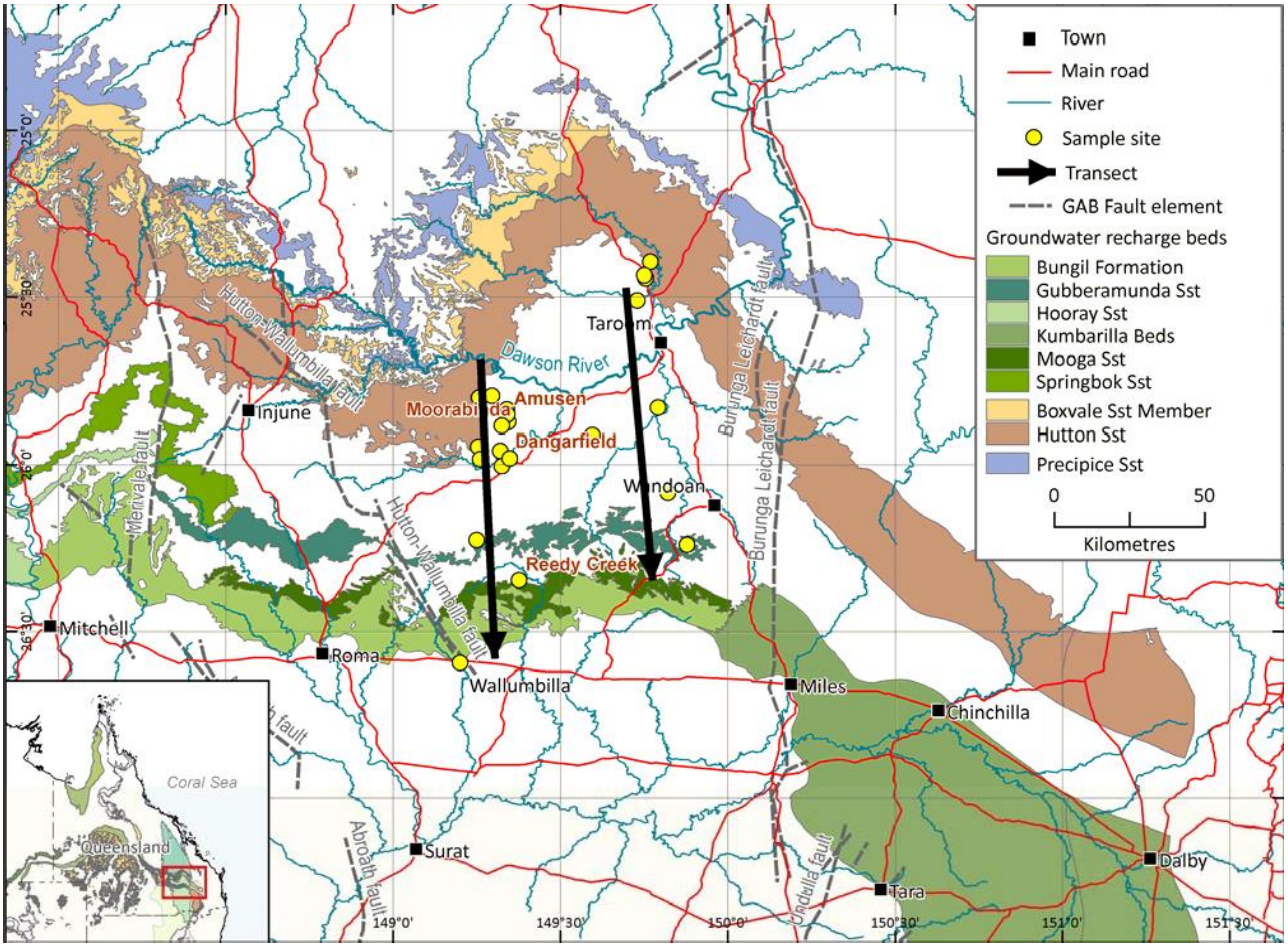

Figure 2.4: Position of the two north-south transects sampled east and west of the Mimosa Syncline with focus on the Hutton Sandstone.

Samples were obtained during two field trips by CSIRO, one in November 2012 with focus on spring complexes and another one in late October–November 2013. These two sampling trips were complemented by a dataset obtained from Steve Clohessy from OGIA (called "OGIA dataset" in the following) and by additional opportunistic sampling by Origin.

2.3 Field sampling methods

2.3.1 PURGING OF BORES

At each bore, groundwater was carefully purged to ensure representative water samples from the aquifer were obtained. Purging at a given bore was conducted using existing infrastructure, which varied from headworks on artesian bores, to Mono pumps, Grundfos submersible pumps and windmills on sub-artesian bores. Hydraulic head and bore construction data obtained from the QDGWD was used to calculate the total purge volume at each site, usually three standing water columns. On occasions, some bore sites needed less purging due to recent pumping or natural artesian flow. Conversely, some bore sites required additional purging volumes until monitored chemical parameters (electrical conductivity (EC), pH and temperature) stabilised.

2.3.2 CHEMICAL PARAMETERS

Chemical parameters were monitored and recorded during purging and sampling under gently flowing conditions, including EC, pH, temperature, total dissolved gas pressure (TDGP). Electrical conductivity, pH

and temperature were monitored using a handheld submersible TPS WP-81 water quality meter. TDGP was monitored using a Pentair Aquatic Eco-Systems Point Four Tracker handheld submersible meter. The presence of H_2S was noted qualitatively when detected (odour) during sampling as was the amount of gas bubbles.

2.3.3 SAMPLE COLLECTION

Sampling for all tracers was conducted by initially establishing a gas-tight connection to existing headworks (on artesian bores) and discharge hose (on sub-artesian bores). In the case of artesian bores, a gas-tight connection was established by securing copper or nylon tubing using Swagelok fittings directly to the headworks. For sub-artesian bores, copper or nylon tubing was secured to agricultural pipe using Philmac adaptors. These gas-tight connections are most important to prevent sample contamination with the atmosphere, as well as any soft plastic components that possibly contain CFCs.

Groundwater samples were collected for laboratory analysis of general chemistry (pH, EC and alkalinity) as well as major and minor ions. Duplicate samples for major and minor ions were collected, filtered with a 0.45 µm Acrodisc syringe filter and placed in 125 mL PET plastic bottles. Dissolved oxygen concentration was determined by Winkler titration using a HACH dissolved oxygen test kit. Samples for cation analysis were acidified with nitric acid (HNO_3). For δ^2H and $\delta^{18}O$, duplicate samples were collected, filtered with a 0.45 µm syringe filter, and placed in a 28 mL gas-tight glass bottle (McCartney bottle) to prevent evaporation. Strontium isotope samples were collected in 500 mL PET bottles under gently flowing conditions. Tritium samples were collected in 1 L PET plastic bottles under gently flowing conditions to avoid excessive air contact and capped without a head space to avoid contact with the atmosphere. Duplicate samples for dissolved noble gases were collected in copper tubes following Weiss (1968). Briefly, this involved creating a gas tight connection between the copper tube and the discharge outlet on the bore, gently flushing the tube, and applying a back pressure using a flow regulator before clamping the copper tube at each end without trapping any gas bubbles. However, for the deepest bores pumping hot water (>50°C), degassing was not always avoidable. In these cases, a fractionation of noble gas values cannot be excluded, although samples were taken such that gas bubbles were not enclosed within the copper tubes. This was achieved by turning the copper tube upside down after closing the first clamp and letting the gas bubbles escape to the connecting tubing.

Samples for ^{14}C were collected in 5 L PET plastic jerry cans. Samples for CFCs were collected following protocols of the CSIRO Environmental Tracer Laboratory (ETL). Briefly, this involved connecting a nylon discharge hose to the bore discharge outlet, placing the nylon hose into the bottom of a 125 mL glass bottle that is placed inside a 10 L steel bucket. Samples were collected using a gentle pumping rate and bottles were reverse- or bottom-filled until the 10 L bucket overflows. Samples were collected in triplicate and capped under water to prevent exposure to the atmosphere. Samples for SF_6 were collected also following a similar protocol where samples were collected in a 1 L glass bottle placed inside the 10 L bucket and were capped under water after the 10 L bucket had overflowed several volumes. Samples for ^{36}Cl were collected in 1 L PET plastic bottles filled to the top and capped tightly without any head space.

2.4 Analytical methods

Major and minor ion concentrations were determined at CSIRO Analytical Services Unit (ASU) Waite Campus Adelaide. Cations were analysed by inductively coupled plasma optical emission spectrometry (ICP-OES) and anions by ion chromatography. Samples for δ^2H and $\delta^{18}O$ were analysed by GNS Science (Te Pü Ao, New Zealand) where measurements were made using an Isoprime mass spectrometer following, for δ^2H, reduction at 1100°C using a Eurovector Chrome HD elemental analyser and for $\delta^{18}O$, by water equilibration at 25°C using an Aquaprep device. Strontium isotope ratios ($^{87}Sr/^{86}Sr$) of all groundwater samples were analysed at the University of Adelaide School of Earth and Environmental Sciences with a Finnigan MAT262 Thermal Ionisation Mass Spectrometer.

Samples for ^{14}C analysis were measured by single stage accelerator mass spectrometry (AMS) at the Australian National University (ANU), Canberra. Samples were prepared by first precipitating the dissolved inorganic carbon from 5 L of groundwater as strontium carbonate ($SrCO_3$) under alkaline conditions (pH >11). The $SrCO_3$ precipitate is then acidified and purified cryogenically into aliquots of carbon dioxide (CO_2) for measurement by AMS (Fallon *et al.* 2010). SF_6 and CFC samples were measured at the CSIRO Environmental Tracer Laboratory (ETL) Waite Campus Adelaide. SF_6 samples were measured using a specific gas chromatograph with an electron capture detector as an aliquot of high purity nitrogen that had been equilibrated with 300 mL of groundwater at 25°C. CFC samples (CFC-11 and CFC-12) were also measured by gas chromatography with an electron capture detector after quantitative stripping from water aliquots of defined volume under a stream of high purity nitrogen (Busenberg and Plummer 1992). Samples for ^{36}Cl were measured by accelerator mass spectrometry at ANU, Canberra (Fifield *et al.* 2010). Prior to measurement samples are prepared as pure silver chloride (AgCl) following methods outlined in Conard *et al.* (1986). Samples for tritium were analysed at the tritium laboratory of GNS Science in New Zealand by electrolytic enrichment and subsequent liquid scintillation counting (Morgenstern and Taylor 2009). Noble gas concentrations (He, Ne, Ar) were determined at the CSIRO Environmental Tracer Laboratory (ETL), Waite Campus, Adelaide using high vacuum extraction, gettering of reactive gases and quadrupole mass spectrometry.

2.5 Lumped Parameter Models

A single scalar 'age' (e.g. '30 years-old') is not appropriate to describe a groundwater sample because, due to dispersion and mixing, groundwater samples contain water recharged at different times, represented as an age distribution. This holds especially true in aquifers with very long timescales of groundwater flow (larger than several thousand years) because mixing, dispersion and diffusion of tracers become more important for longer times. It is also not necessary to determine groundwater 'age' from tracers because many hydrogeological processes can be inferred from tracer concentrations alone. Therefore, no attempt is made here to deduce any 'apparent ages' (Suckow 2014), as this was regarded as not appropriate. Instead, binary tracer-tracer plots, tracer depth profiles and tracer transect profiles were interpreted using zero-dimensional lumped parameter models (LPMs), one-dimensional flow interpretation or other simple approaches. Lumped parameter models are simplified representations of aquifers and flow systems that can be used to understand what are the key hydrogeological processes (advection, dispersion, mixing, etc.) impacting on tracer distribution (see (Suckow 2014) and Appendix A for additional discussion on the concept of groundwater age).

The lumped parameter models used here were the Piston flow Model (PM), the Exponential Model (EM) and the Binary Mixing Model (BMM). The PM assumes that no mixing takes place and that all water particles within the sample represent the same age. This corresponds to the conventional (human) understanding of the word age (Suckow 2014) and also to the particle tracking approach in discretised numerical flow models (Pollock 1994) – see section below. The EM assumes an exponential age distribution in the samples. Mathematically this is equivalent to the flow system in an extremely simplified aquifer with homogeneous recharge, homogeneous transmissivity and porosity and constant depth, sampled using a well screened over the whole aquifer (Vogel 1967). It is also mathematically consistent with a well-mixed system (e.g. a lake) with constant inflow and outflow. As a special property, the youngest water always has the largest relative contribution in an Exponential Model. The BMM assumes that the sample consists of exactly two water sources with a widely differing age – one assumed to be very young and the other very old (that is, free of any anthropogenic or radioactive tracers like CFCs, ^{3}H, etc). The interested reader is referred to (Maloszewski and Zuber 1985; Cook and Böhlke 1999; Solomon *et al.* 2006; Suckow 2013) for more detailed information on LPMs and mean residence times. All data handling and lumped parameter model calculations were performed with the LabData database and laboratory management system (Suckow and Dumke 2001) which includes 'Lumpy', a package for lumped parameter models (Suckow 2012).

To further evaluate the effect of geochemistry (such as dead ^{14}C and ^{36}Cl inputs from aquitards) or of the flow system (single versus double porosity aquifer) on tracer distribution, additional simple models were

used. These included the Phillips (IAEA 2013) ^{36}Cl model and the Sudicky and Frind (1981) model for diffusion-dominated tracer transport. These are described in more details in Appendix A.

2.6 Interpretation of tracer data by particle tracking

Within the GISERA sub-project 'CSG Water Reinjection Impacts: Modelling, Uncertainty and Risk Analysis' (Sreekanth and Moore 2015), an attempt was made to model the groundwater age distribution at selected wells by particle tracking (Pollock 1994). The numerical trial used the "Subregional model" (Sreekanth and Moore 2015) which covers a smaller region than the 'OGIA model' described in QWC (2012). The advantage of using the Subregional model and not the OGIA model itself was a finer horizontal discretization (500 m instead of 1500 m) and a focus on the study area where most of the tracer samples came from. Both the OGIA and the Subregional model are based on MODFLOW (McDonald and Harbaugh 1988) and adapted to the hydrogeological setting by the Queensland Office of Groundwater Impact Assessment (OGIA) and CSIRO (Subregional model). The MODFLOW ADV2 package was used to calculate travel times in groundwater (Anderman and Hill 2001, 2003). These are 'idealized ages' in the terminology of Suckow (2014).

Different strategies can be used to estimate the age distribution in a groundwater sample by particle tracking (Frenzel *et al.* 1997a, 1997b; Troldborg *et al.* 2007; Troldborg *et al.* 2008). Here, backward particle tracking was performed, centred on the middle of the grid cell where a given well was situated. Thus, the particle tracking started <500m away from the well. Each simulation created a stochastic ensemble of 350 different fields of hydraulic conductivities and porosities in the aquifer, and each was automatically calibrated against hydraulic heads. Particle tracking was performed on these 350 flow fields, resulting in a distribution of 350 ages for each well investigated.

This backward calculation was not always possible because particles did not always reach a recharge area within reasonable computation times because they got 'stuck' alternating between aquifers through an aquitard. Thus, the scheme had a practical limitation to determine the older part of an age distribution. In those cases where all 350 particles reached the groundwater surface, an age distribution was calculated (and represented as a histogram of particle numbers with a certain age range). These age distributions were used to calculate tracer concentrations with a convolution integral using the lumped parameter modelling code 'Lumpy' (Suckow 2012). This process used also estimated input concentrations of ^{14}C and ^{36}Cl and resulted in a comparison to the corresponding measured tracer values at the well.

3 Results

Combining the historical and the new information collected during this study, a significant environmental tracer database was assembled for the Hutton Sandstone in the Mimosa Syncline. A stepwise evaluation of the data was made to focus the interpretation on the most useful tracers in this environment. In a first step, tracer-tracer cross plots were evaluated to determine which combination of tracers was most useful to infer flow direction and velocity in the Hutton Sandstone. This analysis also enabled to evaluate some of the parameters required for further interpretation of the data, such as the likely initial ^{14}C and ^{36}Cl concentrations entering the aquifer (which are required to evaluate groundwater velocity). Relevant tracers were then evaluated to infer the potential flow lines and the horizontal and vertical groundwater velocities. Further evaluation of groundwater velocities were made by exploring how geochemical effects and a different representation of the aquifer permeability impacts on tracer distribution. It will be demonstrated that, when the Hutton is considered as a double porosity aquifer, groundwater velocities inferred using ^{36}Cl and ^{14}C are consistent and similar to values estimated using alternative methods.

- Tracers for young groundwater (decades) were at the detection limit, indicating that the Hutton contains no groundwater younger than 50 years.
- Lack of young groundwater indicates the sampled bores were suitable, i.e. do not leak groundwater from shallower aquifers.
- There is a possibility for underground production of SF_6 that requires further investigation.
- A simple piston flow interpretation of ^{14}C and ^{36}Cl to derive flow velocities gave contradicting results.
- The discrepancies between ^{14}C and ^{36}Cl derived flow velocities could not be explained by geochemical alteration introducing 'dead' carbon or chloride into the groundwater.
- A double porosity model can describe both the findings for ^{14}C and ^{36}Cl with one flow velocity and is in agreement with the results for stable isotopes (^{18}O, ^{2}H).
- The double porosity model allows inferring the total groundwater flux to the deeper Hutton Sandstone aquifer.
- Present day state of the art flow modelling combined with the particle tracking approach cannot explain the measured tracer data because it neglects the diffusion effects dominating tracer transport in a double porosity aquifer.

3.1 Cross plots

Tracer-tracer cross plots aimed to: 1) evaluate the presence of 'young' groundwater in the Hutton; 2) determine the initial ^{14}C activity at recharge and 3) determine the initial ^{36}Cl to Cl ratio ($^{36}Cl/Cl$) at recharge. The presence of young groundwater is possible in recharge areas for the Hutton (that is, groundwater with tracer values above background or detection limit for ^{3}H, CFCs or SF_6). However, the presence of young groundwater tracers further along the flow path could represent well leakage (that is, infiltration of rainwater or shallower groundwater along the well casing). Most groundwater samples from the Hutton had ^{3}H values below analytical detection limit (0.25 TU for the GA and GABWRA datasets and 0.03 TU for OGIA and GISERA; Figure 3.1). Only two samples from the OGIA dataset showed a clearly detectable ^{3}H concentration of (0.8±0.03) TU and (0.1±0.03) TU combined with ^{14}C values of 79% and 3.3%. The higher of the two results points towards a correction factor for the initial ^{14}C concentration of 0.8 or lower, corresponding to a 20% dilution of the initial ^{14}C activity by ^{14}C-free carbon from the aquifer; see Appendix A. These samples originate from the recharge area of the Gubberamunda and Springbok Sandstones, respectively. Overall, the Hutton Sandstone aquifer contains water recharged prior to 1960 (see the orange mixing line for the BMM in Figure 3.1 right, assuming the ^{3}H content in rain was never below 1.5–3 TU). There was no evidence for significant well leakage.

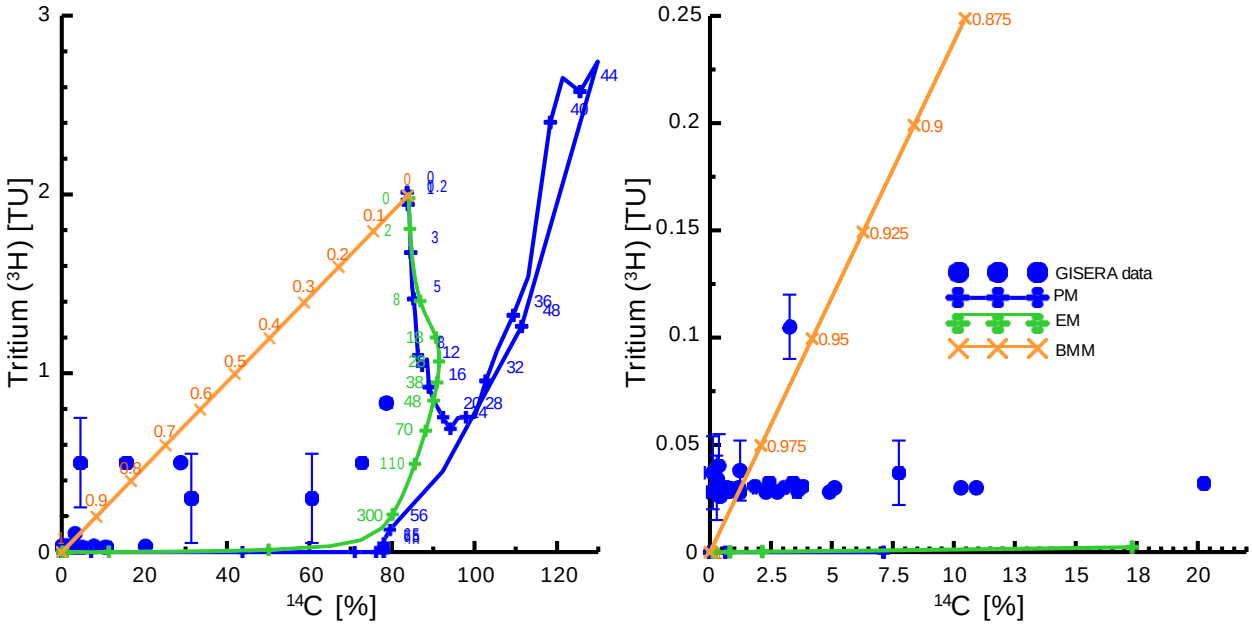

Figure 3.1: Plot of ^{3}H versus ^{14}C for all samples from the area, from the GISERA, OGIA, GA and GABWRA datasets. The right figure is an inset of the left, showing details for small values of ^{3}H and ^{14}C.

The inference about the lack of young groundwater in the Hutton made with ^{3}H was further tested by looking at trends in groundwater CFCs and SF_6 concentrations. In view of anaerobic (oxygen-free) conditions in the Hutton, CFC samples have only been measured on a very small subset for test purposes. CFCs are not always conservative under anaerobic conditions, see Appendix A. CFCs were at the detection limit for all samples measured (data not shown), consistent with either the absence of young groundwater or CFC degradation in the aquifer. However, some ^{3}H-free samples contained SF_6 (Figure 3.2). This could either represent the presence of young groundwater or underground production for SF_6 (Koh *et al.* 2007; Deeds *et al.* 2008; Rohden *et al.* 2010). At least one sample (RN58456, Dangarfield), contained more than 12 fmol/L (shown with broken axis in Figure 3.2), which cannot be explained by equilibration with atmospheric clean air (or any LPM). In this case, natural underground production of SF_6 or a contamination during sampling or transport is possible. However, because other samples measured in the same run resulted in blank concentrations, contamination is unlikely. The RN58456 Dangarfield sample was also collected in duplicate which had similar values, also ruling out a contamination artefact. As most samples were at detection limit, underground SF_6 production (if it occurs) would not be constant across the Hutton. At least one sample (RN123338, SV01) shows a realistic combination of SF_6 and ^{14}C, pointing towards a correction factor for the initial radiocarbon concentration close to 0.9 (see orange line; Figure 3.2 right). Overall, the trends in CFCs and SF_6 were largely consistent with the absence of young groundwater in the Hutton, except in recharge areas.

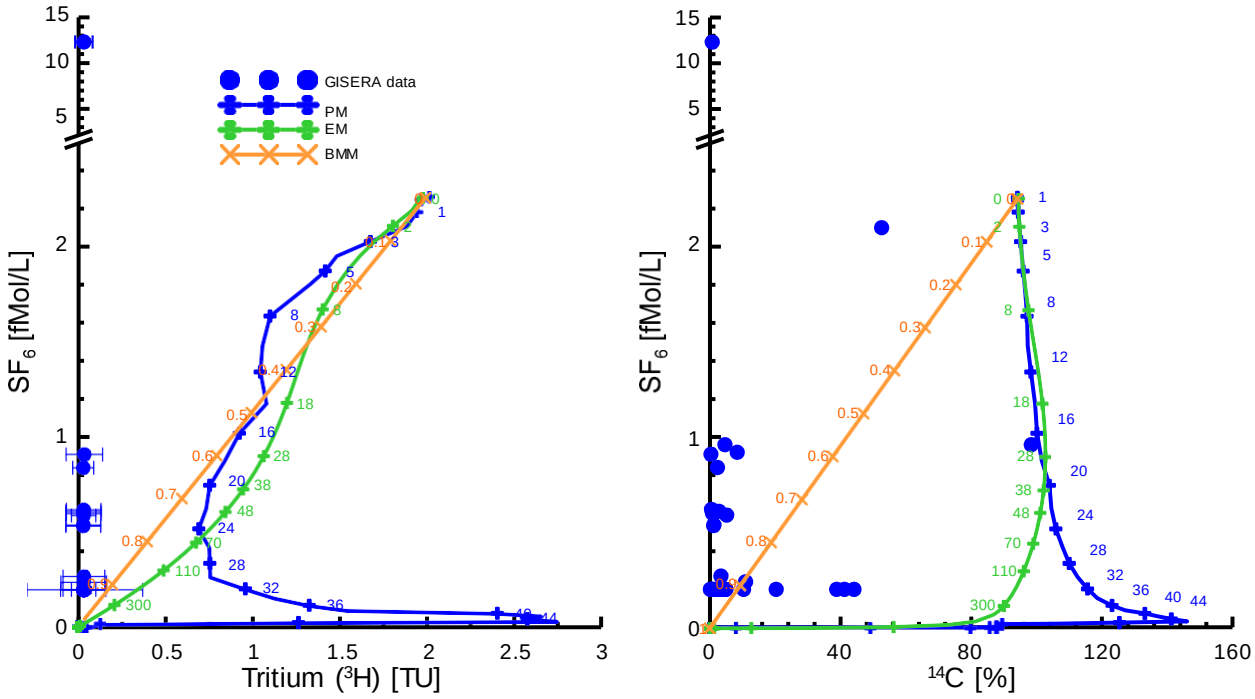

Figure 3.2: Plot of ^{3}H versus SF_6 (left) and SF_6 versus ^{14}C for all samples from the GISERA Baseline project. Model curves are for a recharge altitude of 250 m, a temperature of 15°C, and freshwater recharge without excess air (see Appendix A for a discussion on SF_6 dating)

Comparison of the trends in ^{14}C and $^{36}Cl/Cl$ can also be used to evaluate the initial $^{36}Cl/Cl$ of groundwater entering the Hutton aquifer (Figure 3.3). Hutton groundwater has relatively low ^{14}C (generally <20 %) but shows a wider range in $^{36}Cl/Cl$ ($2–14 \cdot 10^{-14}$), suggesting it is relatively old (that is, because of its shorter half-life, most of the ^{14}C would have decayed). When interpreted with LPMs, the $^{14}C/^{36}Cl$ data could fit either a PM or EM model but not a BMM model (Figure 3.3). Based on samples with relatively high ^{14}C, originating from closer to recharge areas, the initial $^{36}Cl/Cl$ in recharge would be ~$1.2 \cdot 10^{-13}$. The cross plot estimates for the ^{14}C and $^{36}Cl/Cl$ in Hutton recharge are preliminary only because they represent very simple approximations of geochemical processes along the flow path.

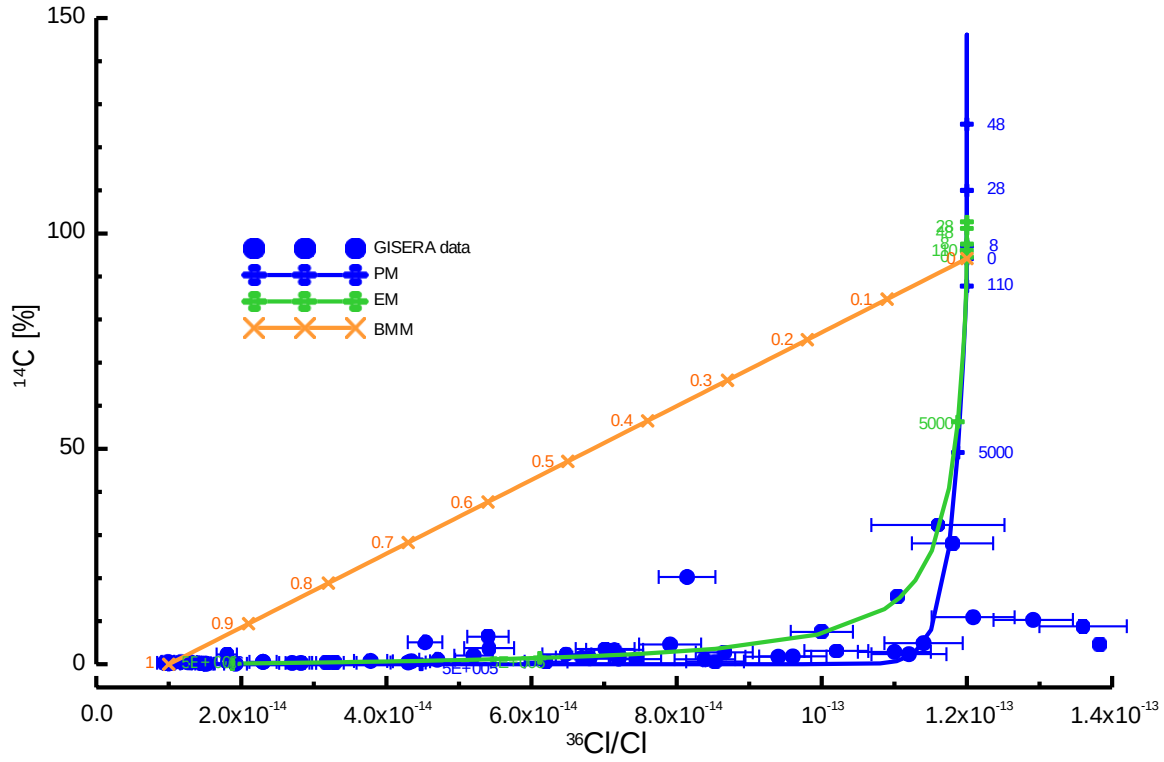

Figure 3.3: Plot of ^{14}C versus ^{36}Cl for all samples from the GABWRA, GA, OGIA and GISERA datasets in the Hutton Sandstone

3.2 General flow direction in the Hutton inferred from ^{14}C and ^{36}Cl

There was a tendency for groundwater ^{14}C and ^{36}Cl to decrease from north to south in the Mimosa Syncline (Figure 3.4 and Figure 3.5), suggesting that the main direction for groundwater flow is from north to south. The highest tracer values were found around two different latitudes, namely around -25.5° N and around -25.9°N latitude, suggesting two main areas of recharge within the outcrop of the Hutton Sandstone. However, because the samples were not evenly distributed throughout the entire recharge area, additional preferential recharge areas are also possible. South of -26.2°N (south of the southmost point of the western branch of the recharge areas) none of the samples contained measurable ^{14}C, whereas the first samples with background-^{14}C showed up as far north as -25.8°N. Very interestingly at the same latitude, some samples were at background for the $^{36}Cl/Cl$ ratio, despite ^{36}Cl having a half-life 53 times larger than ^{14}C. While the trends in ^{14}C and ^{36}Cl are clearly consistent with a general north to south flow direction, at the local scale more diverse flow directions are possible in the Hutton.

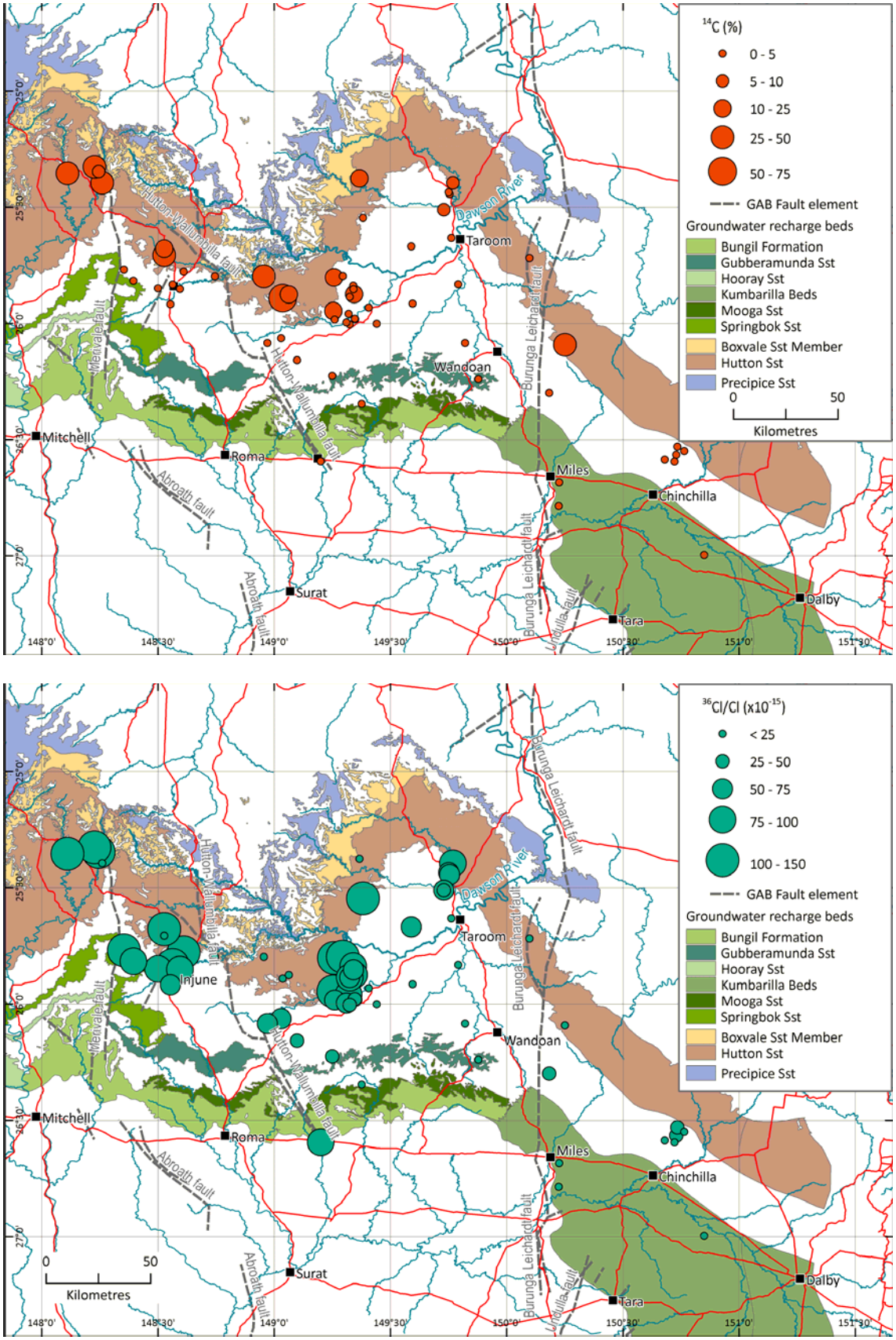

Figure 3.4: All result for ^{14}C and ^{36}Cl/Cl from earlier datasets (GA, GABWRA, OGIA) and acquired during this project.

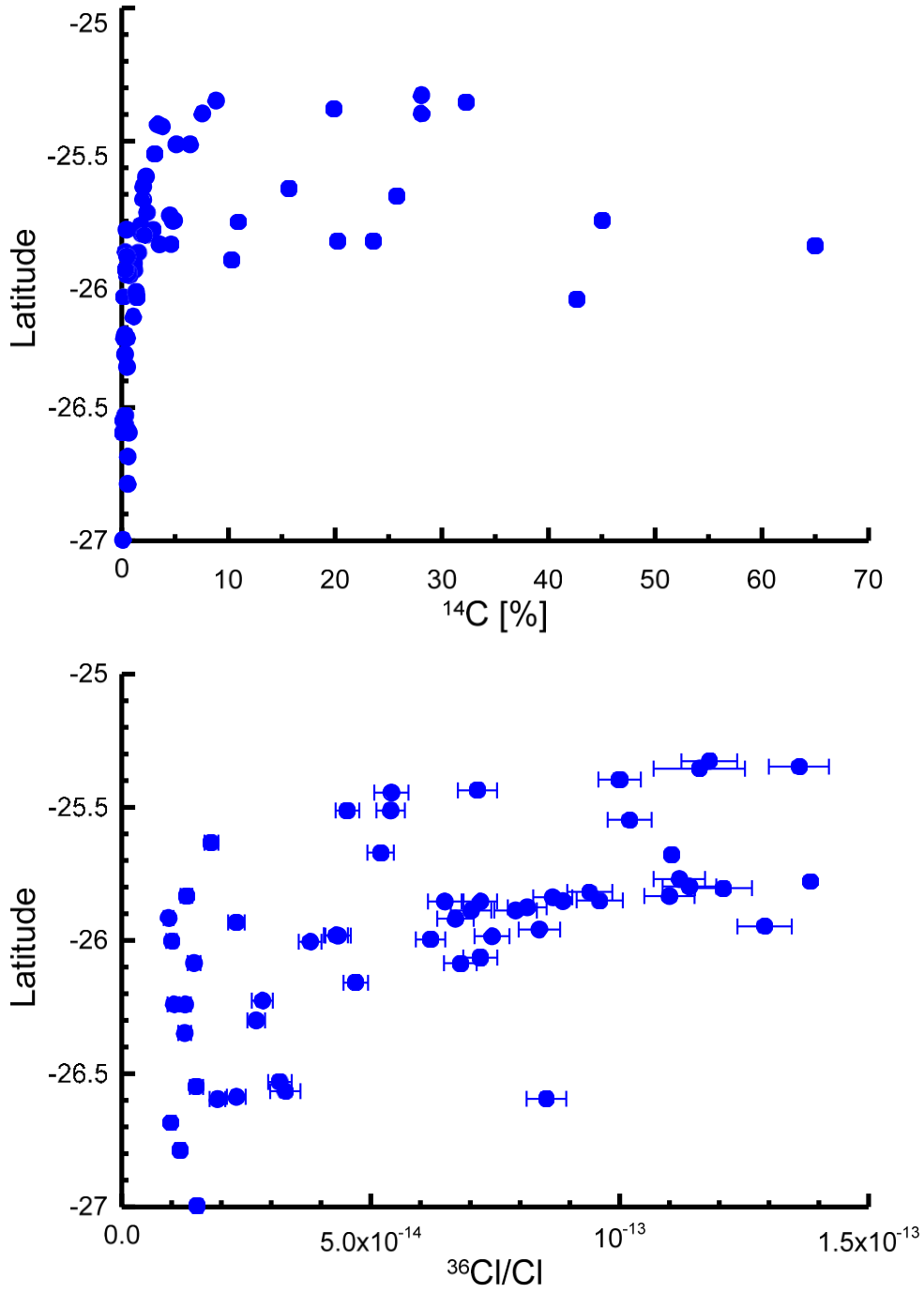

Figure 3.5: All results for ^{14}C and $^{36}Cl/Cl$ in the Hutton Sandstone versus latitude

3.3 Horizontal and vertical flow velocities in the Hutton

Distance from outcrop areas and depth below ground can be used as measures of the horizontal and vertical distance travelled by groundwater at a given well. Changes in tracer activity with distance or depth can then be used to evaluate the horizontal and vertical groundwater velocity in the Hutton, respectively. For the vertical velocity, this is not strictly correct when away from outcrops, because the Hutton is a confined aquifer with a pronounced dip at the Mimosa Syncline. In other words, deeper samples will also tend to be the ones farthest away from outcrops. Ideally, nested piezometers should be used to measure vertical profiles in tracer concentrations, but these were not available here. Despite its limitations the concept of horizontal and vertical groundwater velocity will be used here, primarily to explore the potential effects of geochemical processes and aquifer representation on tracer distribution. Once these processes

are understood, groundwater velocities could be inferred more precisely using a more elaborate numerical groundwater flow model with a more realistic representation of aquifer geometry.

3.3.1 VERTICAL VELOCITIES

Both ^{14}C and $^{36}Cl/Cl$ decrease with depth in the Hutton aquifer (Figure 3.6), consistent with the general tendency for groundwater to be older at depth and for a downward groundwater flow in the Hutton at the Mimosa Syncline. However, when they are compared with similar lumped parameter models, there is a striking discrepancy in vertical velocities inferred using either ^{14}C or $^{36}Cl/Cl$ (Figure 3.6). The best model fits had vertical velocities ranging from 1–10 m/year when using ^{14}C and 0.2–1 m/year when using $^{36}Cl/Cl$. These results demonstrate that the depth profiles cannot be explained by advection only and suggest that a geochemical effect or property of the aquifer not yet taken into account influenced the tracer distribution in the Hutton.

Another interesting insight is that ^{14}C is negligible (defined as <1%) below 300 m depth in the aquifer and $^{36}Cl/Cl$ is down to the underground production value ($\approx 10^{-14}$) below 600 m depth in the aquifer. If ^{14}C loss is only from radioactive decay, this corresponds to apparent ages >10,000 years (1% in ^{14}C corresponds to 38ky if the initial concentration is 100%). However, this is not consistent with the declining trends also observed for $^{36}Cl/Cl$ over the same depth range (i.e. based on ^{14}C apparent ages, the decline in $^{36}Cl/Cl$ over the whole depth gradient should only be ~20% of the initial value). As both tracers go down to background in the profiles, tracer transport is clearly more complex than the simple models used here.

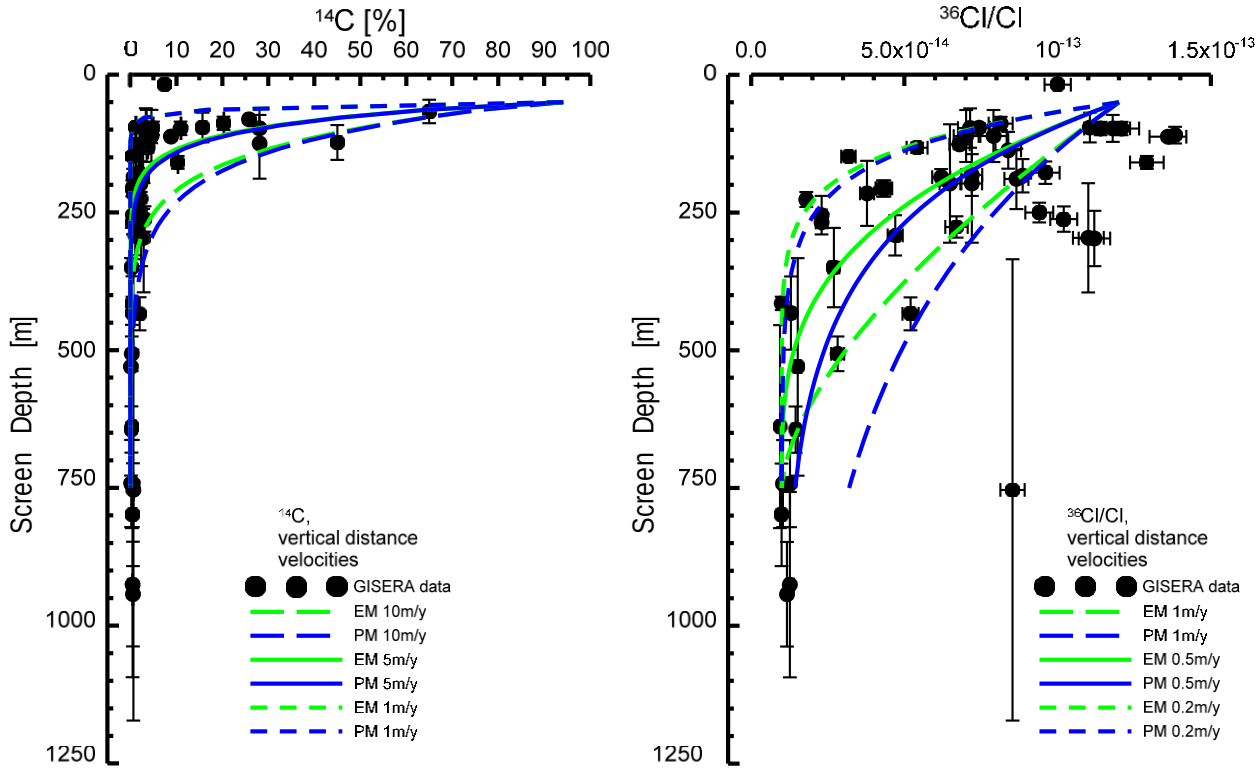

Figure 3.6: Depth profiles for all values of ^{14}C and $^{36}Cl/Cl$ and comparison with vertical model velocities

3.3.2 HORIZONTAL VELOCITIES

Part of the discrepancy between inferred vertical velocities from ^{14}C and $^{36}Cl/Cl$ may have to do with how different recharge areas contribute to groundwater flow in the Hutton. Two approaches were used to evaluate this. Firstly, different starting points were given to the western (149.37°E, -25.38°N) and eastern (149.77°E,-25.4°N) transects (Figure 3.8 left). Corridors around the transects were defined as (149.1-149.5)°E and (149.5-150)°E for the western and eastern transect, respectively. All available data from the GABWRA, GA, OGIA and GISERA datasets were used. The results plotted versus the distance to a reference

point give a clearer picture than when plotted versus latitude, especially for the eastern transect (Figure 3.7). They compare better to the piston flow model (PM). However, there is still a very considerable scatter in the data, especially at the western transect where data is clustered over intermediate distances.

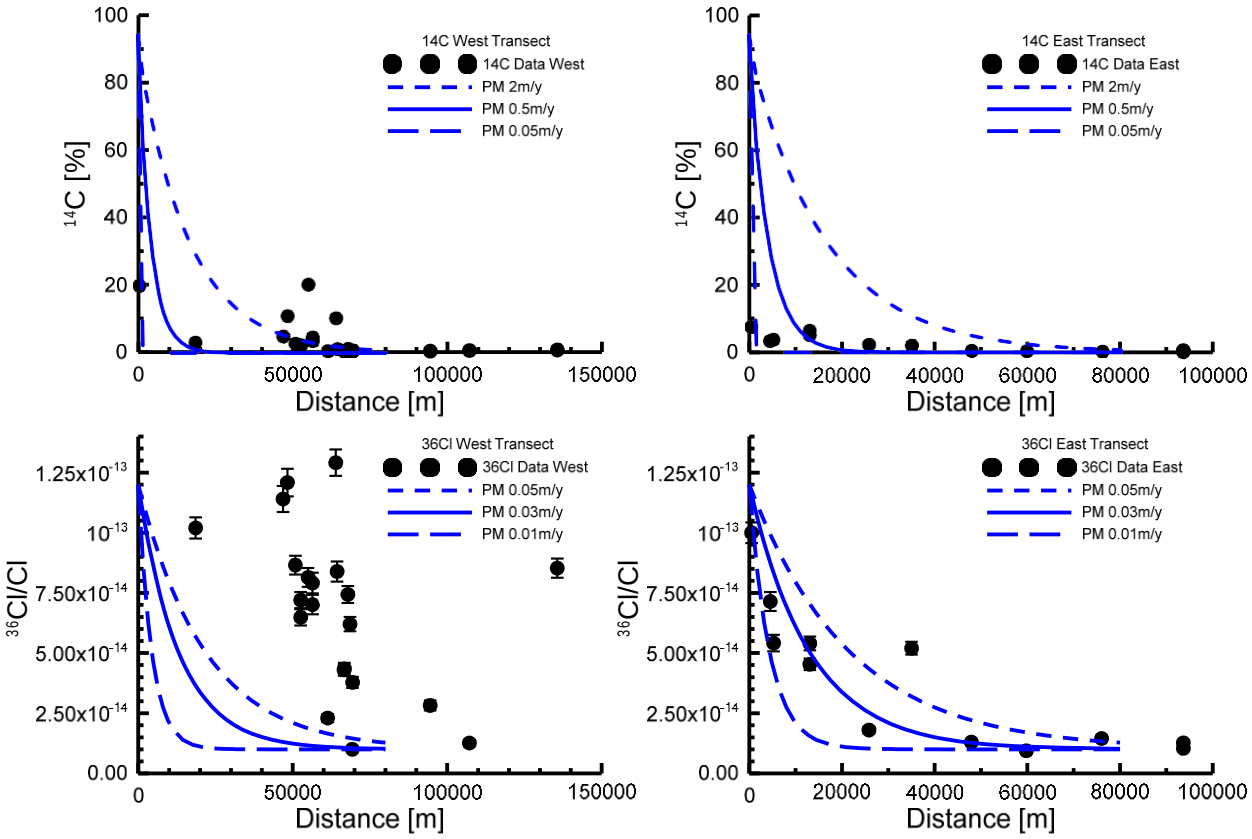

Figure 3.7: North-South transects for all values of ^{14}C in the Hutton Sandstone on the western (top left) and eastern (top right) transect and for $^{36}Cl/Cl$ on the western (bottom left) and eastern (bottom right) transect

In a second approach, the distance was calculated as the shortest distance from a given well to an outcrop (Figure 3.8, right), a more realistic approximation of the flow path to a given well. Even when combining the two transects together, this display shows the smallest scatter and the best agreement with the assumed exponential decrease of ^{14}C and $^{36}Cl/Cl$ versus distance (Figure 3.9). However, the discrepancy in the estimated flow velocity between ^{14}C (0.1–0.5 m/year) and $^{36}C/Cl$ (0.01–0.05 m/year) is still present. As neither ^{14}C nor ^{36}Cl are fully conservative in groundwater, this is not entirely unexpected (see Appendix A). Geochemical processes potentially impacting the tracers include 'dead' (^{14}C-free) carbon inputs from inorganic carbon production in the aquifer (e.g. methane oxidation) and the diffusion of dead (^{36}Cl-free) Cl from adjacent aquitards. These will be discussed in the following.

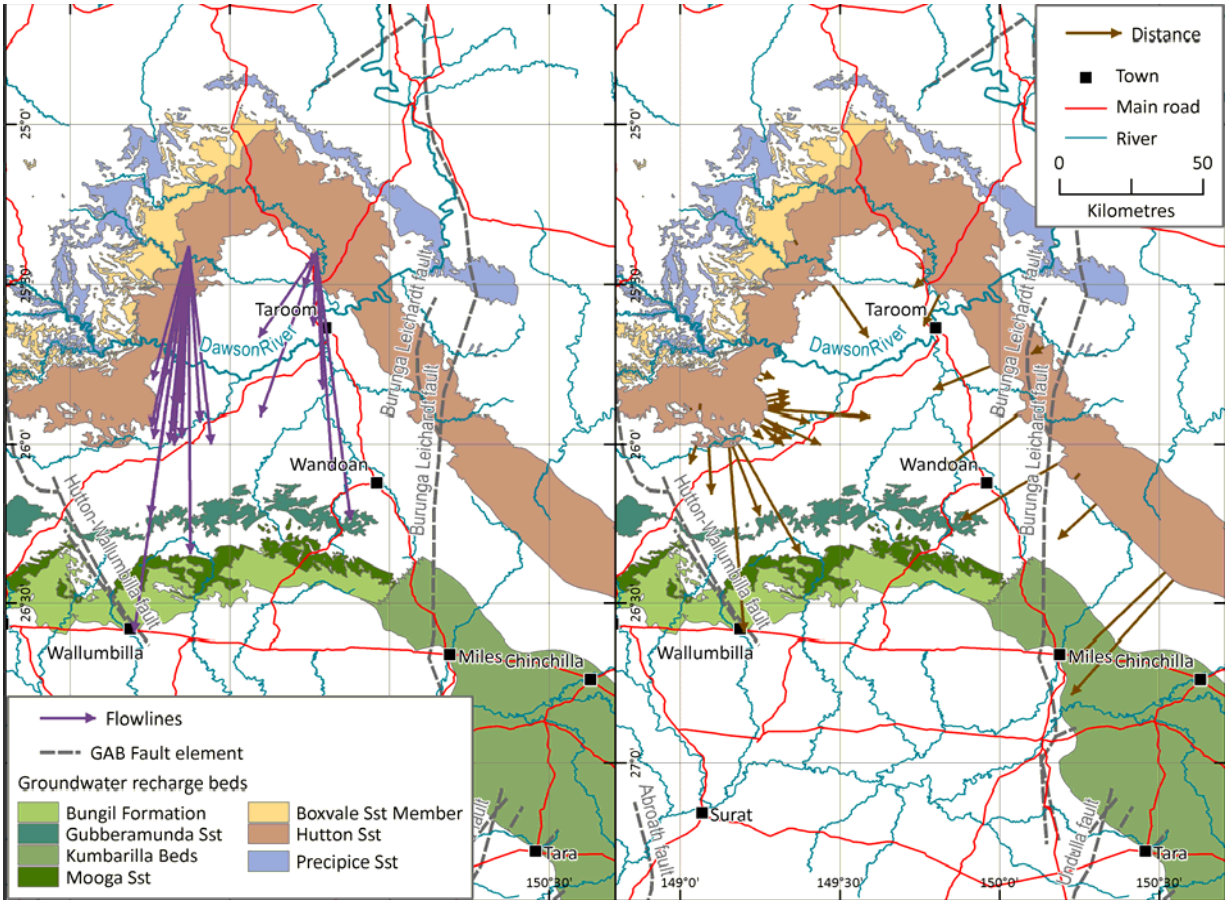

Figure 3.8: Illustration how the flow distances were calculated for the two transects (left) and for different flow lines on the shortest connection from the outcrop (right)

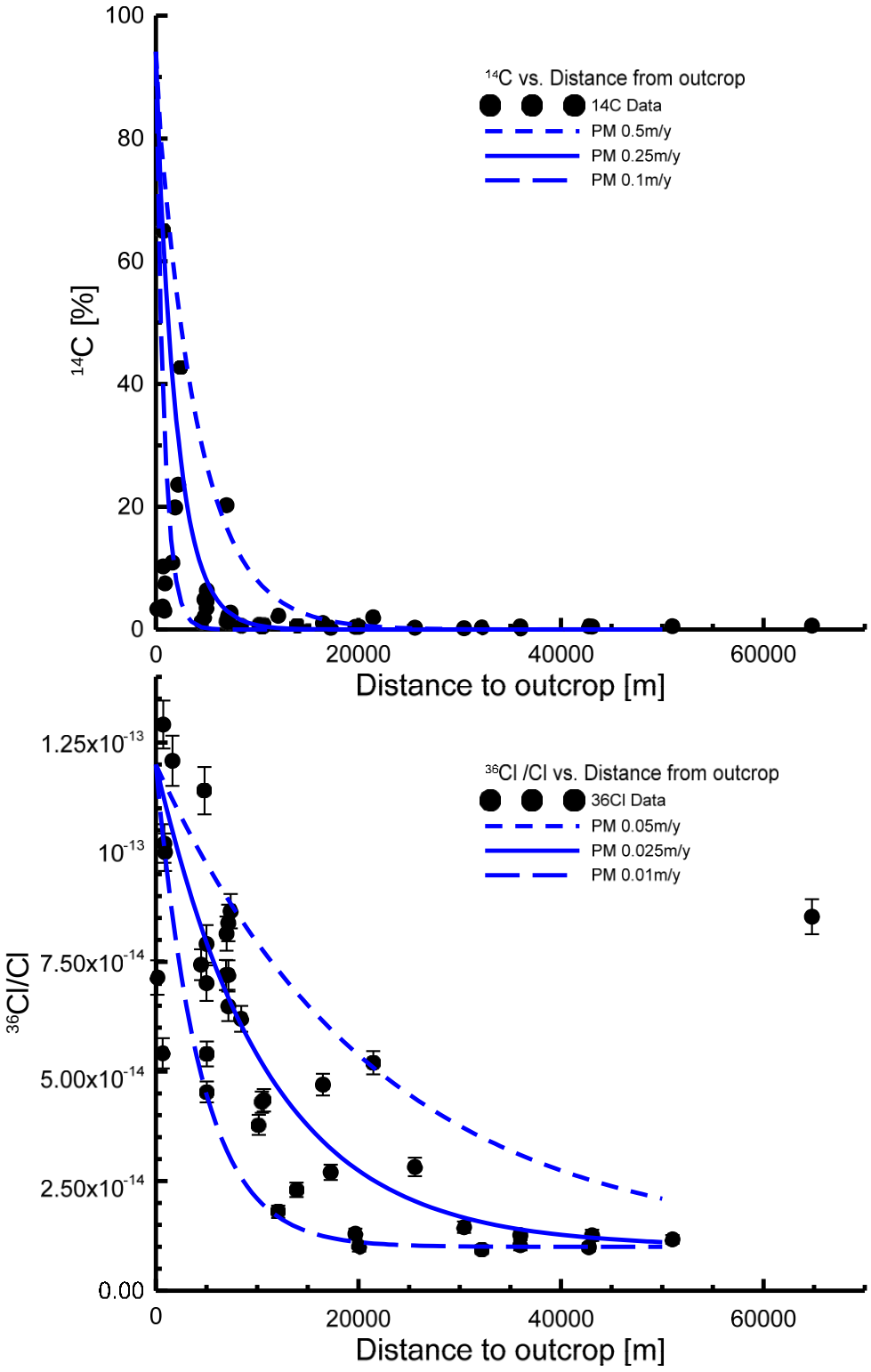

Figure 3.9: Plot of *all* samples from the Hutton Sandstone for ^{14}C (top) and $^{36}Cl/Cl$ (bottom) between longitudes 149°E and 150.5°E versus the distance to the closest point of the outcrop of Hutton Sandstone

3.4 Geochemical influences on ^{14}C and ^{36}Cl

Adding 'dead' C and Cl to a groundwater flow path dilutes the ^{14}C and ^{36}Cl pool and result in groundwater appearing 'older'. Sources of 'dead' C in aquifers include degradation of very old organic matter and the dissolution of carbonate minerals, whilst the main source of 'dead' Cl is diffusion of syn-sedimentary stored chloride from neighbouring aquitards. In the following, simple geochemical corrections are used to account for potential dilution effects on both ^{14}C and ^{36}Cl.

3.4.1 DILUTION OF ^{14}C WITH 'DEAD' CARBON

The measured value of ^{14}C (when expressed in %) is actually a ratio of $^{14}C/C$ where C is Total Dissolved Inorganic Carbon (TDIC). Therefore, the ratio of $^{14}C/C$ will be diluted if the amount of inorganic carbon increases in groundwater. Some increase in inorganic C along groundwater flow paths is a nearly universal process in aquifers, including in the GAB (Radke *et al.* 2000). In the Hutton Sandstone, TDIC increases both with depth and with flow distance (Figure 3.10).

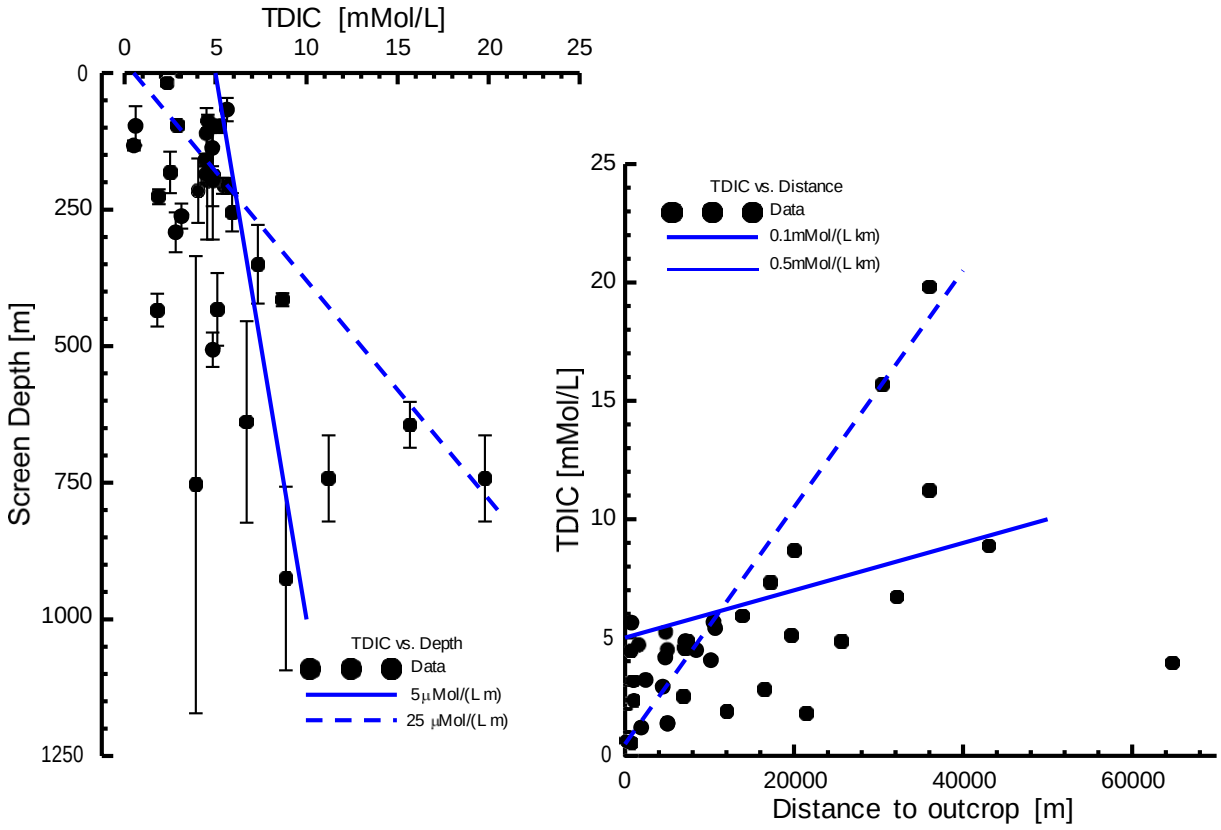

Figure 3.10: Increase of total dissolved inorganic carbon (TDIC) in the Hutton with depth and with distance to outcrop

In the case of the Hutton Sandstone at the Mimosa Syncline, the increase of TDIC can be roughly quantified. In the recharge areas, TDIC ranges from 0.5–5 mmol/L and at maximum depth and flow distance it is in the range of 10 to 20.5 mmol/L. This results in slopes of 0.005–0.025 mmol/L per m depth or 0.1–0.5 mmol/L per km flow distance (Figure 3.10). For both estimates, the extreme value at RN58444 (Wallumbilla) was neglected because it is for a municipal supply well that taps several aquifers from the Gubberamunda Sandstone down to the Hutton Sandstone. Despite the uncertainty in the rate of increase along the flow path, TDIC clearly increases by a factor of two to five. When expressed as a shift in apparent age, a TDIC increase by a factor of five would correspond to an increase in apparent age of more than 10 ky. Thus, a correction for geochemical effects is clearly needed to estimate flow velocity when using ^{14}C.

Two methods were used to account for geochemical effects. Firstly, absolute concentrations of ^{14}C (in atoms/L) were used instead of relative ^{14}C concentrations (expressed in %). A drawback for this approach is that it is sensitive to the absolute ^{14}C concentration in recharge areas, which is not well known, because it combines the uncertainty in TDIC and in ^{14}C in the recharge area. The second approach was the use of a Phillips model (see Appendix A), which is essentially a combined ^{14}C and C mass balance along the flow path. When using absolute ^{14}C concentrations (Figure 3.11 bottom), an initial TDIC of 3 mmol/L was used. Scenarios using increases in TDIC varying between 0.1-0.5 mmol/(L km) along the flow path were evaluated (see case for 0.4 mmol/(L km) on Figure 3.11). Since the absolute concentration of ^{14}C in atoms/L is not affected by the addition of 'dead' TDIC, no Philips model was included (Figure 3.11 bottom). Using either approaches, best fit horizontal groundwater velocities ranged between 0.2 to 1 m/year, depending on the

rate of TDIC increase used. In other words, correction for geochemical effects provided a small *increase* in ^{14}C-inferred horizontal velocities relative to the case without geochemical correction (i.e. 0.1–0.5 m/year; Figure 3.9) and therefore enhances the discrepancy to ^{36}Cl/Cl.

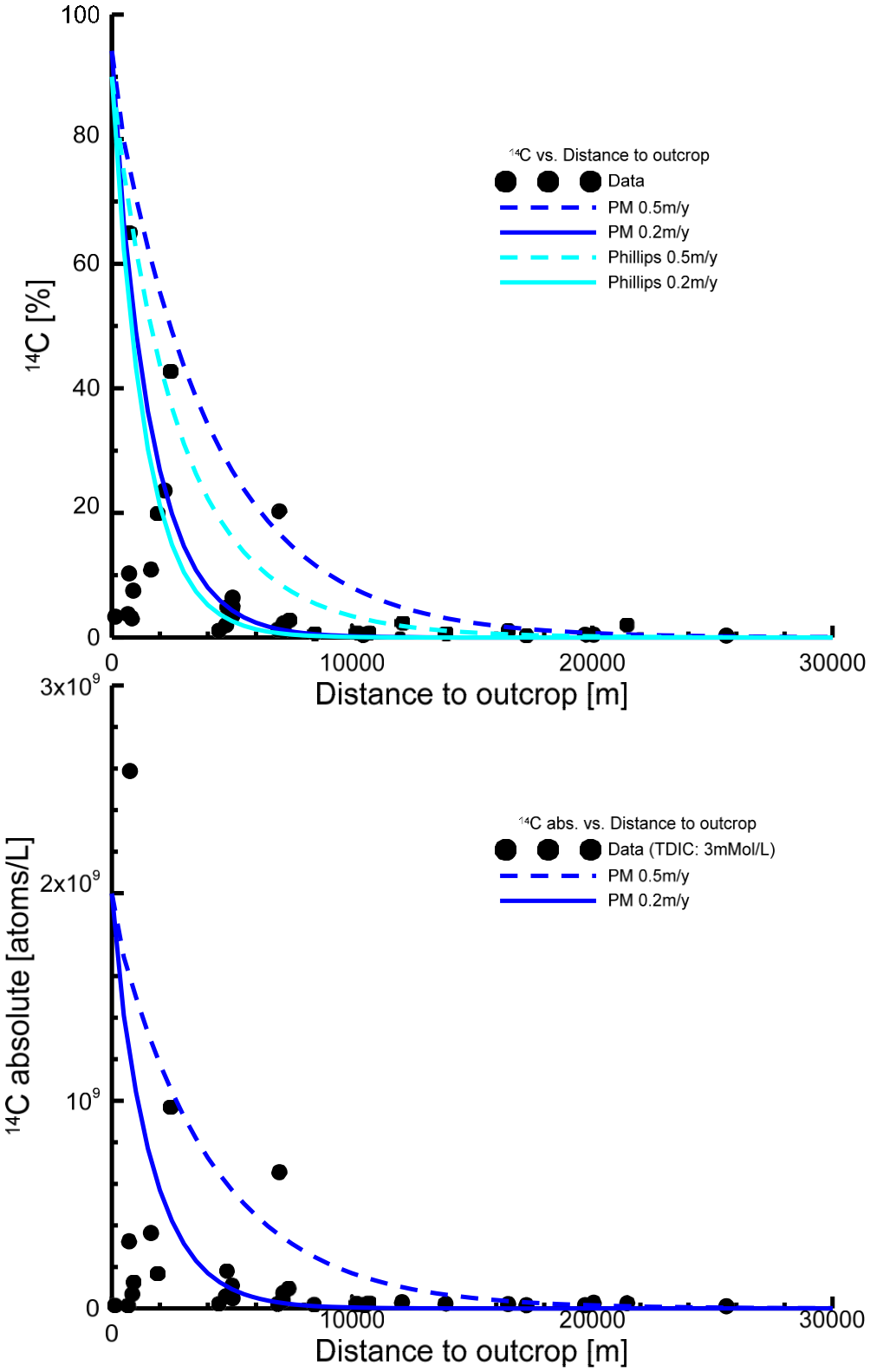

Figure 3.11: Absolute ^{14}C concentration in atoms/L (bottom) and geochemically corrected ^{14}C/C values (top) versus distance to outcrop. Phillips model lines assume a rate of TDIC increase along the flow path of 0.4 mmol/(L km).

3.4.2 DILUTION OF ^{36}CL/CL WITH 'DEAD' CL

The interpretation of ^{36}Cl as a groundwater tracer is influenced by 1) evaporation in the recharge area, 2) underground production of ^{36}Cl, 3) diffusive Cl inputs from aquitards and, to a minor extent, 4) variations in natural atmospheric ^{36}Cl production due to variations in the geomagnetic field (not further discussed here). To see if any significant geochemical effects are likely, the first step is to evaluate if there are variations (in particular an increase) in Cl concentration along the flow path. Most Hutton groundwater samples in the Mimosa Syncline have chloride concentrations in the range of 80–380 mg/L (Figure 3.12). Five samples, generally near outcrops to the east, are outside this range and have concentrations as high as 1120 mg/L (Figure 3.13). Even if the five eastern samples are excluded, there was no clear trend for increasing Cl concentration with depth or with distance to outcrops. This indicates that Cl diffusion from aquitards does not occur or is small relative to the background variation in aquifer Cl concentration.

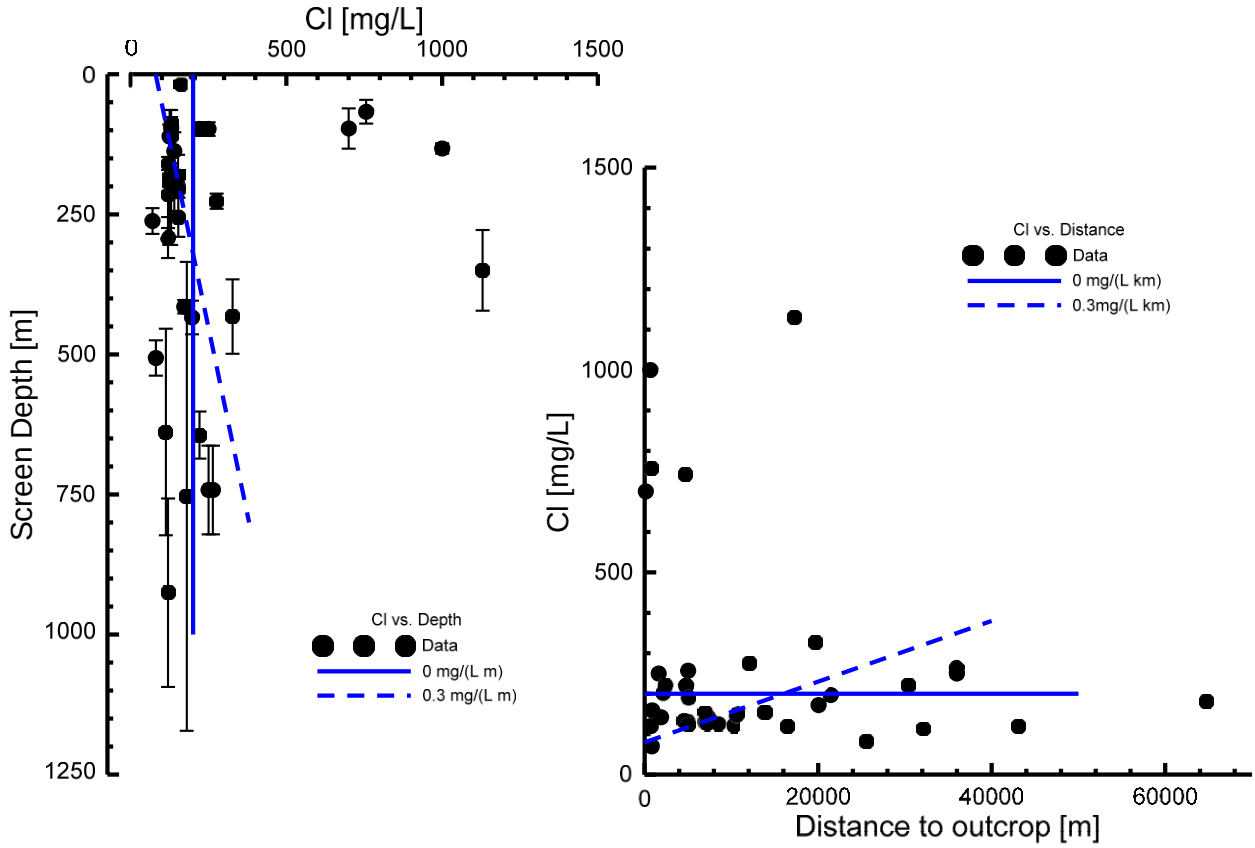

Figure 3.12: Depth profile and transect of chloride concentration in groundwater (samples from this study only)

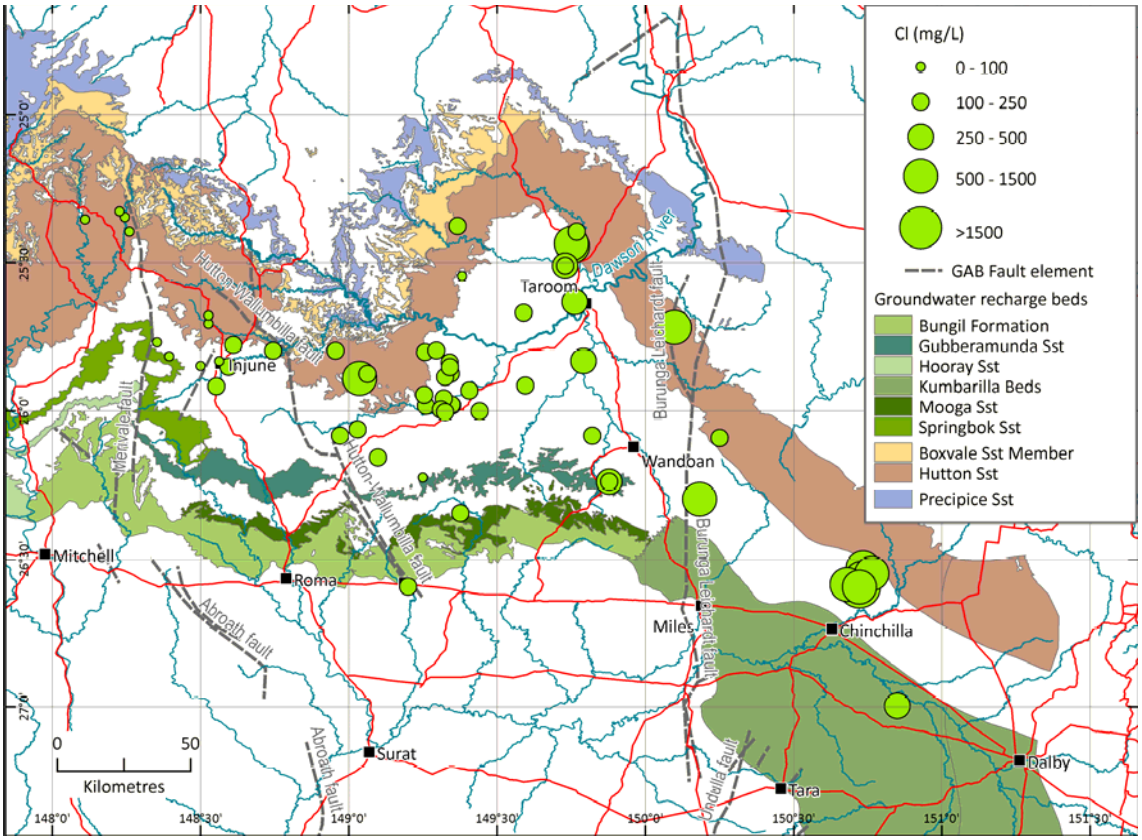

Figure 3.13: Cl concentration in the Hutton Sandstone in the vicinity of the Mimosa Syncline.

To illustrate how dilution by dead Cl could impact on inferred groundwater velocities, the effects of small gradients in chloride (0–0.3 mg/L per m depth and 0–6 mg/L per km distance) were evaluated for the Hutton Sandstone. Firstly, Cl – ^{36}Cl/Cl cross plots were examined to evaluate which components of the Cl and ^{36}Cl mass-balances are most likely to control patterns observed in the aquifer (Figure 3.14). These plots show that, for most samples, a combination of radioactive decay, some underground production and possibly some minor extent of Cl diffusion from nearby aquitards can explain the observed trends. The eastern samples with higher concentrations cannot be fitted by a model assuming $1.3 \cdot 10^{-13}$ and 100 mg/L for initial ^{36}Cl/Cl and Cl concentration, respectively. These may represent a source of groundwater possibly exposed to a higher degree of evapotranspiration at the time of recharge, resulting in a different initial Cl and ^{36}Cl concentration than the other samples, or exposed to some other process that increased their Cl concentration (leakage through a fault, etc).

Including potential geochemical effects had little impact on ^{36}Cl-inferred groundwater velocities (Figure 3.15). In case of the absolute ^{36}Cl concentration the Phillips model and the Piston Flow model do not produce the same model curves, in contrast to ^{14}C. This is related to ^{36}Cl underground production in the aquifer and the aquitard, causing a slight increase of ^{36}Cl atoms per litre with time and distance. As in case of ^{14}C, taking input of dead Cl into account *increases* groundwater velocities also for ^{36}Cl and the discrepancy between ^{14}C and ^{36}Cl derived groundwater velocities persists. The best estimate of groundwater velocity for the Phillips model is 1.5 and 3 cm/year, still a factor of ten smaller than the possible flow velocities for ^{14}C under this model. Thus, geochemical effects alone cannot explain the differences in inferred velocities between ^{14}C and ^{36}Cl.

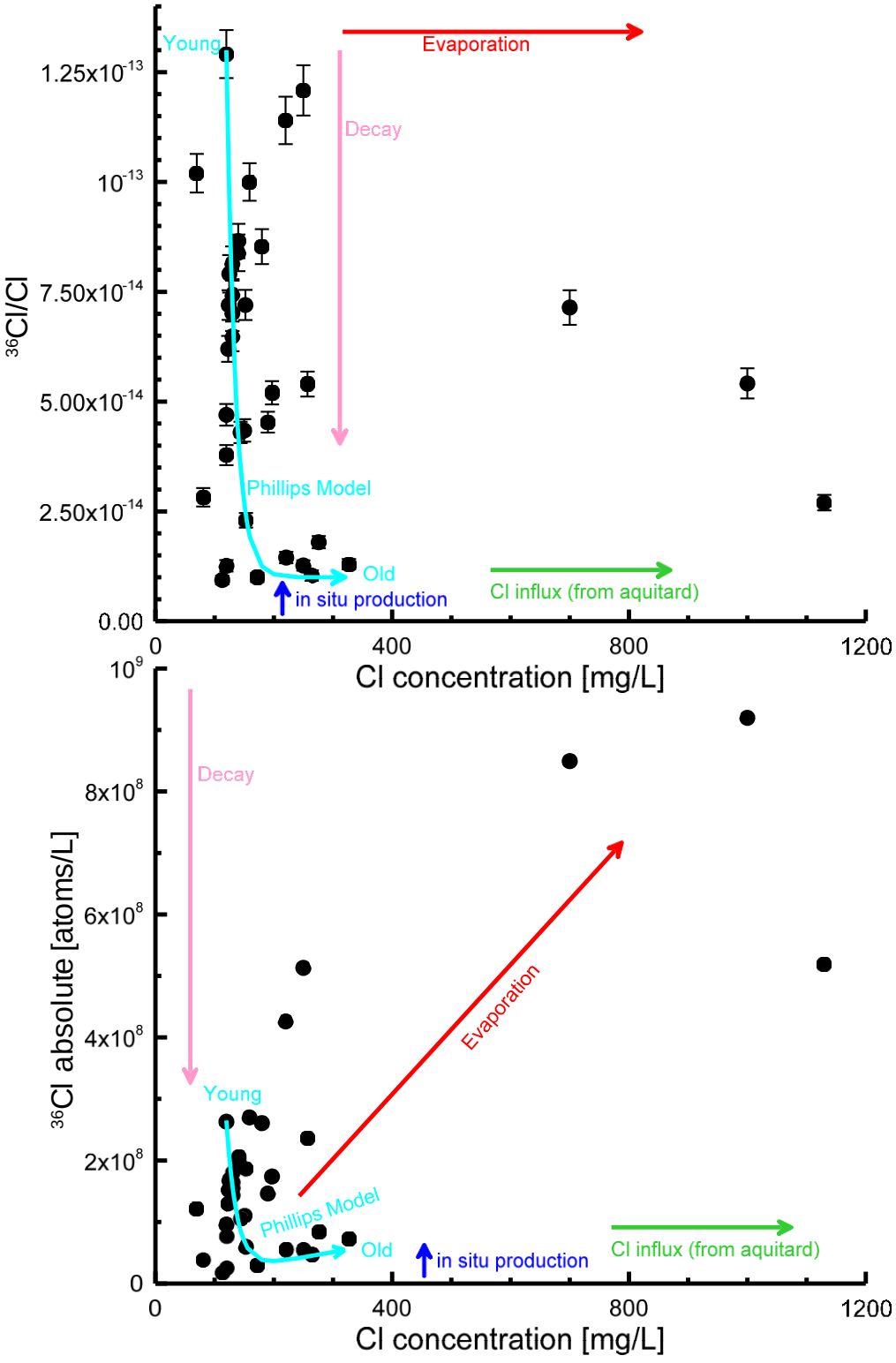

Figure 3.14: Geochemical cross-plots of th ^{36}Cl-Cl system: ^{36}Cl/Cl versus Cl (top) and ^{36}Cl versus Cl (bottom). The mass-balance was evaluated using the Phillips model for an initial Cl concentration of 120 mg/L, a ^{36}Cl/Cl ratio of $1.3 \cdot 10^{-13}$ and for a diffusive chloride increase flux of 0.04 µg/(L·year). Arrows indicate how different components of the mass-balance for ^{36}Cl and Cl could impact on observed concentrations.

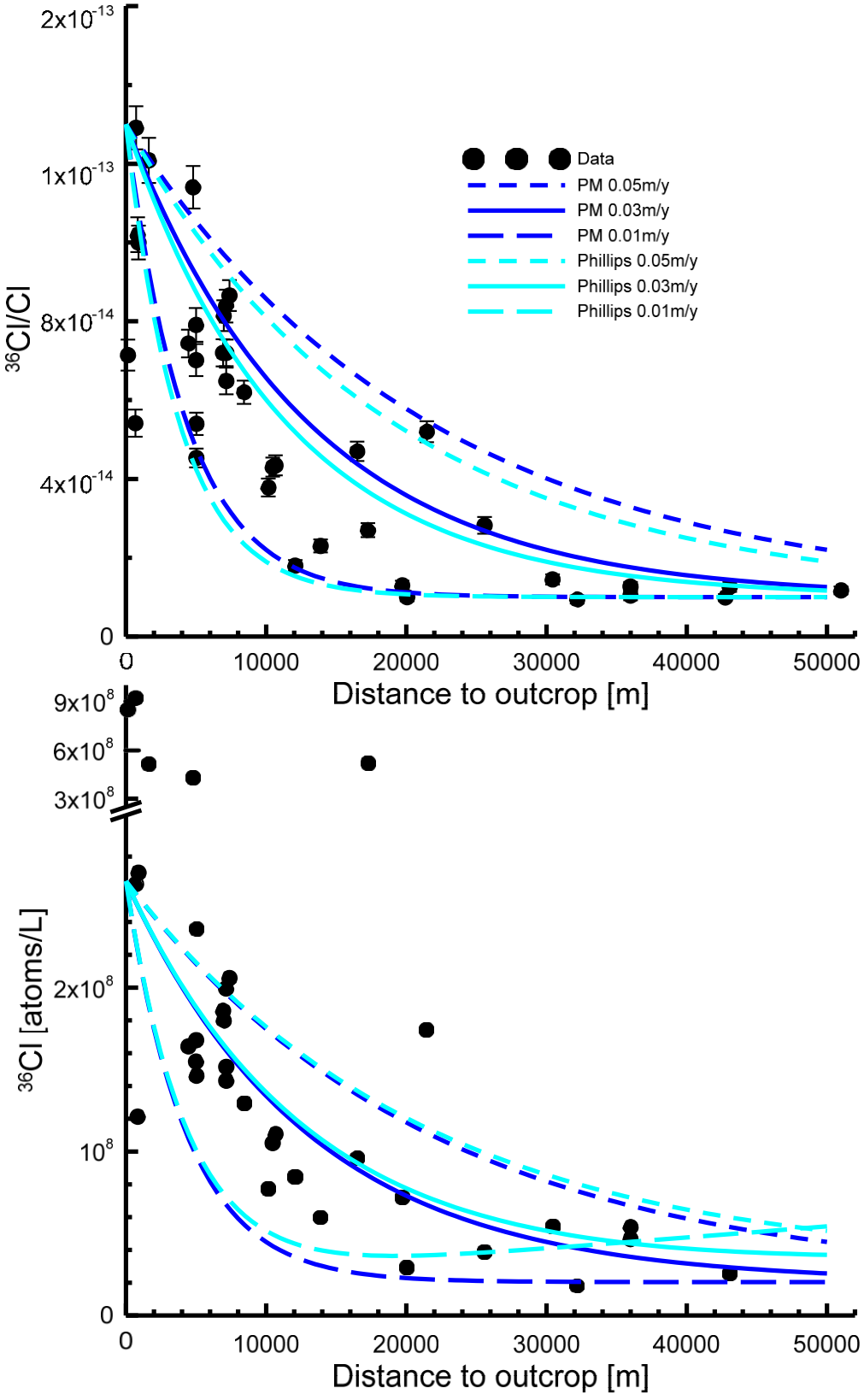

Figure 3.15: Above ^{36}Cl concentration (bottom) and geochemically corrected $^{36}Cl/C$ values (top) versus distance to outcrop. For the Philips model, the initial Cl concentration was 120 mg/L, the $^{36}Cl/Cl$ ratio $1.3 \cdot 10^{-13}$ and the diffusive chloride flux 0.04 µg/(L·year).

3.5 Influence of double porosity on ^{14}C and ^{36}Cl in the Hutton

Double porosity is a common feature of many aquifers, including in the Hutton Sandstone (APLNG 2014). In a double porosity aquifer, most of the groundwater will travel through more permeable areas, often also referred to as 'mobile zones', but solute can still be exchanged by diffusion with nearby 'stagnant' zones where advection is much smaller or negligible. Here, the one-dimensional analytical model of solute transport developed Sudicky and Frind (1981) was used to evaluate whether double porosity can account for the differences in inferred groundwater velocity between ^{14}C and ^{36}Cl (see also Appendix A for the model description). For the Sudicky and Frind model, the Hutton is represented as a thin aquifer (a few meters) surrounded by much thicker aquitards (>50 m). When using realistic parameters to describe the properties of the aquifers and the aquitards, the inferred horizontal velocities obtained with ^{14}C and ^{36}Cl are similar (Figure 3.16) ranging between 0.5–2 m/year. The double porosity model is therefore the first description of groundwater flow in Hutton Sandstone that resolves the apparent discrepancy between ^{14}C and ^{36}Cl results. Here ^{36}Cl-inferred velocities were more sensitive to double porosity effects than the ^{14}C ones, which is illustrated by the much larger difference between Sudicky model and piston flow model for ^{36}Cl (lower plot in Figure 3.16) than for ^{14}C (upper plot in Figure 3.16). This was expected because the longer half-life of ^{36}Cl makes it more sensitive to diffusive transport. Also, the fit was insensitive against dispersivity in the aquifer and the fit described only the product of aquifer thickness and groundwater velocity. Increasing flow velocity by a factor of two and decreasing aquifer thickness by a factor of two resulted in the same quality of fit. This allows for a robust estimate of total groundwater flux in the deeper part of the Hutton Sandstone (see discussion in next chapter).

While a good agreement between tracers is encouraging, the inferred velocities should be considered preliminary estimates because of the simplified nature of the modelling methods used. The key finding here is that the Hutton Sandstone has a very low effective porosity, with most of the groundwater flow occurring within the higher mobility zones that occupy only a few m thickness of the aquifer.

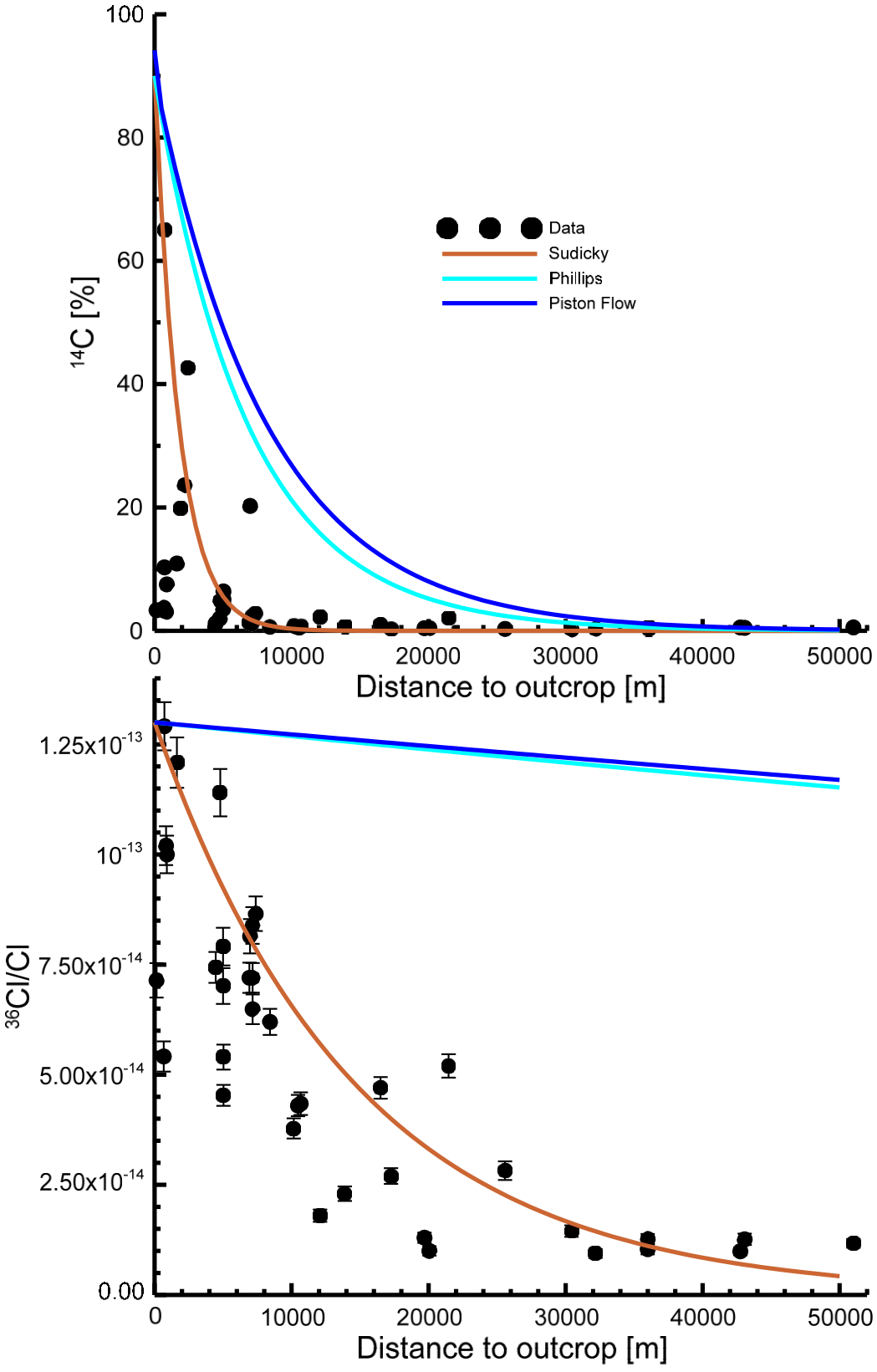

Figure 3.16: Flow-velocities as described by the Sudicky and Frind (1981) model. This model assumes *the same* flow velocity of 1 m/year in the mobile zone for both tracers (^{14}C and ^{36}Cl). The displayed brown curve is for an aquifer thickness (mobile zone) of 10 m, a dispersivity α_L of 10 m, and porosities of aquifer and aquitard of 20% and 30%, respectively.

3.6 Support of the double porosity model by other tracers

Two additional tracers were measured that could further constrain the flow velocities in the Hutton: the stable isotopes ^{2}H and ^{18}O of the water molecule and the noble gas ^{4}He. This occurs because rainfall during the cooler Pleistocene (which concluded ~12ky ago) had a lower isotopic signature than current rainfall (by ~2.5‰ and ~20‰ for $\delta^{18}O$ and $\delta^{2}H$, respectively). In contrast, ^{4}He accumulates over time in the aquifer. These results will be discussed in the following sections.

3.6.1 STABLE ISOTOPE RESULTS AND THE PALEOCLIMATE SHIFT

There is a pronounced decreased in groundwater $\delta^{18}O$ and $\delta^{2}H$ versus distance to outcrop in the Hutton Sandstone aquifer at ca. 10–20 km (Figure 3.17). The data show a scatter of –5.5±0.5‰ and –32±5‰ for modern water in $\delta\ ^{18}O$ and $\delta\ ^{2}H$, respectively, which corresponds to the known values for stable isotopes in precipitation for this area (IAEA/WMO 2015). For groundwater beyond 20 km, the shift in isotopic signature is consistent with water recharged during the Pleistocene (–8±0.5‰ and –50±5‰ for $\delta\ ^{18}O$ and $\delta\ ^{2}H$, respectively). Using a simple advection-dispersion model and assuming dispersivity ~ 750 m which is a valid assumption for transport distances of 20 km or more (Gelhar *et al.* 1992), the isotopic shift would correspond to a horizontal velocity of ~1.2 m/year, very similar to the estimate obtained with ^{14}C and ^{36}Cl (~1 m/year).

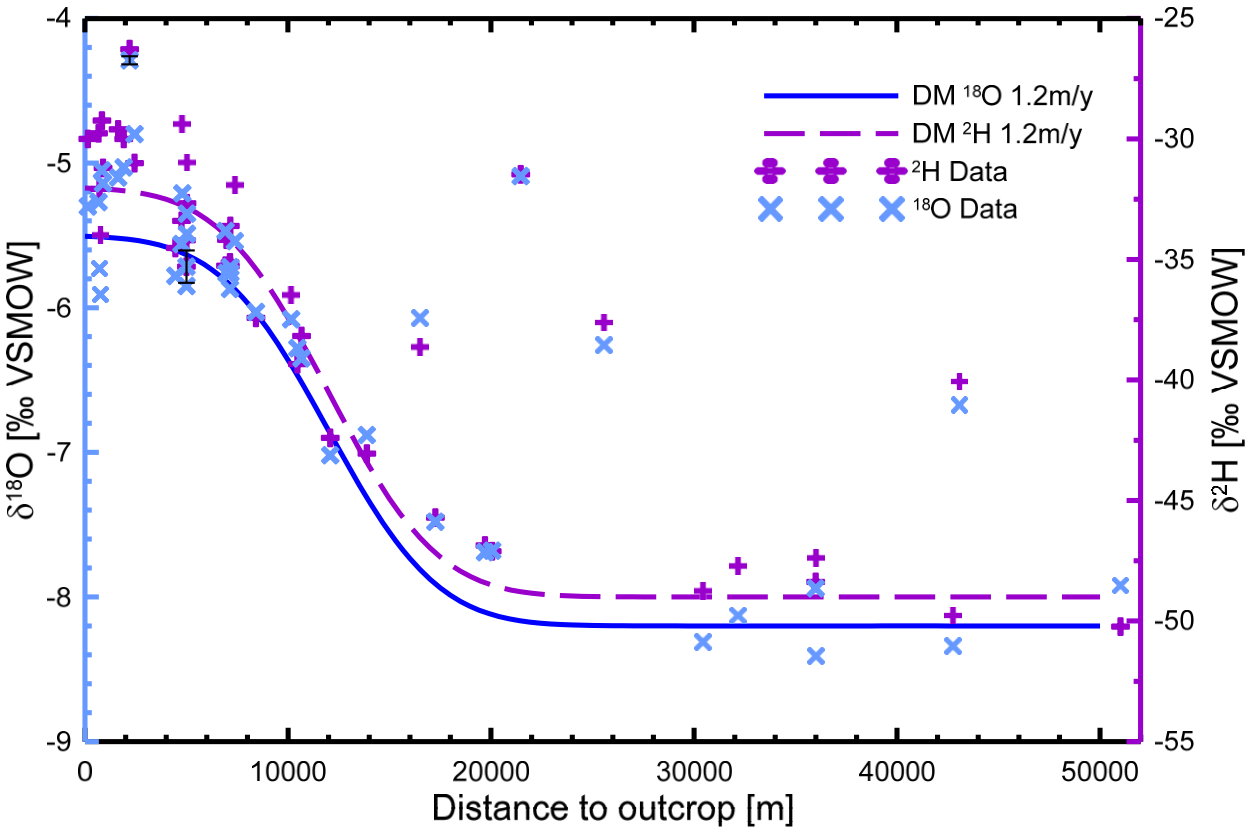

Figure 317: Stable isotope results plotted versus the distance from Hutton outcrop. Indicated are model results for a palaeoclimatic shift of 2.5‰ and 20‰ in ^{18}O and ^{2}H respectively and 1.2m/year distance velocity

Not all groundwater samples had a 'Pleistocene' signature beyond 20 km (Figure 3.17). This includes the municipal supply well of Wallumbilla, which is probably unrepresentative because it taps several aquifers. The Reedy Creek bore INJ3-H also had a more modern signature, but may also not be representative for the Hutton because it was the site for an injection test at the time of the study. The two other wells at 25 km and 22 km flow distance (Caenby Bore and bore 35458) also have a more modern signature – suggesting that the distance to their recharge area is shorter than what was estimated here. The map in $\delta^{18}O$

distribution in the Hutton Sandstone also indicates higher isotopic values at the eastern side of the Mimosa Syncline, suggesting a different recharge environment there (as was also observed for Cl).

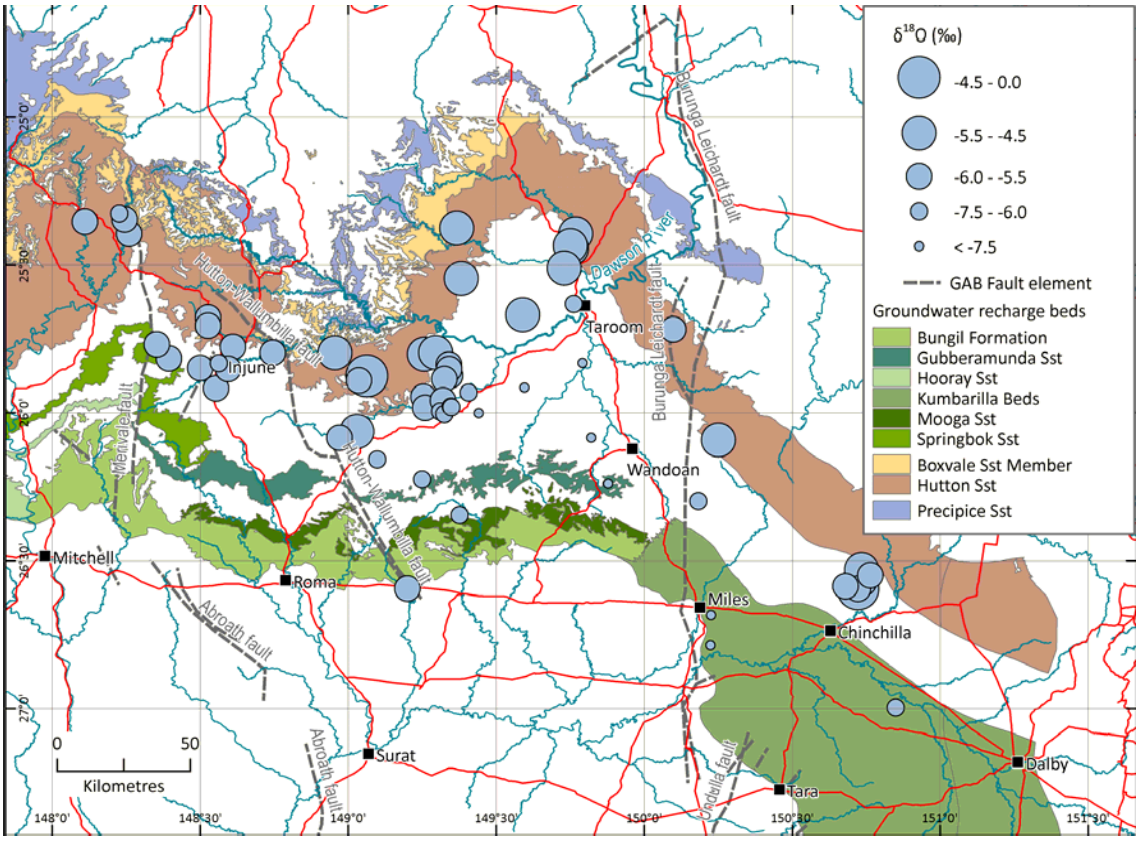

Figure 3.18: Map of ^{18}O values in groundwater in the Hutton Sandstone

3.6.2 NOBLE GAS RESULTS

Ideally, the palaeoclimatic signal in ^{18}O and ^{2}H would be further tested with noble gas palaeotemperatures derived from the concentrations of Ar, Kr and Xe in groundwater (Stute *et al.* 1992; Stute and Sonntag 1992; Stute and Schlosser 1993; Stute *et al.* 1995a; Beyerle *et al.* 1998; Aeschbach-Hertig *et al.* 1999; Aeschbach-Hertig *et al.* 2002). Unfortunately, there is no facility in Australia at present to measure heavier noble gases. The CSIRO facility for this purpose is under construction and will be operational in late 2016. Therefore the confirmation of the palaeoclimate signal could be undertaken at a later date.

Helium concentrations in groundwater, however, were measured and can also indicate groundwater flow direction. Sampling for noble gases was complicated by observed degassing of groundwater and hot groundwater temperatures (>50°C) in the deeper bores. Hot water has smaller helium solubilities and the diffusion constant increases with temperature. Furthermore groundwater pumped from a deep well observes higher de-pressurization during transport to the surface. All these processes increase the possibility for degassing, so the ^{4}He data used here should be considered a qualitative tool. A large range in ^{4}He concentration was measured in the Hutton Sandstone. These ranged from solubility equilibrium concentration (ca. $5 \cdot 10^{-8}$ cc(STP)/g, found in rain water, surface water and groundwater younger than a century) to among the highest values previously found in groundwater (10^{-4} cc(STP)/g; Figure 3.20).

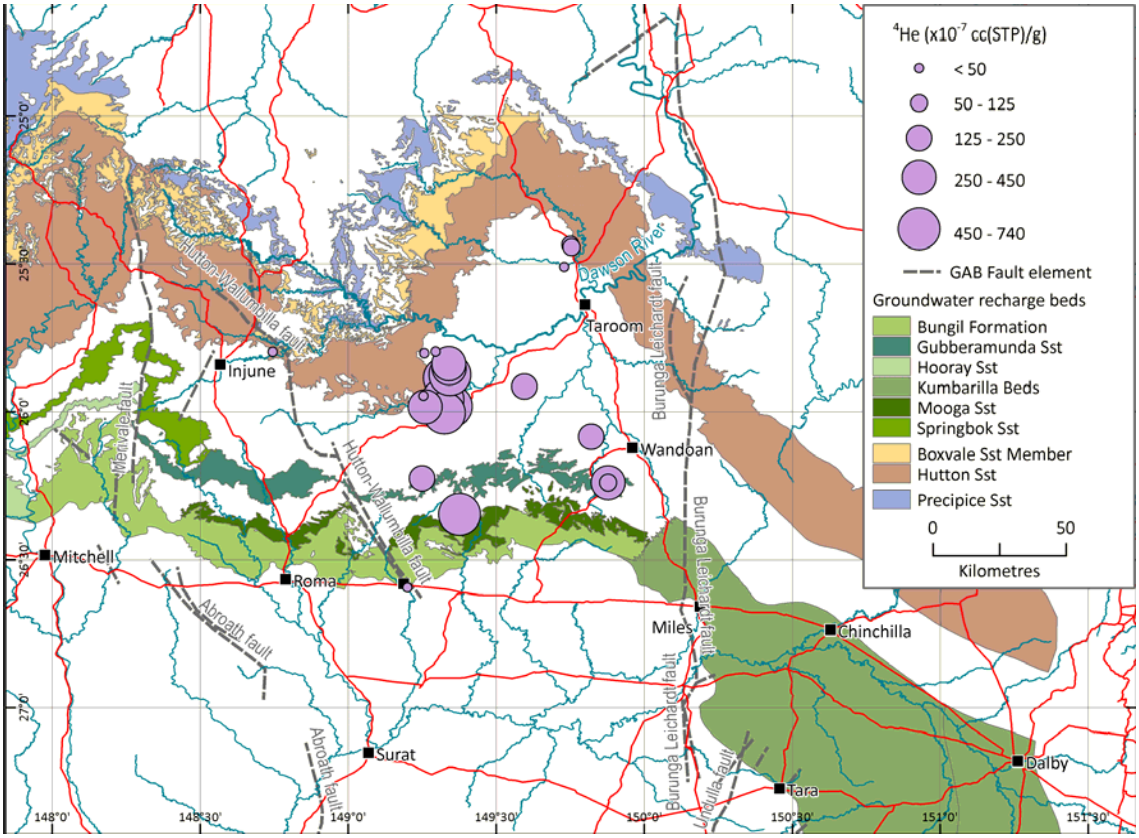

Figure 3.19: Map of helium concentrations in groundwater of the Hutton Sandstone.

Two patterns are discernible in the helium concentration map in Figure 3.19: The first pattern is a group of samples close to the southern part of the western recharge area, which shows exceptionally high helium at shallow depths. These results come from the wells at the farms Amusen, Dangarfield and Moorabinda (see Figure 2.4 and Figure 3.20) and were reproducible across two sampling campaigns for one of the wells (Moorabinda artesian house bore sampled in November 2012 and October 2013). A possible explanation for this finding is a small input of very old, deep water coming up in this area and admixing helium into local groundwater. This upward flow may have happened further upstream, closer to the Hutton-Wallumbilla fault system. Such an admixture of old water is not necessarily detected in the radioactive tracers (^{14}C and ^{36}Cl) because these are very sensitive for small admixtures of young water in old water, but much less sensitive when old water is mixed into young water. It would also not be visible in the stable isotopes, unless the water mass added is significant (20% or more). In contrast to ^{14}C, ^{36}Cl/Cl and stable isotopes, where maximum differences between values for old and young water is a factor of two to 100 only (see Figure 3.16 and Figure 3.17), concentrations of helium in groundwater can vary much more, over a factor of 100,000. Therefore, admixtures of a few % of very old groundwater may explain this local pattern of high helium concentrations.

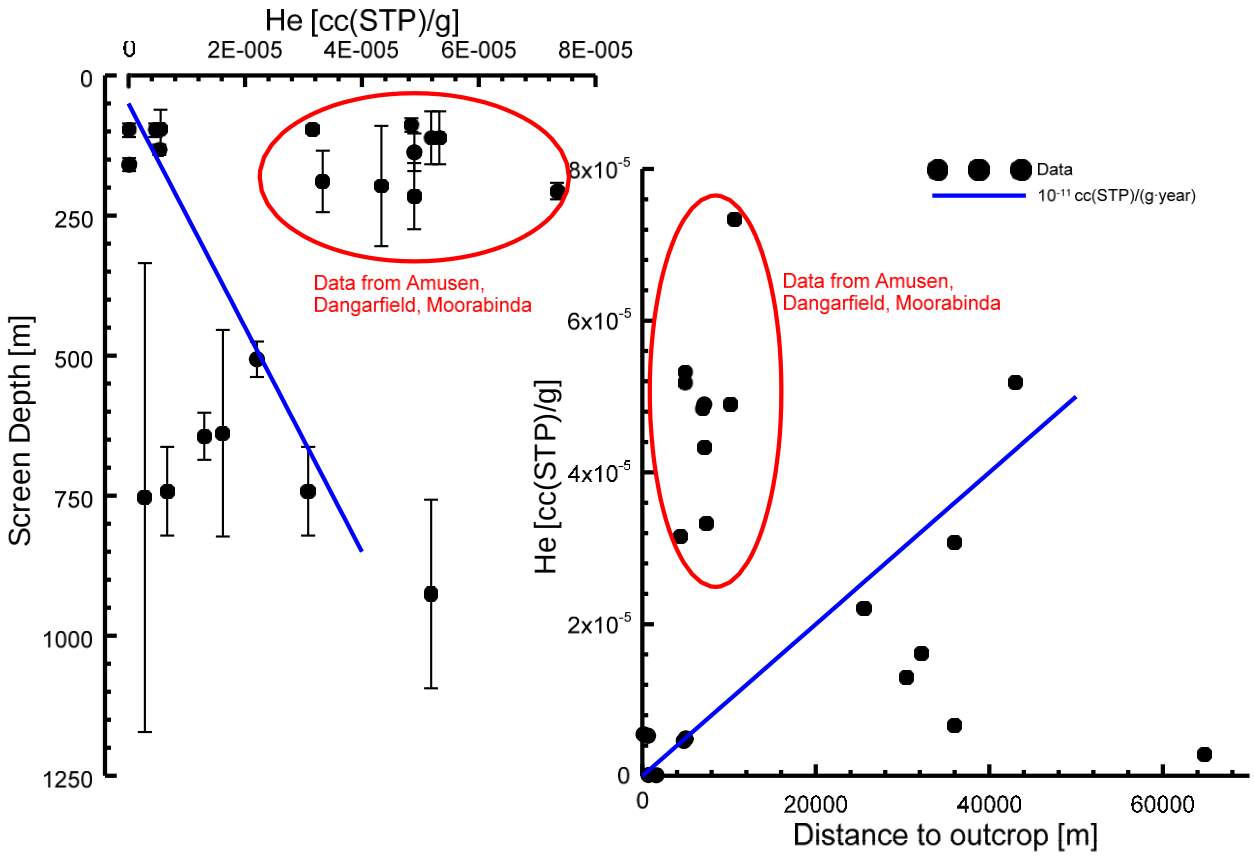

Figure 3.20: Depth profile (left) and transect of helium concentration versus distance to Hutton outcrop (right)

The other group of helium results shows a more gradual increase with depth and with length of flow path up to the highest values in the range of $5 \cdot 10^{-5}$ cc(STP)/g, which was measured in the INJ3-H bore at Reedy Creek. Despite the considerable scatter in the data, this gradual increase is of the right magnitude for a moderate rate of terrigenic ^{4}He production in the aquifer (10^{-11} cc(STP)/(g·year); Figure 3.20). Comparison with ^{36}Cl and ^{14}C also suggests a different mixture of groundwater sources for the Amusen, Dangarfield and Moorabinda wells relative to the other sites (Figure 3.21). Evaluating horizontal velocities using ^{4}He was not attempted here because the behaviour of this tracer in aquifer-aquitard systems can be quite complex (because of its high diffusivity). However, the trends in ^{4}He suggest an old fluid input into parts of the Hutton.

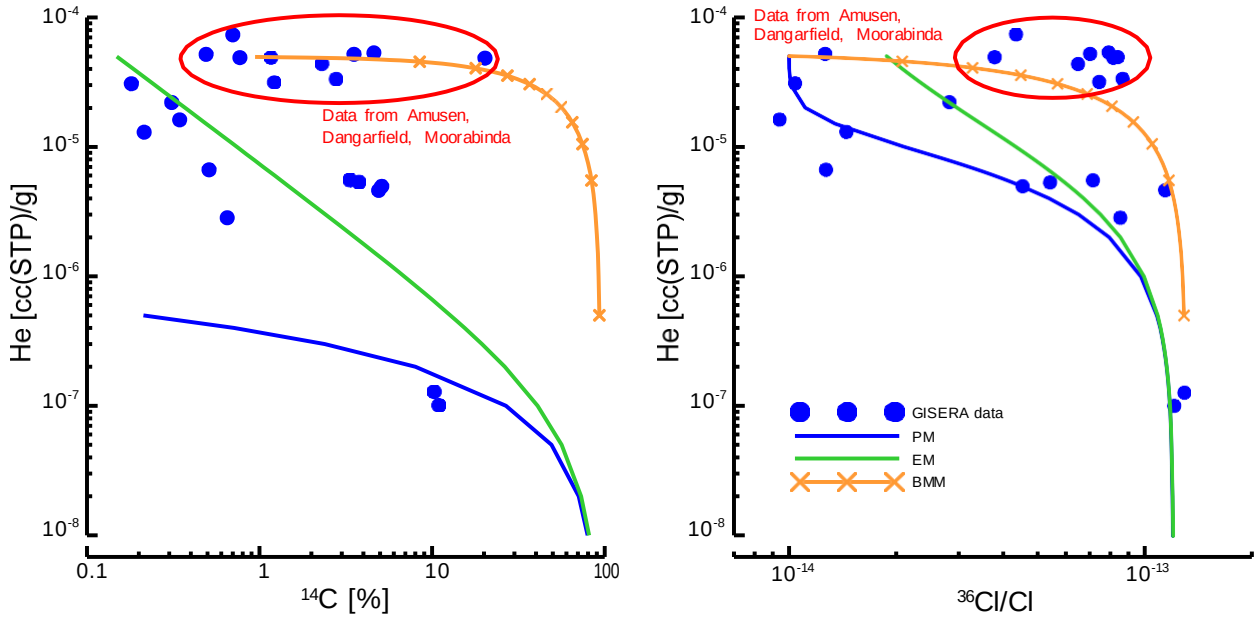

Figure 3.21: Cross plots for ^{4}He with ^{14}C (left) and ^{36}Cl/Cl (right) with their best matching piston flow (PM), exponential (EM) and binary mixing models (BMM). The PM and EM models used a helium production rate of 10^{-11} cc(STP)/(g·year).

3.7 Particle tracking

The particle tracking calculations did provide insights into the origin of groundwater at a given bore (that is: what is the recharge area), but was less successful to predict the tracer data (that is: concentrations and age distributions). Particle tracking did demonstrate that groundwater from a relatively large area can be sampled at a given well (Figure 3.22). This is consistent with the tendency found in many groundwater samples to have a tracer make-up representative of more than one water source (see example above for ^{4}He). However, the comparison between observed concentrations versus predicted by particle-tracking age distributions was inconclusive for ^{14}C and poor for ^{36}Cl. Most of the wells selected for the comparison were down-gradient in the Hutton (that is, had relatively old groundwater) and had low predicted and observed ^{14}C concentrations (Figure 3.22). On the other hand, there was no correlation between observed and predicted ^{36}Cl concentrations (Figure 3.22). There are many potential reasons for the poor fit. However, the key one would be that particle tracking cannot account for diffusive exchange of tracers in a double porosity aquifer like the Hutton.

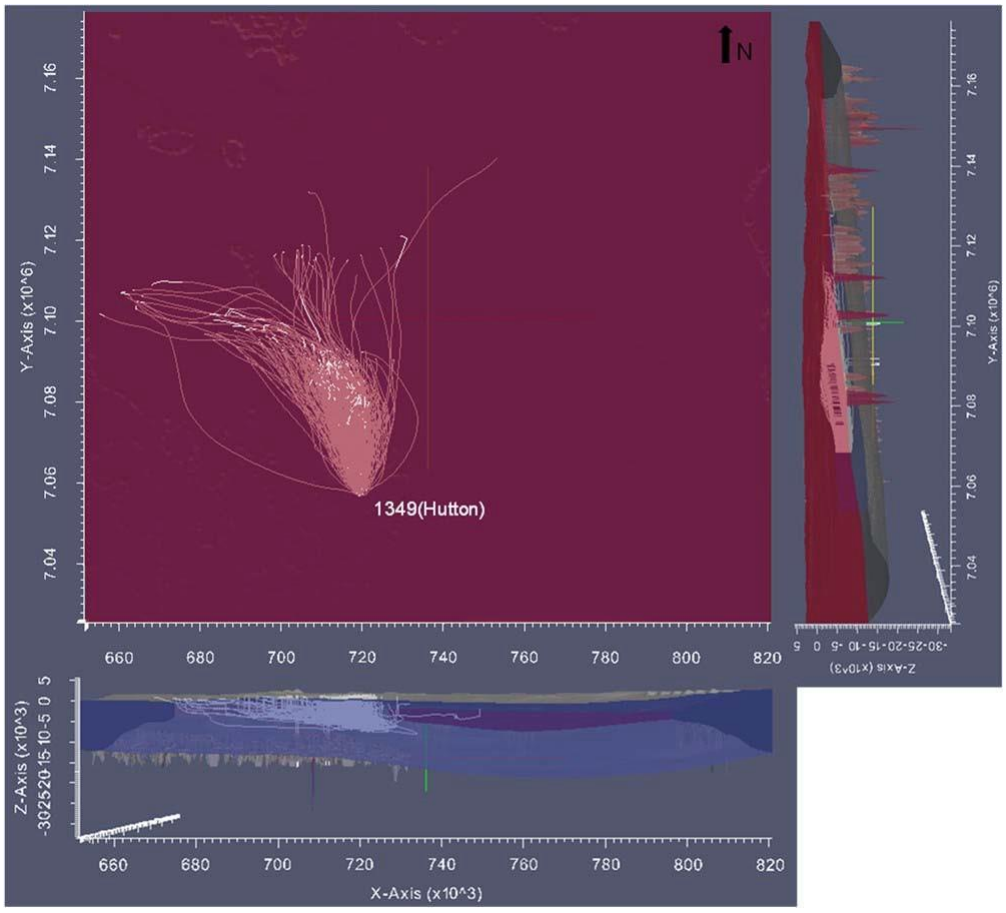

Figure 3.22: Example for a visualisation of MODFLOW-ADV2 generated particle tracks for a sample well (Sreekanth and Moore 2015). The starting point of each track represents a possible source (recharge) area for water pumped in the well.

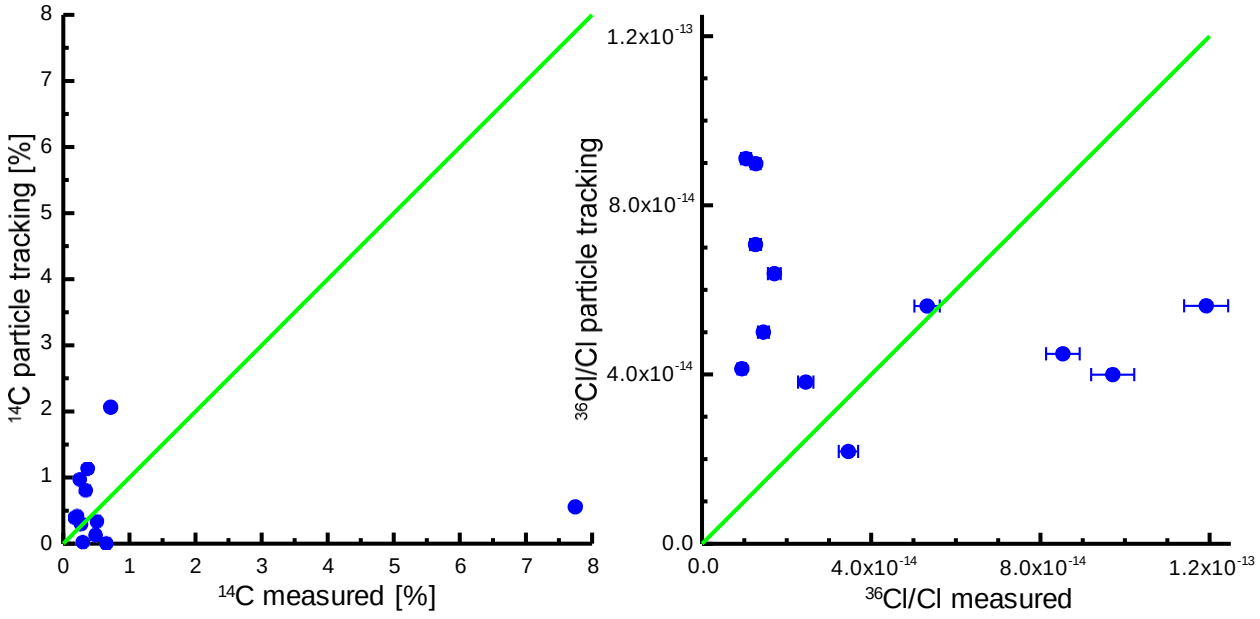

Figure 3.23: Comparison of particle-tracking derived ^{14}C (left) and ^{36}Cl/Cl (right) values with the actually measured tracer concentrations

3.8 Precipice Sandstone

The present study had its focus on the Hutton Sandstone aquifer. The Precipice Sandstone aquifer was only sampled when there was an opportunity to directly combine tracer values for both aquifers at the same location. Despite this limitation, this study roughly doubled the existing dataset of environmental tracer values in this aquifer in the area of the Mimosa Syncline (nine measurements from all datasets). All values for ^{14}C are smaller than 3.5%. This is still higher than the analytic detection limit of an AMS ^{14}C-analysis but, given the depth of the formation (some of the sampled wells were deeper than 1000 m) and the poor state for some of the wells, the presence of small amounts of ^{14}C may be a sampling artefact. $^{36}Cl/Cl$ in contrast is higher in the Precipice than in the Hutton Sandstone (Figure 3.23). The highest $^{36}Cl/Cl$ value found was $1.8 \cdot 10^{-13}$. The chloride content is lower in the Precipice Sandstone than the Hutton – 50% of the samples measured in the Precipice contained less than 20 mg/L and all have less than 120 mg/L. This probably indicates less evaporation during recharge, thus increasing the $^{36}Cl/Cl$ ratio. Therefore, the initial ratios determined for the Hutton Sandstone cannot be transferred to the Precipice. Since all samples are at the practical detection limit for ^{14}C, a plot of ^{14}C versus $^{36}Cl/Cl$ cannot be used to determine the initial $^{36}Cl/Cl$ ratio at recharge for the Precipice. The sample closest to the outcrop of Precipice Sandstone is at a distance of about 30 km from it. Thus, flow velocities cannot be evaluated for the Precipice because no $^{36}Cl/Cl$ values in the recharge area are available.

Sampling for noble gases in the Precipice Sandstone was extremely difficult due to the deep wells and high water temperatures, leading to degassing during sampling. Despite these difficulties the results of the three helium samples taken during this study show concentrations in a narrow range between $1.5 \cdot 10^{-5}$ and $2.2 \cdot 10^{-5}$ cc(STP)/g. No trend with any inferred flow direction is discernible from these results.

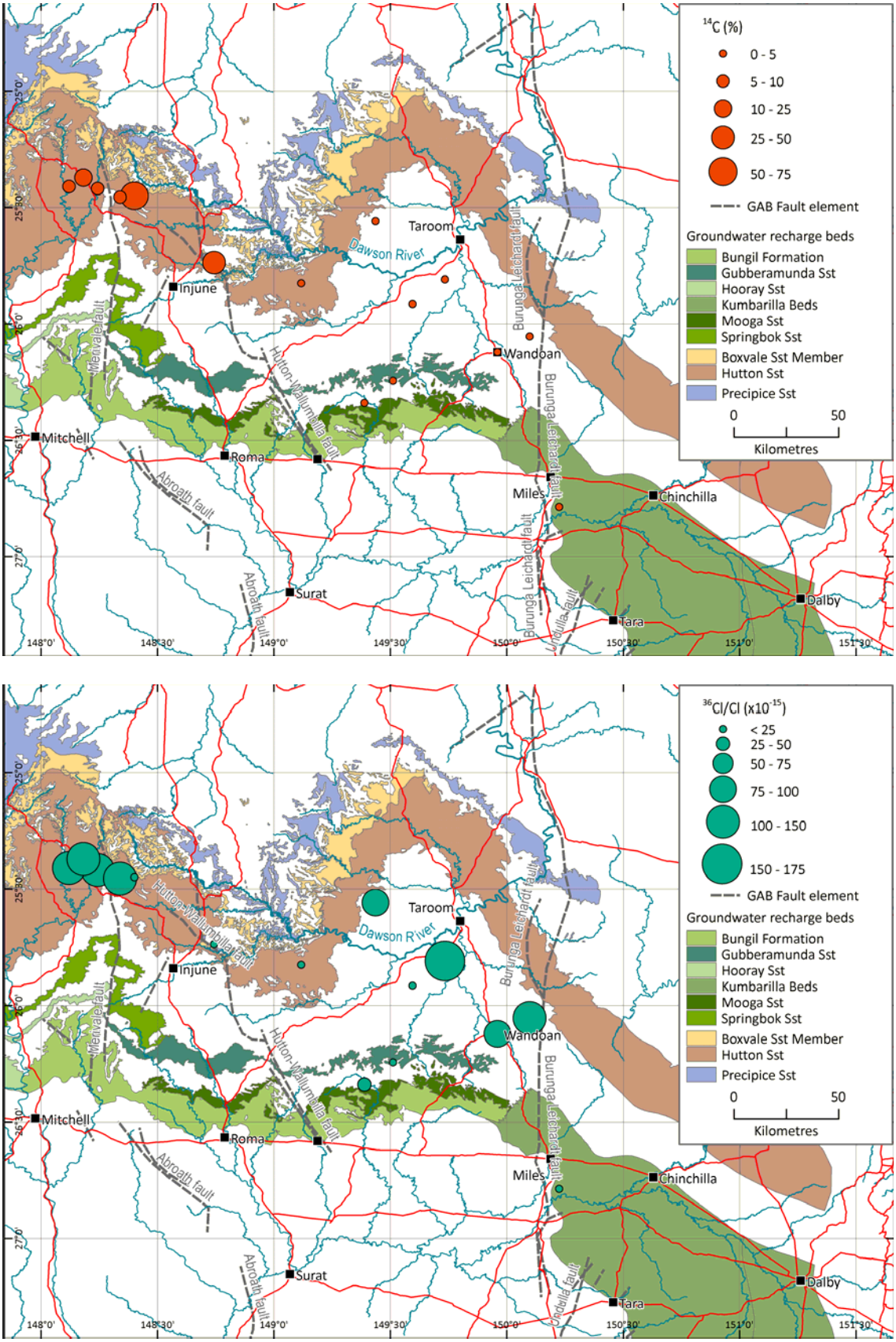

Figure 3.24: Map of ^{14}C (top) and ^{36}Cl/Cl (bottom) for all samples from the GABWRA, GA, OGIA and GISERA datasets in the Precipice Sandstone

4 Discussion

This multi-tracer investigation provided several new insights into the hydrogeology of the Hutton Sandstone aquifer, including that it has more diverse flow paths than previously considered, a lower effective porosity and therefore transmissivity than earlier assumed, which results in higher vulnerability of the aquifer towards extraction. Whilst using environmental tracers to infer hydrogeological processes in GAB aquifers is not new, additional information was gained here by using a variety of tracers that could characterise the system at different spatial and temporal scales. In particular, the matching of age-dating tracers covering different timescales provided additional information. These are inferences about initial tracer concentrations at the beginning of the flow path and a preliminary quantification of the double porosity properties of the Hutton Sandstone.

- This study provided the best estimate to date for the water balance of the deeper Hutton Sandstone aquifer.
- As recharge rates are much lower than previously estimated, this aquifer is more vulnerable to over-extraction than previously thought.
- Tracer results reflect the natural flow system before human influence.
- The Hutton Sandstone is probably not at steady state with respect to past climate change and present extraction.
- To constrain the water balance of the aquifer system as a whole, the connectivity *between* aquifers requires further investigation
- Tracer knowledge for the Precipice is insufficient to derive a similar simple assessment as done for the Hutton.
- The combined use of numerical modelling and tracer measurements needs further refinement.

In the following, the Hutton aquifer flow system is reviewed, the deeper Hutton groundwater flux estimated, and key recommendations to further characterise the Hutton and Precipice Sandstone aquifers are provided.

4.1 Hutton flow system

The environmental tracer survey highlighted that the Hutton Sandstone flow system is complex, with several recharge areas, flow pathways and discharge zones. The study design (two north-south piezometer transects) could exclude a northward flow direction but not an eastward or westward one. However, the maps of $^{36}Cl/Cl$ distribution do not exclude flow towards the southeast or east (e.g. towards the Dawson River). Thus, the Hutton Sandstone north of the Great Dividing Range may not represent one large flow system contributing recharge to the Great Artesian Basin but instead would decompose into several regional flow systems, each discharging into tributaries of the Dawson River (Hodgkinson *et al.* 2010). Discharge in the Dawson River catchment would explain why Hutton groundwater southeast of the line connecting Roma and Taroom is at background values for both ^{14}C and $^{36}Cl/Cl$. This section of the aquifer may not have a flow connection to the northern recharge area and may represent a 'stagnant' or very slowly flowing groundwater body. A more detailed study at the scale of outcrop areas would be needed to describe local flow systems and to quantify groundwater flow towards the Dawson River.

The level of connectivity between the Hutton Sandstone and neighbouring geological formations remains unclear. In the companion study, Smith (2015) could not determine the level of connectivity between the Walloon Coal Measures and the Hutton Sandstone using environmental tracers because of limited available information. Smith (2015) suggested that the Hutton and the Precipice are probably poorly or not connected based on ^{4}He profiles in the Evergreen Formation. However, the presence of very high ^{4}He in western parts of the Hutton Sandstone suggests that an input of older fluids (possibly through faults) is locally possible. The inferences about flow processes in the Hutton aquifer made using ^{14}C and ^{36}Cl are probably representative of natural flow conditions during the Holocene and late Pleistocene in general, but

not of the current conditions. The reason is that groundwater abstraction from this aquifer is a relatively recent phenomenon (<200 y) whereas these tracers operate at timescales of many thousand years. Any possible change in the flow system and water mass transport cannot be captured by a single measurement of these tracers. Only a repeated measurement of the same wells after some years can reveal changes in tracer concentrations with time and thus a change in the flow system within human time scales. The discrepancy between the flow paths inferred from current potentiometric surfaces and from tracers indicates that the Hutton aquifer is not at steady-state, but gradually adjusting to its current extraction and (Holocene) climate regimes.

4.1.1 GROUNDWATER FLUX

Using the estimates for the horizontal groundwater velocity (v) as derived from ^{36}Cl, ^{14}C and stable isotopes (^{18}O, ^{2}H), and an estimate of effective porosity in the Hutton Sandstone (n_a), the groundwater flux at depth in the Hutton Sandstone (Q) can be estimated (see Equation 12-14 in section A.3 in Appendix A for further reasoning). This estimate uses the fact that the double porosity model estimates effective flux through the whole formation thickness as:

$$Q = v \cdot n_a \cdot a \cdot l \qquad (1)$$

Here a is the effective thickness of the Hutton Sandstone and l the length of the recharge segment of the outcrop. A simple GIS analysis (red line in Figure 4.1) estimated l to be ≈226 km. When assuming that a = 10 m, v = 1 m/year and n_a = 0.2, Q is calculated to be 452 ML/y.

This number is much smaller than the recharge value derived from a chloride mass balance assessment of the area. The CMB assessment amounts to 17 GL/year and was derived from re-assessing the recharge area of the Hutton between the Hutton-Wallumbilla fault and the Burunga-Leichardt fault with the methods of Smerdon and Ransley (2012) (Figure 4.1). The tracer-derived recharge for the Hutton therefore represents only 2.7% of the CMB value. However, the two assessments do not necessarily represent the same process. The chloride mass balance estimates the recharge rate at the outcrop, while Q in the current study is more representative of the groundwater flux deeper in the aquifer. Aside for measurement and modelling uncertainties, the difference between the two fluxes may represent loss by groundwater discharge near outcrop areas. This process (also called 'rejected recharge'; (Herczeg 2008)) is a common feature of GAB aquifers and is known to provide baseflow to several rivers.

The groundwater flux for the Hutton estimated here should be considered preliminary. The main purpose for the simple modelling approaches used in this study was to determine the key processes impacting on tracer concentration across the aquifer. A more spatially-explicit numerical model of groundwater flow and solute (tracer) transport in the Hutton aquifer could provide a more rigorous estimate of groundwater velocity and flux. A key finding is that the Hutton aquifer is transmissive only over a limited part of its whole stratigraphic depth (<50m versus 150m respectively), suggesting that most of the groundwater flow occurs through a small section of the whole thickness of the Hutton Sandstone.

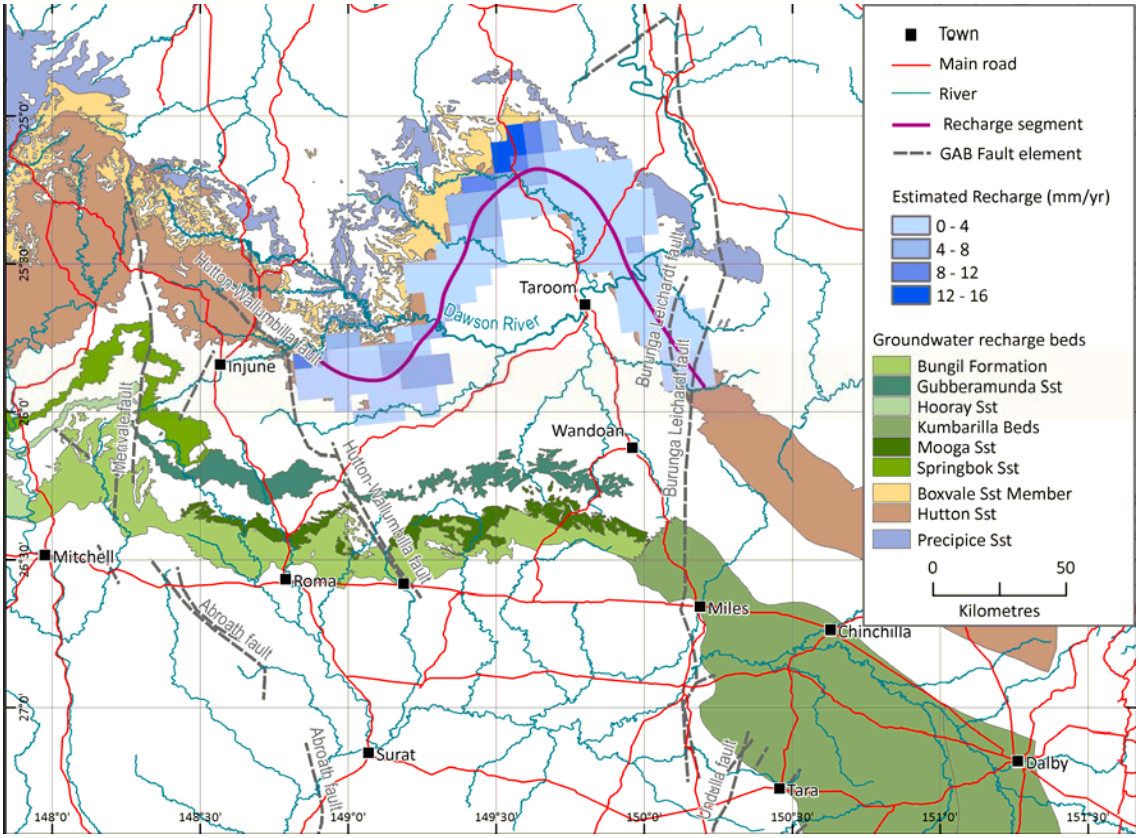

Figure 4.1: Length of recharge segment of Hutton Sandstone between the two dominant fault systems and recharge values according to the Chloride Mass Balance approach (Smerdon and Ransley 2012)

4.2 Other tracers

4.2.1 SULFUR HEXAFLUORIDE

The Hutton Sandstone provided the first evidence for apparent underground SF_6 production in a Queensland aquifer, but this process has also been observed elsewhere in Australia (Leaney *et al.* 2013; Kretschmer and Wohling 2014; Taylor *et al.* 2015). The mechanism for a possible underground production of SF_6 is not yet understood. At present, the most favoured model is radiogenic activation (by alpha particles) of chemical reactions between organic matter and fluorite minerals (Harnisch and Eisenhauer 1998; Harnisch *et al.* 2000). Underground production does not happen everywhere in the Hutton because many of the samples had concentrations below the detection limit. As atmospheric concentrations are steadily increasing, SF_6 should remain a useful tracer for young groundwater for many decades. However, its usefulness will be increased if underground production in Australian aquifers could be identified and quantified, such that the fraction of SF_6 originating from recharge and from underground production can be differentiated.

4.2.2 HELIUM

Establishing the connectivity between aquifers remains one of the key knowledge gaps for quantifying potential impacts of unconventional gas development. Perhaps the most useful tracer for this purpose is ^4He. Helium has a key advantage – it is often found in large quantities in 'old' groundwater (Torgersen and Clarke 1985; Torgersen and Ivey 1985; Torgersen and Clarke 1987; Torgersen and Stute 2013; Aggarwal *et al.* 2015) whereas the abundance of all other tracers decreases in old groundwater. Helium-4 (the main

form of He in groundwater) is an end-product of the radioactive decay of U- and Th-bearing minerals, which are found in essentially all geological formations. Being a stable isotope, ^{4}He produced from U and Th slowly accumulates over time in aquifers, and may create higher relative concentration gradients between aquifers than any other tracer (factor 100,000 as compared to a maximum of 100 for ^{14}C). Even though its production rates are not well known for Australian aquifers, Helium enables to detect the input of very old groundwater into aquifers or surface waters. This is also true if the amount of 'old' groundwater in 'young' groundwater is relatively small (Gardner *et al.* 2011) because the large relative concentration differences allow the detection of small admixtures. However, the high diffusivity of helium is both an advantage and a potential drawback. The high diffusivity of He makes it an especially useful tracer to evaluate diffusion-dominated solute transport in aquitards (Smith 2015). Under particulate circumstances a high diffusivity complicates significantly its use to quantify groundwater and solute transport in aquifers. In a context like the Hutton, where a thin aquifer is surrounded by relatively thick aquitards, diffusion in and out of aquitards can be a large component of the He mass-balance, but one that is not easy to quantify. In extreme cases, a high diffusive He flux through an aquitard separating two aquifers may give the impression that a flow connection exists, whereas the actual exchange of groundwater between aquifers is negligible. Thus, future groundwater modelling exercises aiming to assess 'connectivity' in layered aquifer- aquitard systems should be developed with the aim to properly characterise He transport processes, including localised inputs through faults and fractures and diffusive fluxes through aquitards.

4.3 Tracers and numerical models

Whilst the use of particle tracking to interpret tracers did not allow to uniquely predict tracer concentrations, a number of steps could be taken to improve the interface between environmental tracer application and modelling and to better demonstrate the usefulness of tracers to improve models. One clear outcome of the particle tracking modelling exercise was to help understand the likely flow paths leading to a particular well in a three-dimensional space. Other than for flow path demonstration, the particle tracking scheme used had several restrictions:

- Particle tracking calculations on the comparably coarse discretization of the OGIA flow model (1500m) turned out to be not accurate. Calculations therefore needed a grid refinement (500m), which increased computation times by a factor of 9.
- Despite the finer discretization, Hutton was represented as a homogenous layer, instead of several layers with different transmissivities.
- To obtain an age distribution, a large number of particles was required – the number used here (350) was a compromise dictated by feasibility, several thousand would be desirable.
- Particle tracking neglects any mixing effects caused by dispersion or diffusion.

The model predicted the measured ^{14}C values comparably well, that is, it predicted to have little or no ^{14}C in the samples. In contrast, ^{36}Cl was much less well represented by the model. For three wells 36Cl values predicted by particle tracking were smaller than those measured. This can be explained by "windows" in the aquitards between two aquifers not represented in the model and enabling faster groundwater flow. All other particle tracking results indicate much larger tracer values than were actually measured. In view of the diffusive loss of tracer to the adjacent aquitard discussed earlier, this is not unexpected. The particle tracking approach does not take into account any diffusion process and its related tracer loss.

Future intercomparison between numerical modelling and environmental tracers in the Hutton aquifer will need several refinements. These include to:

- Compare the age distribution determined for a certain control volume around the well with the age distribution obtained with stochastically simulated flow fields introducing a different spatial variability of *K* in each run;
- Systematically evaluate the effect of grid discretization on particle tracking traveltime;
- Use a transport model to describe the tracer concentrations and directly use tracer concentrations to constrain the flow field rather than use them for post hoc comparison;

- Consider transient flow conditions: the flow field in the Hutton is probably not at steady state. A climate shift in the region occurred ~11ky ago, probably influencing recharge, and the aquifer is possibly still adjusting to this.

The most realistic comparison of tracer values with numerical models will come from a direct transport modelling exercise describing the isotopic composition of the tracer itself. However, because of the model complexity involved, this has been done up to now only for two-dimensional vertical cross sections, and only for helium and ^{36}Cl (Castro *et al.* 1998; Zhao *et al.* 1998; Park *et al.* 2002; Castro *et al.* 2007). Thus, the modelling approach to be used needs to be problem- and context-dependent. Simple lumped and analytical models appeared sufficient in this study to improve the conceptual understanding of the Hutton Sandstone aquifers. However, they are of limited usefulness when models are to be used to infer how the system could evolve in the future under different conditions. Particle tracking and more complex groundwater and solute transport numerical models need to be developed; the problem (CSG impact) and the available information (tracer and geochemical data) warrant the investment in developing these models.

4.4 Conclusions and recommendations

The differences in the inferred groundwater flow direction in the Hutton Sandstone between the contemporary potentiometric surface and tracers suggest that this system may be in a transition phase. The contemporary piezometric surface could reflect in part ongoing changes driven by climate (that is, the Holocene-Pleistocene climate shift) and more recent groundwater extraction, whilst tracers would reflect the natural flow system prior to development. The environmental tracers supported the concept of the low effective transmissivity of the Hutton, potentially making this system more vulnerable than anticipated to groundwater extraction or to depressurisation in neighbouring geological formations. In other words, as only a small proportion of the aquifer effectively transmits water, the sustainable yield for this aquifer is probably low. This is important for sustainable management of this aquifer and the definition of groundwater allocations.

The study highlighted other knowledge gaps, including that:

- The initial tracer values at the far northern and south-eastern (east of the Burunga-Leichardt fault) recharge areas for the Hutton are not known and are required to assess flow velocities there;
- The magnitude of groundwater flow from the south-eastern recharge area towards the centre of the Mimosa Syncline is not known;
- The initial tracer values in recharge areas for the Precipice Sandstone are unknown and tracer data in general is lacking for this aquifer;
- The water balances for the Hutton and the Precipice sandstones remain sketchy, complicating the assessment of the potential impacts of groundwater extraction from the aquifer system;
- The connectivity of the Walloon Coal Measures to the Hutton Sandstone should still be considered a key knowledge gap; the companion study (Smith 2015) is the only one known to date that assesses this parameter with measurements on the scale of the formation thickness;

Key recommendations from the study include to:

- Strategically sample additional wells in the Hutton and Precipice aquifers to improve the spatial coverage for tracer distribution, especially in recharge areas;
- Strategically sample for ^{39}Ar in recharge areas and ^{81}Kr farther along flow paths to help constrain the more numerous ^{14}C and ^{36}Cl data. Whilst more complicated to sample in the field, ^{39}Ar and ^{81}Kr can quantify groundwater flow velocity at the right timescales (intermediate for ^{39}Ar and very old for ^{81}Kr) and are relatively easy to interpret;
- Evaluate groundwater velocity and recharge rates for the Precipice Formation;
- Re-evaluate tracer distribution in the Hutton using a numerical groundwater flow and solute transport model;
- Continue efforts to quantify the connectivity between the Walloon Coal Measures and neighbouring geological formations.

References

Aeschbach-Hertig, W, Clark, JF, Stute, M, Reuter, RF, Schlosser, P (2002) A paleotemperature record derived from dissolved noble gases in groundwater of the Aquia Aquifer (Maryland, USA). *Geochimica et Cosmochimica Acta* **66**, 797-817.

Aeschbach-Hertig, W, Peeters, F, Beyerle, U, Kipfer, R (1999) Interpretation of dissolved atmospheric noble gases in natural waters. *Water Resources Research* **35**, 2779-2792.

Aggarwal, PK, Matsumoto, T, Sturchio, NC, Chang, HK, Gastmans, D, Araguas-Araguas, LJ, Jiang, W, Lu, Z-T, Mueller, P, Yokochi, R, Purtschert, R, Torgersen, T (2015) Continental degassing of 4He by surficial discharge of deep groundwater. *Nature Geosci* **8**, 35-39.

Anderman, ER, Hill, MC (2001) MODFLOW-2000, the U. S. Geological Survey modular ground-water model – Documentation of the Advective Transport Observatikon (ADV2) Package, Version 2. U. S. Geological Survey.

Anderman, ER, Hill, MC (2003) MODFLOW-2000, the U. S. Geological Survey modular ground-water model – Documentation of effective porosity parameters in the Advective Transport Observatikon (ADV2) Package. U. S. Geological Survey.

Andrews, JN, Davis, S, Fabryka-Martin, J, Fontes, JC, Lehmann, BE, Loosli, HH, Michelot, J-L, Moser, H, Smith, B, Wolf, M (1989) The in-situ production of radioisotopes in rock matrices with particular reference to the Stripa granite. *Geochimica et Cosmochimica Acta* **53**, 1803–1815.

Andrews, JN, Lee, DJ (1979) Inert gases in groundwater from the Bunter Sandstone of England as indicators of age and palaeoclimatic trends. *Journal of Hydrology* **41**, 233-252.

APLNG (2014) Australia Pacific LNG Upstream 2013-2014 Groundwater Assessment Report. Available at http://www.aplng.com.au/pdf/Q-LNG01-75-RP-0001 Annual_GW Report_Rev1_Final.pdf.

Bentley, HW, Phillips, FM, Davis, SN, Habermehl, MA, Airey, PL, Calf, GE, Elmore, D, Gove, HE, Torgersen, T (1986) Chlorine 36 Dating of Very Old Groundwater 1. The Great Artesian Basin, Australia. *Water Resources Research* **22**, 1991-2001.

Beyerle, U, Purtschert, R, Aeschbach-Hertig, W, Imboden, DM, Loosli, HH, Wieler, R, Kipfer, R (1998) Climate and groundwater recharge during the last glaciation in an ice-covered region. *Science* **282**, 731-734.

Busenberg, E, Plummer, LN (1992) Use of chlorofluorocarbons CCl3F and CCl2F2 as hydrologic tracers and age-dating tools: the alluvium and terrace system in central Oklahoma. *Water Resources Research* **28**, 2257-2283.

Castro, MC, Goblet, P, Ledoux, E, Violette, S, Marsily, Gd (1998) Noble gases as natural tracers of water circulation in the Paris Basin 2. Calibration of a groundwater flow model using noble gas isotope data. *Water Resources Research* **34**, 2467-2483.

Castro, MC, Hall, CM, Patriarche, D, Goblet, P, Ellis, BR (2007) A new noble gas paleoclimate record in Texas – Basic assumptions revisited. *Earth and Planetary Science Letters* **257**, 170-187.

Conard, NJ, Elmore, D, Kubik, PW, Gove, HE, Tubbs, LE, Chrunyk, BA, Wahlen, M (1986) The chemical preparation of AgCl for measuring 36Cl in polar ice with accelerator mass spectrometry. *Radiocarbon* **28**, 509-515.

Cook, PG, Böhlke, J-K (1999) Determining Timescales for Groundwater Flow and Solute Transport. In 'Environmental Tracers in Subsurface Hydrology.' (Eds PG Cook, AL Herczeg.) pp. 1-30. (Kluwer Academic Press: Boston, Mass.)

Craig, H (1961) Isotopic variations in meteoric waters. *Science* **133**, 1702-1703.

Deeds, DA, Vollmer, MK, Kulongoski, JT, Miller, BR, Mühle, J, Harth, CM, Izbicki, JA, Hilton, DR, Weiss, RF (2008) Evidence for crustal degassing of CF4 and SF6 in Mojave Desert groundwaters. *Geochimica et Cosmochimica Acta* **72**, 999-1013.

DNRM, 2013. Queensland Department of Natural Resources and Mines groundwater database. Queensland Department of Natural Resources and Mines,

Einstein, A (1905) Über die von der molekularkinetischen Theorie der Wärme geforderte Bewegung von in ruhenden Flüssigkeiten suspendierten Teilchen. *Annalen der Physik* **17**, 549-560.

Fallon, SJ, Fifield, LK, Chappell, JM (2010) The next chapter in radiocarbon dating at the Australian National University: Status report on the single stage AMS. *Nuclear Instruments and Methods in Physics Research Section B: Beam Interactions with Materials and Atoms* **268**, 898-901.

Fifield, LK, Tims, SG, Fujioka, T, Hoo, WT, Everett, SE (2010) Accelerator mass spectrometry with the 14UD accelerator at the Australian National University. *Nuclear Instruments and Methods in Physics Research Section B: Beam Interactions with Materials and Atoms* **268**, 858-862.

Frenzel, H, Kessels, W, Lengnick, M, Suckow, A, Geyh, MA (1997a) Kalibrierung eines numerischen Grundwasserströmungsmodells für das Testgebiet Golpa-N/Gröbern durch Vergleich von Bahnlinienlaufzeiten mit 14C-Grundwasseraltern. Niedersächsisches Landesamt für Bodenforschung - Geowissenschaftliche Gemeinschaftsaufgaben (NLfB-GGA) No. Archiv-Nr. 116 2934, Hannover.

Frenzel, H, Kessels, W, Lengnick, M, Suckow, A, Geyh, MA (1997b) Numerische Modellierung des Grundwasseralters mit dem Bahnlinienverfahren für das Modellgebiet Golpa-N/Gröbern und Vergleich mit Isotopendaten. In '3. GBL Kolloquium. Halle/Saale', 19-21. Februar 1997. (Ed. Ad GBL-Gemeinschaftsvorhabens) Volume 4 pp. 168-174. (E. Schweizerbart: Stuttgart)

Gardner, WP, Harrington, GA, Solomon, DK, Cook, PG (2011) Using terrigenic 4He to identify and quantify regional groundwater discharge to streams. *Water Resour. Res.* **47**, W06523.

Gelhar, LW, Welty, C, Rehfeldt, KR (1992) A critical review of data on field-scale dispersion in aquifers. *Water Resources Research* **28**, 1955-1974.

Gonfiantini, R (1986) Environmental Isotopes in Lake Studies. In 'Handbook of Environmental Isotope Geochemistry. Vol. 2, The Terrestrial Environment B.' (Eds P Fritz, J-C Fontes.) Vol. 2 pp. 113-168.

Habermehl, MA (1980) The Great Artesian Basin, Australia. *BMR Journal of Australian Geology & Geophysics* **5**, 9-38.

Harnisch, J, Eisenhauer, A (1998) Natural CF4 and SF6 on Earth. *Geophyscal Research Letters* **25**, 2401-2406.

Harnisch, J, Frische, M, Borchers, R, Eisenhauer, A, Jordan, A (2000) Natural fluorinated organics in fluorite and rocks. *Geophysical Research Letters* **27**, 1883-1886.

Heaton, THE, Vogel, JC (1981) "Excess Air" in Groundwater. *Journal of Hydrology* **50**, 201-216.

Herczeg, AL (2008) Background report on the Great Artesian Basin. CSIRO.

Hodgkinson, J, Hortle, A, McKillop, M (2010) The Application of Hydrodynamic Analysis in the Assessment of Regional Aquifers for Carbon Geostorage: Preliminary Results for the Surat Basin, Queensland. *APPEA Journal* 1-18.

Hoffmann, G, Jouzel, J, Masson, V (2000) Stable water isotopes in atmospheric general circulation models. *Hydrological Processes* **14**, 1385-1406.

IAEA (2006) 'Use of Chlorofluorocarbons in Hydrology. A Guidebook.' (International Atomic Energy Agency: Vienna)

IAEA (2013) 'Isotope Methods for Dating Old Groundwater.' (International Atomic Energy Agency: Vienna)

IAEA/WMO (2015) Global Network for Isotopes in Precipitation. The GNIP Database. Release 3, October 1999.

Jähne, B, Heinz, G, Dietrich, W (1987) Measurement of the diffusion coefficients of sparingly soluble gases in water. *Journal of Geophysical Research: Oceans* **92**, 10767-10776.

King, DB, Saltzman, ES (1995) Measurement of the diffusion coefficient of sulfur hexafluoride in water. *Journal of Geophysical Research: Oceans* **100**, 7083-7088.

Koh, D-C, Plummer, LN, Busenberg, E, Kim, Y (2007) Evidence for terrigenic SF6 in groundwater from basaltic aquifers, Jeju Island, Korea: Implications for groundwater dating. *Journal of Hydrology* **339**, 93-104.

Kretschmer, P, Wohling, D (2014) Groundwater recharge in the Anangu Pitjantjatjara Yankunytjatjara Lands, South Australia., Government of South Australia, through the Department of Environment, Water and Natural Resources, Adelaide. Available at http://www.waterconnect.sa.gov.au.

Königer, P, Leibundgut, C, Link, T, Marshall, JD (2010) Stable isotopes applied as water tracers in column and field studies. *Organic Geochemistry* **41**, 31-40.

Königer, P, Leibundgut, C, Stichler, W (2009) Spatial and temporal characterisation of stable isotopes in river water as indicators of groundwater contribution and confirmation of modelling results; a study of the Weser river, Germany. *Isotopes in Environmental and Health Studies* **45**, 289 - 302.

Lamontagne, S, Taylor, AR, Batlle-Aguilar, J, Suckow, A, Cook, PG, Smith, SD, Morgenstern, U, Stewart, MK (2015) River infiltration to a subtropical alluvial aquifer inferred using multiple environmental tracers. *Water Resources Research* n/a-n/a.

Leaney, FW, Taylor, AR, Jolly, ID, Davies, PJ (2013) Facilitating Long TermOut-Back Water Solutions(G-FLOWS). Task 6: Groundwater recharge characteristics across key priority areas. Goyder Institute for Water Research, Adelaide, South Australia.

Maloszewski, P, Zuber, A (1985) On the theory of tracer experiments in fissured rocks with a porous matrix. *Journal of Hydrology* **79**, 333-358.

McDonald, MG, Harbaugh, AW (1988) MODFLOW, a modular three-dimensional finite-difference ground-water flow model.

Mook, WG, Plicht, Jvd (1999) Reporting 14C activities and concentrations. *Radiocarbon* **41**, 227-239.

Morgenstern, U, Taylor, CB (2009) Ultra low-level tritium measurement using electrolytic enrichment and LSC. *Isotopes in Environmental and Health Studies* **45**, 96-117.

Park, J, Bethke, CM, Torgersen, T, Johnson, TM (2002) Transport modeling applied to the interpretation of groundwater 36Cl age. *Water Resources Research* **38**, 1-1-1-15.

Phillips, FM (2013) Chlorine-36 dating of old groundwater. In 'Isotope Methods for Dating Old Groundwater.' (Eds A Suckow, PK Aggarwal, LJ Araguas-Araguas.) pp. 125-152. (International Atomic Energy Agency: Vienna)

Plummer, LN, Glynn, PD (2013) Radiocarbon Dating in Groundwater Systems. In 'Isotope Methods for Dating Old Groundwater.' (Eds A Suckow, PK Aggarwal, LJ Araguas-Araguas.) pp. 33-89. (International Atomic Energy Agency: Vienna)

Pollock, DW (1994) User's guide for MODPATH/MODPATH-PLOT, Version 3: A particle post-processing package for MODFLOW, the U. S. Geological Survey finite-difference ground-water flow model. U. S. Geological Survey.

Purtschert, R, Yokochi, R, Sturchio, NC (2013) 81Kr dating of old groundwater. In 'Isotope Methods for Dating Old Groundwater.' (Eds A Suckow, PK Aggarwal, LJ Araguas-Araguas.) pp. 91-124. (International Atomic Energy Agency: Vienna)

QWC (2012) Underground Water Impact Report for the Surat Cumulative Management Area. Queensland Water Commission.

Radke, BM, Ferguson, J, Cresswell, RG, T.R., R, Habermehl, MA (2000) 'Hydrochemistry and implied hydrodynamics of the Cada-owie-Hooray Aquifer Great Artesian Basin.' (Bureau of Rural Sciences, Australia:

Ransley, TR, Smerdon, BDe (2012) Hydrostratigraphy, hydrogeology and system conceptualisation of the Great Artesian Basin. CSIRO Water for a Healthy Country Flagship, Australia.

Rohden, Cv, Kreuzer, A, Chen, Z, Aeschbach-Hertig, W (2010) Accumulation of natural SF6 in the sedimentary aquifers of the North China Plain as a restriction on groundwater dating. *Isotopes in Environmental and Health Studies* **46**, 279-290.

Rozanski, K (1985) Deuterium and Oxygen-18 in European groundwaters - Links to atmospheric circulation in the past. *Chemical Geology (Isotope Geoscience Section)* **52**, 349-363.

Smerdon, BD, Ransley, TRe (2012) Water resource assessment for the Surat region. CSIRO Water for a Healthy Country Flagship, Australia.

Smith, SD (2015) Geochemical baseline monitoring: quartz-helium trial. CSIRO, Adelaide.

Solomon, DK, Cook, PG, Plummer, LN (2006) Models of Groundwater Ages and Residence Times. In 'Use of Chlorofluorocarbons in Hydrology. A Guidebook.' pp. 73-88. (International Atomic Energy Agency (IAEA): Vienna)

Sonntag, C, Schoch-Fischer, H (1985) Deuterium and Oxygen 18 in Water Vapour and Precipitation: Application to Atmospheric Water Vapour Transport and to Paleoclimate. *Isotopenpraxis* **21**, 193-198.

Sreekanth, J, Moore, C (2015) CSG Water Reinjection Impacts: Modelling, Uncertainty and Risk Analysisanalysis; Groundwater flow and transport modelling and uncertainty analysis to quantify

the water quantity and quality impacts of a coal seam gas produced water reinjection scheme in the Surat Basin, Queensland. CSIRO Land and Water Flagship.
Stuiver, M, Polach, HA (1977) Discussion of Reporting of 14C Data. *Radiocarbon* **19**, 355-363.
Stute, M, Clark, JF, Schlosser, P, Broecker, WS, Bonani, G (1995a) A 30,000 yr continental paleotemperature record derived from noble gases dissolved in groundwater from the San Juan Basin, New Mexico. *Quaternary Research* **43**, 209-220.
Stute, M, Forster, M, Frischkorn, H, Serejo, A, Clark, JF, Schlosser, P, Broecker, WS, Bonani, G (1995b) Cooling of Tropical Brazil (5°C) During the Last Glacial Maximum. *Science* **269**, 379-383.
Stute, M, Schlosser, P (1993) Principles and applications of the Noble Gas Paleothermometer. In 'Climate Change in Continental Isotopic Records, Geophysical Monograph.' (Eds PK Swart, KC Lohmann, J McKenzie, S Svin.) Vol. 78 pp. 89-100. (American Geohysical Union:
Stute, M, Schlosser, P, Clark, JF, Broecker, WS (1992) Paleotemperatures in the southwestern United States derived from noble gas measurements in groundwater. *Science* **256**, 1000-1003.
Stute, M, Sonntag, C (1992) Palaeotemperatures derived from noble gases dissolved in groundwater and in relation to soil temperature.
Stute, M, Talma, S (1997) Glacial temperatures and moisture transport regimes reconstructed from noble gases and d18O, Stampriet aquifer, Namibia.
Suckow, A (2009) Chapter 9 Analysis of Radionuclides. In 'Radioactivity in the Environment.' (Ed. F Klaus.) Vol. Volume 16 pp. 363-406. (Elsevier:
Suckow, A (2012) 'Lumpy - an interactive Lumped Parameter Modeling code based on MS Access and MS Excel., EGU 12.' Vienna. (European Geosciences Union. Available at http://meetingorganizer.copernicus.org/EGU2012/EGU2012-2763.pdf
Suckow, A (2013) System Analysis using Multi-Tracer Approaches. In 'Isotope Methods for Dating Old Groundwater.' (Eds A Suckow, PK Aggarwal, LJ Araguas-Araguas.) pp. 217-244. (International Atomic Energy Agency: Vienna)
Suckow, A (2014) The age of groundwater – Definitions, models and why we do not need this term. *Applied Geochemistry* **50**, 222-230.
Suckow, A, Dumke, I (2001) A database system for geochemical, isotope hydrological, and geochronological laboratories. *Radiocarbon* **43**, 325-337.
Sudicky, EA, Frind, EO (1981) Carbon 14 dating of groundwater in confined aquifers: Implications of aquitard diffusion. *Water Resources Research* **17**, 1060-1064.
Tadros, CV, Hughes, CE, Crawford, J, Hollins, SE, Chisari, R (2014) Tritium in Australian precipitation: A 50 year record. *Journal of Hydrology* **513**, 262-273.
Taylor, AR, Pichler, MM, Olifent, V, Thompson, J, Bestland, EA, Davies, PJ, Lamontagne, S, Suckow, AO, Robinson, NI, Love, A (2015) Groundwater Flow Systems of North Eastern Eyre Peninsula: a multi-disciplinary approach: hydrogeology, geophysics and environmental tracers. Facilitating Long Term Outback Water Solutions —Stage 2. Goyder Institute for Water Research.
Torgersen, T, Clarke, WB (1985) Helium accumulation in groundwater, I: An evaluation of sources and the continental flux of crustal 4He in the Great Artesian Basin, Australia. *Geochimica et Cosmochimica Acta* **49**, 1211-1218.
Torgersen, T, Clarke, WB (1987) Helium accumulation in groundwater, III. Limits on helium transfer across the mantle-crust boundary beneath Australia and the magnitude of mantle degassing. *Earth and Planetary Science Letters* **84**, 345-355.
Torgersen, T, Ivey, GN (1985) Helium accumulation in groundwater. II: A model for the accumulation of the crustal 4He degassing flux. *Geochimica et Cosmochimica Acta* **49**, 2445-2452.
Torgersen, T, Purtschert, R, Phillips, FM, Plummer, LN, Sanford, W, Suckow, A (2013) Defining Groundwater Age. In 'Isotope Methods for Dating Old Groundwater.' (Eds A Suckow, PK Aggarwal, LJ Araguas-Araguas.) pp. 21-32. (International Atomic Energy Agency: Vienna)
Torgersen, T, Stute, M (2013) Helium (and other Noble Gases) as a Tool for Understanding Long Timescale Groundwater Transport. In 'Isotope Methods for Dating Old Groundwater.' (Eds A Suckow, PK Aggarwal, LJ Araguas-Araguas.) pp. 179-216. (International Atomic Energy Agency: Vienna)
Troldborg, L, Jensen, K, Engesgaard, P, Refsgaard, J, Hinsby, K (2008) Using Environmental Tracers in Modeling Flow in a Complex Shallow Aquifer System. *Journal of Hydrologic Engineering* **13**, 1037-1048.

Troldborg, L, Refsgaard, JC, Jensen, KH, Engesgaard, P (2007) The importance of alternative conceptual models for simulation of concentrations in a multi-aquifer system. *Hydrogeology Journal* **15**, 843–860.

Vogel, JC (1967) Investigation of groundwater flow with radiocarbon. In 'Isotopes in Hydrology. Vienna'. pp. 255-368. Vienna)

Weiss, RF (1968) Piggyback samplers for dissolved gas studies on sealed water samples. *Deep Sea Research* **15**, 659-699.

Zhao, X, Fritzel, TLB, Quinodoz, HAM, Bethke, CM, Torgersen, T (1998) Controls on the distribution and isotopic composition of helium in deep groundwater flows. *Geology* **26**, 291-294.

Appendix A Using environmental tracers to quantify groundwater time scales

Using environmental tracers as age indicators relies on time-dependent concentrations of trace substances in water. The trace substances have a known time-dependent input function as indicated on the left of Figure A.1. Tracers can be stable and conservative, like for example ^{18}O and ^{2}H, CFCs and SF_6. Other trace substances can be radioactive, and in this case the natural radioactivity can provide time information also when the input function at recharge is constant, as for example, with ^{14}C and ^{36}Cl. Also, a combination of time-dependent input and radioactive decay is possible such as with ^{3}H and ^{85}Kr, as long as the time-dependent input is quantified. Or, the concentration of the tracer can increase with time along the flow path, e.g. due to underground production, as is the case with ^{4}He. Any age deduced from the measured concentration of an environmental tracer, however, is never unique, no matter what tracer is used. Figure A.1 illustrates this.

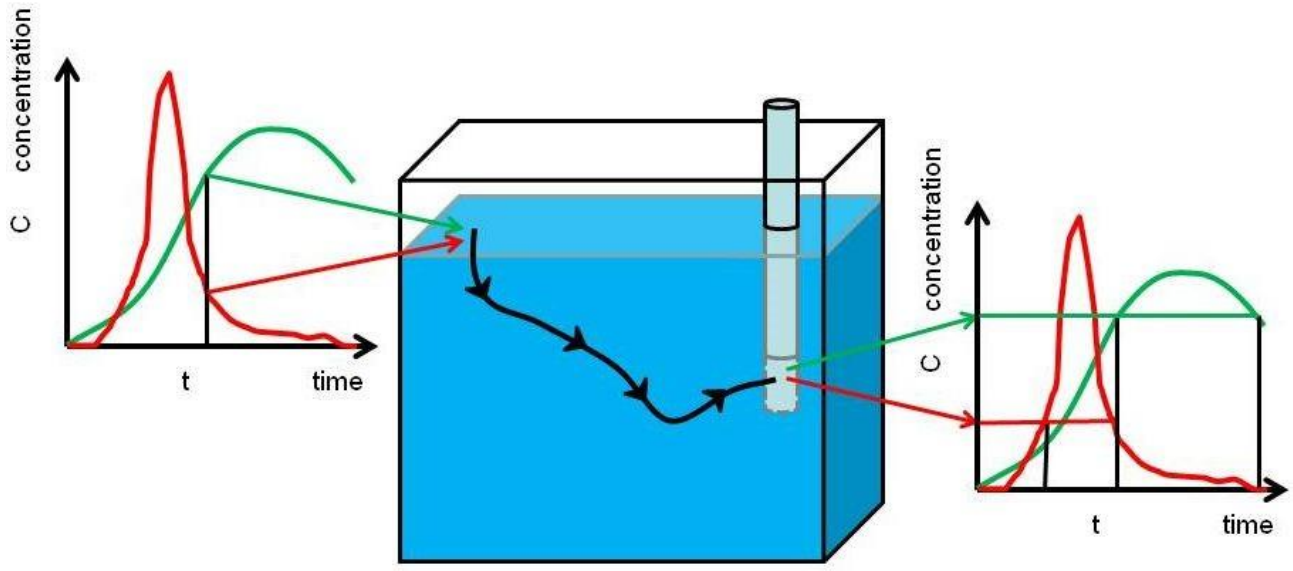

Figure A.1: Principle of the application of environmental tracers to deduce groundwater age (Suckow 2014)

The tracer concentration always needs to be known at the recharge site ("input function", represented by the red and green curve on the left, indicating two different tracers). However, the measured concentration at the well screen allows for several moments in time to be deduced (horizontal red and green lines on the right, each giving two ages, represented as vertical black lines). Therefore every application needs a combination of several tracers to derive a unique value on the time axis (middle black line agreeing both to the red and green concentrations on the input curve). Details of different age definitions and how they relate to common conceptions of human age can be found in Suckow (2014). Only those tracer properties will be discussed in the following sections that are important in the context of the present project. It is, however, important to note that all tracer methods determine the distance velocity v within the aquifer (unit: m/year). This is related to the Darcy velocity q (volumetric groundwater flux in cubic meters per square meter aquifer cross section and year; also expressible as m/y) by the (effective) porosity n_e via $v=q/n_e$. Tracer derived velocities are therefore always larger than Darcy velocities and the factor n_e between v and q needs an independent assessment.

A.1 Tracers used

Tracers used in this report to interpret flow velocities were the stable isotopes of water (^{18}O and ^{2}H), CFCs, SF_6, tritium (^{3}H), ^{14}C, ^{36}Cl and ^{4}He. They will be introduced shortly in the following sections. The chemical compounds CFCs and SF_6 are of anthropogenic origin, are dissolved in water and recharge times can be deduced from their known atmospheric concentration. The other tracers are radioactive (^{14}C, ^{36}Cl, ^{3}H) or stable isotopes (^{2}H, ^{18}O, ^{4}He) of elements. Isotopes (from the Greek word 'iso topos' for 'same place' – meaning the same place in the periodic table of the elements) are varieties of atoms of one element with identical chemical behaviour (since they belong to the same element) but slightly different mass, which can result in fractionation during physical or biological processes. This difference in mass is due to different number of neutrons. Since the chemical properties are determined by the number of electrons in the hull, which in a neutral atom equals the number of protons in the nucleus, all isotopes show the same chemical behaviour of the element. This makes isotopes ideal tracers. Too few or too many neutrons relative to protons renders a core unstable, which is why some isotopes are radioactive. Environmental tracers use all these properties to investigate natural processes – known concentration at the time of recharge, identical chemical behaviour since it is the same element, differences in mass that lead to fractionation, and radioactive decay that provides a natural 'clock' for natural processes.

A.1.1 STABLE ISOTOPES OF WATER

The water molecule H_2O is formed of the elements hydrogen and oxygen. While the most abundant isotopes of hydrogen and oxygen are ^{1}H and ^{16}O, respectively (forming $^{1}H_2{}^{16}O$), both elements have a stable and rare isotope, ^{2}H and ^{18}O. In the natural water cycle these isotopes behave as normal water. In fact they *are* water, forming molecules with slightly different masses (e.g. $^{2}H^{1}H^{16}O$ and $^{1}H_2{}^{18}O$). Nevertheless, the different isotopic species of water are slightly enriched during different natural processes, the most important being phase transitions (e.g. from liquid to gas phase). The heavier molecules, containing ^{2}H and ^{18}O, are slightly enriched (by a few ‰ only) in the less mobile phase. For example, the ocean will contain slightly more ^{2}H and ^{18}O per gram water than the water vapour formed from it, and the raindrop will contain slightly more ^{2}H and ^{18}O than the cloud it formed from. The magnitude of this isotopic difference depends on the temperature prevailing during the phase transition (evaporation or condensation). These slight differences in the isotopic ratio *R* are expressed as per mil deviation of a standard, called SMOW (Standard Mean Ocean Water) using the delta notation:

$$\equiv \frac{R_{Sample}-R_{Standard}}{R_{Standard}} = \frac{R_{Sample}}{R_{Standard}} - 1 \cdot 1000‰ \qquad (2)$$

Since the standard is ocean water and since, as mentioned, the water vapour derived from it will have less of the heavy isotopic species, and since nearly the entire global water cycle happens after this phase transition, most isotopic values for $\delta^{18}O$ and $\delta^{2}H$ in water samples are negative. One has to keep in mind that the fractionation effects in stable isotopes are very small, per mil only, whereas the effects of radioactivity (^{3}H, ^{14}C, ^{36}Cl) or concentration (CFCs, SF_6) are comparably large: several percent or a factor of two to ten. As a consequence of natural isotopic enrichment processes, several effects can be observed.

Continental effect

Air masses losing water as rain when moving inland will gradually deplete in the heavy isotopes. This means that rain falling further inland will be more negative in $\delta^{18}O$ and $\delta^{2}H$ than close to the coast. The effect was first described for Europe (Sonntag and Schoch-Fischer 1985) and later verified all over the world, see http://www-naweb.iaea.org/napc/ih/documents/userupdate/Waterloo/. The magnitude of this effect is on the order of 0.2‰/100 km in $\delta^{18}O$. For the study here the effect is unimportant, because the size of the whole study area is not much more than 100 km and the typical measurement precision for $\delta^{18}O$ is 0.1‰.

Evaporation effect

If a water body evaporates, the water vapour will be isotopically lighter (more negative in δ values) than the remaining water body. As a consequence, the remaining water body will gradually develop more positive values in $\delta^{18}O$ and $\delta^{2}H$. This is a useful tool in water balance investigations of lake studies (Gonfiantini 1986) and allows determining the evaporated fraction of lakes, channels and rivers. Evaporation can be easily determined in a plot of $\delta^{2}H$ versus $\delta^{18}O$ because the slope of evaporating waters in this plot is characteristically smaller – around 4 to 6 – than the global meteoric water line GWML (Craig 1961) on which most other precipitation and groundwater values are situated and which has a slope of 8. The slope of the evaporation line depends on relative humidity, for tropical conditions with 100% relative humidity it approaches the slope of 8 of the GMWL. For the present study the evaporative effect is only important in case groundwater infiltrates from rivers, which is not to be expected.

Temperature effect

The isotopic fractionation is temperature dependent, and at lower temperatures the heavy species will be even less mobile than at higher temperatures. Therefore rain in winter will have a hydrogen and oxygen isotopic composition slightly lighter (less heavy isotopes, more negative delta values) than in summer. The magnitude of this effect is 0.5‰/°C in $\delta^{18}O$ as global average but can vary considerably on a local scale. This seasonal effect is most pronounced in precipitation itself and meanwhile used to calibrate General Circulation Models (GCM) of the atmosphere (Hoffmann *et al.* 2000). The seasonal temperature effect in stable isotopes is also discernible in the runoff signal in rivers (Königer *et al.* 2009), and in the soil zone (Königer *et al.* 2010). In groundwater this seasonal signal in stable isotopes is only discernible for very young groundwater (typically <4years), which makes this seasonality a useful tool in Karst systems.

Another temperature effect is more important when studying old groundwater; Pleistocene precipitation was recharging groundwater under colder conditions than today and these colder temperatures are reflected by isotope values that are typically 20‰ more negative in $\delta^{2}H$ for Pleistocene palaeowaters than for modern waters in Europe (Rozanski 1985). This corresponds to ≈2.5‰ more negative values in $\delta^{18}O$ for Pleistocene palaeowaters. The reason for this variation between the last glaciations and today is, however, not only due to temperature. Since during the last glaciations 3% of the global water volume was stored in the ice caps and since this ice-stored water was depleted in ^{18}O and ^{2}H (had more negative isotope values) the remaining ocean water was roughly 1.2‰ more positive than today. The actual temperature effect in Europe therefore corresponds to 3.7‰ in ^{18}O. The global effect will vary from place to place and only few palaeoclimate records exist on the southern hemisphere (Stute *et al.* 1995b; Stute and Talma 1997). Some of these show positive and some negative shifts in ^{18}O values during the last ice-age, with no reliable record published to date for Australia. In any case, stable isotope measurements may allow discerning water recharged 10 ky ago from those recharged today. This is a useful application to confirm other tracers, like ^{14}C and ^{36}Cl, used to derive flow velocities.

A.1.2 ANTHROPOGENIC DECADAL TRANSIENT TRACERS (^{3}H, CFCS, SF_6)

The transient tracers of anthropogenic origin can be used for timescales of years to a few decades. These comprise ^{3}H, CFCs and SF_6 and are called transient because their input concentration changes with time.

Tritium

Tritium (^{3}H) is the radioactive isotope of hydrogen and as such is part of the water molecule. Tritium is commonly measured in Tritium Units (TU), where one tritium unit corresponds to a ratio of ^{3}H to normal hydrogen of 10^{-18}, or to a tritium related specific radioactivity of 0.119 Bq per kg water. The ^{3}H presently observed predominantly in shallow groundwater is largely a result of atmospheric hydrogen bomb tests carried out in the sixties. Natural background of tritium in Australia is below 5 TU. Figure A.1 shows the time series of ^{3}H content in precipitation in Kaitoke, New Zealand, where the longest record on the southern hemisphere is available. For comparison, this record is displayed together with some stations in Australia (IAEA/WMO 2015). Evidently, the tritium fallout in precipitation in Australian stations was slightly

higher around the bomb era than it was in New Zealand, which is due to a higher continental effect in Australia equivalent to higher dilution of the tritium input by oceanic (tritium-free) moisture in New Zealand. While the highest measurement in NZ was 76 TU in September 1966, some results in Adelaide, Melbourne, Brisbane and Alice Springs have values between 100 and 300 TU until 1972, which corresponds to the last French nuclear tests in the 100kt range in Mururoa. Unfortunately, while there is a recent evaluation of ^{3}H data in precipitation (Tadros *et al.* 2014), these contain no numerical values and have not been uploaded to the GNIP record as of August 2015 (IAEA/WMO 2015). Therefore, no Australian values are available for precipitation later than 1990.

Since ^{3}H is radioactive, Figure A.2 also displays how radioactive decay from some dates onward decreases the ^{3}H signal (blue lines). These lines give evidence that tritium alone cannot distinguish different recharge years uniquely, since rain from many different rainfall events would have 3-6 TU today. Therefore, although ^{3}H is radioactive, the way to use it as a groundwater tracer is largely like a dye, that is like CFCs and SF_6 are used, and hardly as a radioactive substance, as is the case for ^{14}C and ^{36}Cl (see below). A groundwater sample containing ^{3}H of more than 0.2 TU is an indication that part of the water recharged later than 1963, which corresponds to the peak in ^{3}H in precipitation in Figure A.2. *How much* of such young water is in the sample or *when* it was infiltrated cannot be uniquely quantified from one tritium measurement alone.

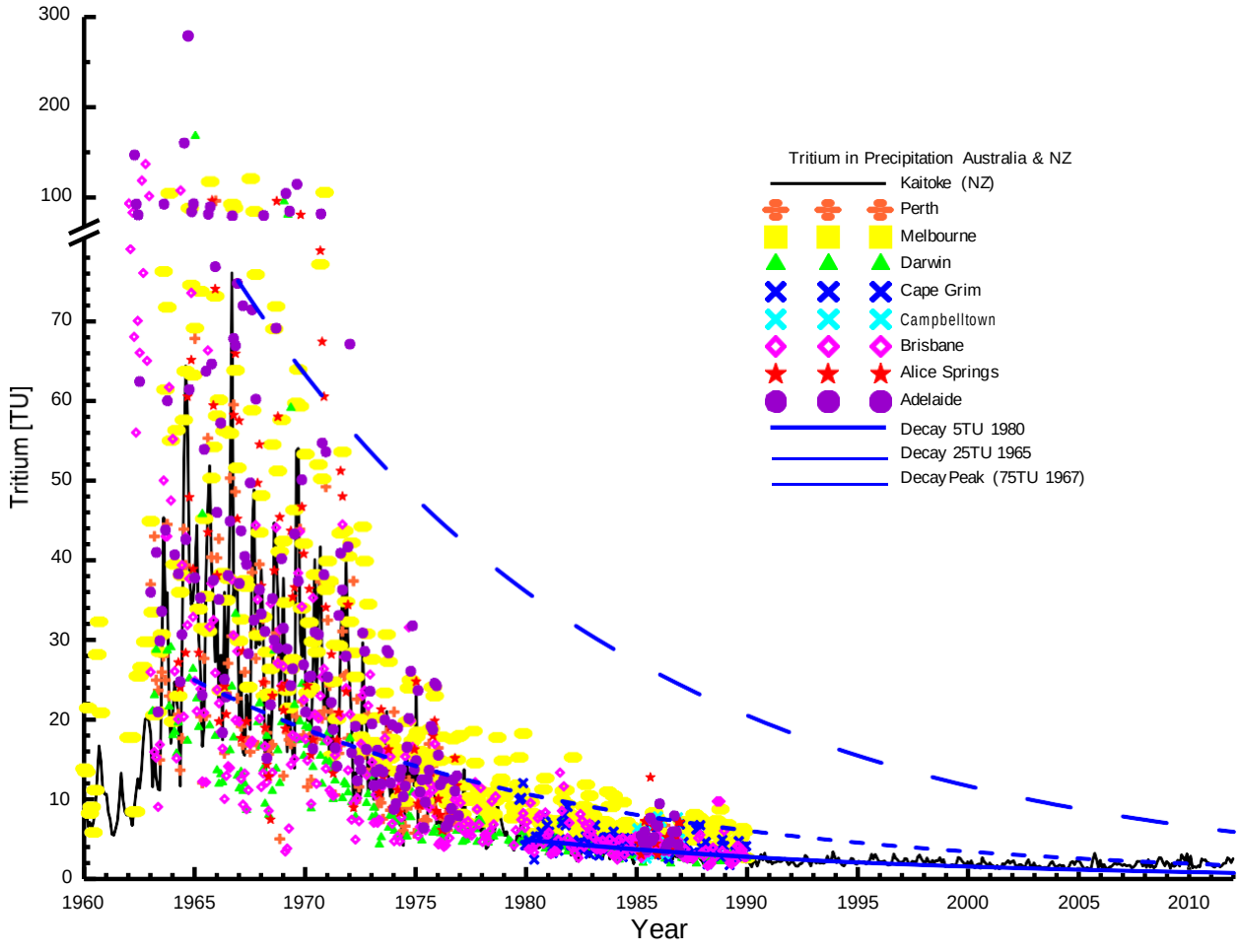

Figure A.2: Input function of tritium in Kaitoke and several Australian stations (IAEA/WMO 2015)

CFCs/SF_6

The environmental tracers Chlorofluorocarbons with the three species CFC-11, CFC-12 and CFC-113 and sulphur hexafluoride (SF_6) are synthetic compounds, volatile at room temperature, that have been used for refrigeration, aerosols and electrical insulation since the 1940s. Their concentrations in the atmosphere

increased steadily since then, reaching a peak in the late 1990s for CFCs and continuing to rise in the case of SF_6 (IAEA 2006). They can be measured down to levels of part per trillion using gas chromatography. During recharge the atmospheric concentration will be preserved in groundwater in accordance to their solubility (Henry's law). Figure A.3 illustrates this principle: known air concentrations (yellow panel left side) are converted with known infiltration temperatures to water concentrations (blue panel right side). Very simplified the infiltration year can then in principle be deduced from the measured concentrations: the horizontal lines in the right panel, symbolizing the measured concentrations, lead to a common infiltration year following the vertical line. In general terms, the mean residence time can be determined from the measured concentration, assuming an age distribution which needs assessment of the flow field and sampling condition (Suckow 2014). If no information concerning the flow field is available, several model assumptions are tested against the measured values of different tracers in binary tracer plots.

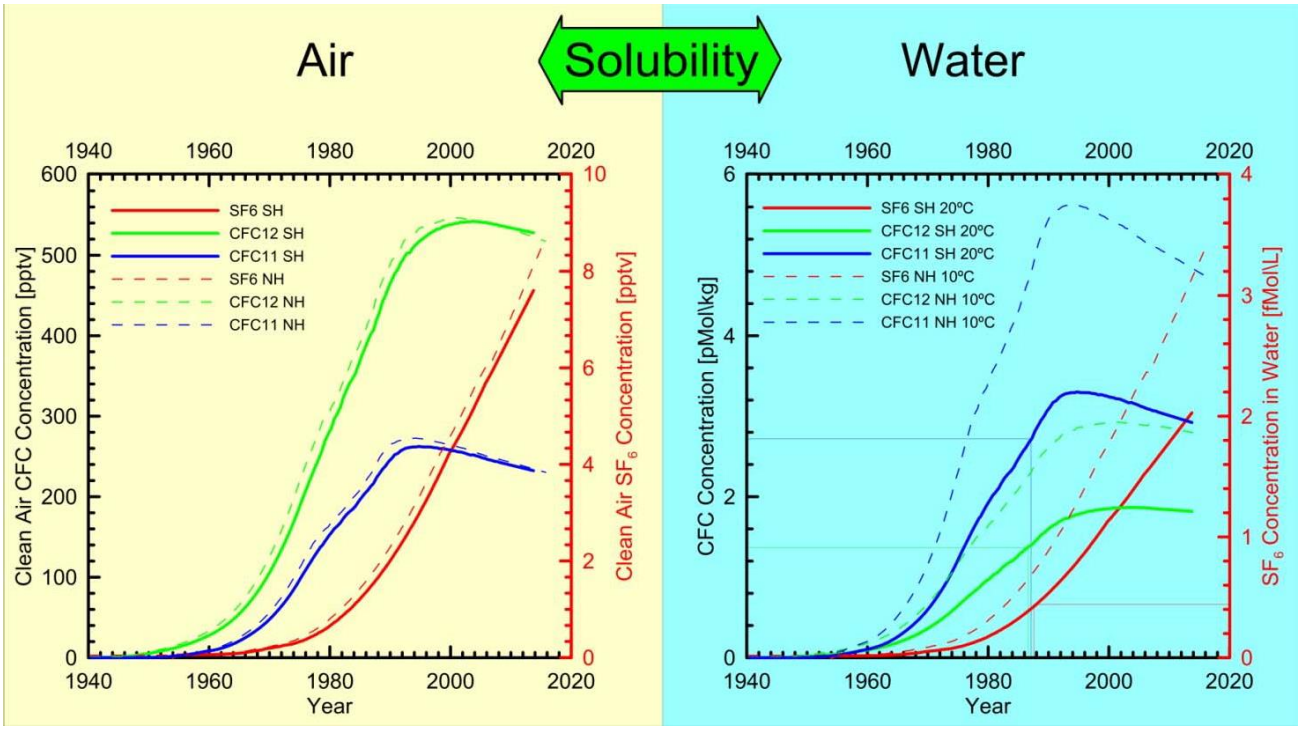

Figure A.3: The principle how CFCs and SF_6 are used to deduce time, SH and NH being 'southern' and 'northern' hemisphere respectively

In practice several processes can complicate the application of CFCs and SF_6: the recharge temperature has to be deduced as soil temperature by adapting information from nearby meteorologic stations, or needs concentrations of all noble gases in another sample aliquot, which is not always possible. Sulphur hexafluoride is influenced strongly by excess air (Heaton and Vogel 1981), which can only be assessed by analysing concentrations of all noble gases in another sample aliquot. Furthermore, CFCs can be degraded in anaerobic groundwater and there is an ongoing discussion about natural underground production of SF_6 in the subsurface (Koh *et al.* 2007; Deeds *et al.* 2008; Rohden *et al.* 2010).

A.1.3 RADIOACTIVE TRACERS FOR OLD WATER (^{14}C, ^{36}Cl)

Radioactive tracers used for the longer timescales are ^{14}C and ^{36}Cl. Both are cosmogenic nuclides, naturally produced in the upper atmosphere from cosmic radiation. For radioactive tracers with known or constant input function, an apparent age can be derived from concentrations using the equation of radioactive decay:

$$c(t) = c_0 \exp(-At) \Leftrightarrow t = \frac{1}{A} \ln\left(\frac{C_0}{C(t)}\right) \qquad (3)$$

Here t is the apparent age (Suckow 2014), λ is the decay constant, corresponding to $\ln(2)/t_{1/2}$ and $t_{1/2}$ is the half-life. $C(t)$ is the measured concentration in the sample and C_0 the concentration at recharge. For most groundwater tracers C_0 is insufficiently known *a priori* and needs to be determined in the recharge area. Such an empirical determination involves a cross-plot with a tracer for the next younger timescale (Suckow 2013). For ^{14}C this may be ^{3}H, CFCs, SF_6 and ^{85}Kr. For the initial value of $^{36}Cl/Cl$, ^{14}C can be favourably used as this young tracer. For ^{14}C in combination with CFCs or ^{3}H, input functions for both tracers can be compared with measured values on a dual tracer plot and a constant factor to the atmospheric ^{14}C ratio can be fitted, as successfully demonstrated in Lamontagne *et al.* (2015) or Taylor *et al.* (2015). For $^{36}Cl/Cl$ the initial value would be obtained from those samples that still contain radiocarbon, if mixtures between water of different age can be excluded. Typical applications allow the determination of timescales up to five half-lives, so how far a tracer can be used into the past strongly depends on the kind of tracer.

Radiocarbon

Radiocarbon or ^{14}C is probably the most used tracer for 'dating' groundwater in Australia. Radiocarbon has a half-life of 5730 years, which allows determining flow velocities and constraining timescales between some thousand and approximately 30,000 years. For ^{14}C, the actually measured value is not the absolute concentration of ^{14}C in water, but the isotopic ratio of $^{14}C/^{12}C$ in the Total Dissolved Inorganic Carbon (TDIC), which is the sum of dissolved CO_2, HCO_3^- and CO_3^{2-}. The unit for this ratio of $C/^{14}C$ was pMC (percent Modern Carbon, (Stuiver and Polach 1977)) or more recently %, where 100% corresponds to the atmospheric $^{14}C/^{12}C$ ratio in 1950 (Mook and Plicht 1999). The basic assumption is that the isotopic ratio of $^{14}C/^{12}C$ changes only by radioactive decay of ^{14}C. Radiocarbon can be measured very precisely (better 0.1%) and with a very low detection limit of less than 0.1% via Accelerator Mass Spectrometry (AMS). In practical groundwater studies, especially in deep aquifers, a few % of ^{14}C should be considered as practical detection limit, since leaky casings or small hydraulic connections in the bore annulus can never completely be excluded.

Very often however, radioactive decay is not the only process decreasing ^{14}C in groundwater. All geochemical changes increasing TDIC or alkalinity can potentially decrease $^{14}C/^{12}C$ (Plummer and Glynn 2013). This is of special importance when fossil sources of carbon are available, as is obviously the case in the coal seam gas districts. Also for the GAB as a whole, an increase in alkalinity (and hence TDIC) is known with flow distance (Radke *et al.* 2000; Ransley and Smerdon 2012). A possibility to avoid this geochemical influence, which causes the water samples to look 'too old', is to consider only the concentration of ^{14}C (e.g. as ^{14}C atoms per litre water), in analogy to general practice for ^{36}Cl (see below). This case is easier than ^{36}Cl, because underground production of ^{14}C is negligible and therefore most underground sources of carbon can be considered ^{14}C-free and would not influence the ^{14}C concentration. If N_A is the Avogadro constant, TDIC is expressed as mmol/L carbon, $^{14}C/^{12}C$ in % and ^{14}C as atoms/L, then the recalculation of % into atoms/L ^{14}C is:

$$^{14}C \text{ atoms/L} = \frac{^{14}C}{^{12}C} \% \cdot \frac{1}{100} \cdot \frac{TD/C}{1000} \cdot N_A \cdot 1.175 \cdot 10^{-12} \quad (4)$$

The number $1.175 \cdot 10^{-12}$ corresponds to the isotope ratio $^{14}C/^{12}C$ of modern carbon, which can be calculated from the specific activity of 0.226 Bq/gC and its physical half-life of 5730 years (Mook and Plicht 1999).

There are many geochemical 'correction' models which are all designed to derive the initial 'no decay' concentration C_0 for Equation 3. Since they will not be applied in this report they are not discussed in detail, and the interested reader is referred to the detailed description by Plummer and Glynn (2013).

Chlorine-36

The application of ^{36}Cl is very analogous to ^{14}C and the basic idea also follows Equation 3, with the important difference that the half-life of ^{36}Cl is much longer (301,000±4,000 years) (Phillips 2013). The applicable time range therefore is between 50,000 and approximately one million years. This means ^{36}Cl behaves in comparison to ^{14}C similarly as ^{14}C behaves in comparison to ^{3}H. Also in the case of ^{36}Cl, the actually measured value is the isotopic ratio of $^{36}Cl/Cl$. A general complication of ^{36}Cl is that it is produced in

the subsurface (Andrews *et al.* 1989), mainly by neutron capture of ^{35}Cl and to a much smaller extent of potassium-39 (^{39}K). The thermal neutrons in both cases come from uranium (U) and thorium (Th) in the aquifer. As a result of this underground production, the ^{36}Cl/Cl ratio normally does not approach zero but a non-zero value that has to be determined empirically in each aquifer. Chloride (Cl) as the carrier for the dating isotope has the advantage of being a much more conservative substance in groundwater than TDIC is for ^{14}C. Nevertheless, already in the first applications in the GAB the basic problems of dilution with 'dead' Cl and underground production of ^{36}Cl were discussed (Bentley *et al.* 1986). The Cl concentration along the flow path is necessary information for the interpretation of ^{36}Cl, as is the knowledge of the final value, to which the ^{36}Cl/Cl ratio develops for groundwater being much older than the dating range of ^{36}Cl. Data interpretation typically involves a discussion of plots of ^{36}Cl/Cl versus Cl concentration, ^{36}Cl/Cl versus ^{36}Cl concentration and ^{36}Cl concentration versus Cl concentration, as discussed in detail by Phillips (2013). In this book chapter, also a sufficiently general model of ^{36}Cl evolution in groundwater is described, which will be summarized next.

The Phillips Model for ^{36}Cl

In Chapter 6 of IAEA (2013) Fred M. Phillips described an easy mass balance equation for the absolute ^{36}Cl concentration in an aquifer. The model incorporates radioactive decay of the recharged ^{36}Cl, underground production in the aquifer towards a secular equilibrium ratio of ^{36}Cl/Cl and an additional source of chloride, like e.g. diffusion from an adjacent aquitard, which may have another ^{36}Cl/Cl ratio in secular equilibrium. The formula for the ^{36}Cl evolution with time is:

$$^{6}\mathrm{Cl}(t) = \mathrm{Cl} = {}_{r}\mathrm{Cl}\,\exp(-\lambda t) - {}_{1}\mathrm{Cl}_{r}\,\frac{F_{Cl}}{A}\,(R_2 - R_1)\,r\,1 - \exp(-\lambda t)\;{}_{2}\,t_{Cl} \quad (5)$$

In this formula ^{36}Cl(t) is the absolute ^{36}Cl concentration [atoms/L], which corresponds to the measured ^{36}Cl/Cl ratio (R_m) multiplied with the measured chloride concentration Cl_m [atoms/L]. Further R_r, R_1 and R_2 are the isotopic ratios of ^{36}Cl/Cl in the recharge area (r), in secular equilibrium in the aquifer (1) and the adjacent aquitard (2) respectively. F_{Cl} is the flux of chloride from the aquitard to the aquifer [atoms/(L·year)], and λ is the decay constant of ^{36}Cl.

The model is general enough, that it can be applied to radiocarbon as well. In this case R_1 and R_2 are both zero, since no underground production takes place for ^{14}C, and it describes the dilution of the (measured) ^{14}C/C ratio with 'dead' TDIC. In any case it is necessary to support the findings from ^{14}C and ^{36}Cl with other tracers such as helium.

A.1.4 HELIUM AS A TRACER

The helium isotope ^{4}He is produced in the underground from the U/Th decay chains since these two elements are abundantly present at ppm concentration level in the rock matrix. Every alpha particle from the decay chains contributes a ^{4}He atom and most of these are released to the groundwater and pore water (Torgersen and Stute 2013). Figure A.4 displays the decay chain of ^{238}U (Suckow 2009) and each yellow arrow in it represents an alpha particle, corresponding to the creation of a helium atom. One atom of ^{238}U therefore will produce a total of eight ^{4}He atoms when decaying to ^{206}Pb.

The easiest, but seldom fulfilled assumption is that ^{4}He in groundwater increases constantly with time according to the formula (Andrews and Lee 1979):

$$\frac{dc\,^{4}\mathrm{He}}{dt} = \frac{\rho_R}{\rho_W} A \frac{1-n_{tot}}{n_{eff}} \left(1.19 \cdot 10^{-16}\ \mathrm{U} \quad 2.88 \cdot 10^{-14}\ \mathrm{Th}\right) \quad (6)$$

Here $c(^{4}\mathrm{He})$ is the measured concentration of ^{4}He in groundwater and $dc(^{4}\mathrm{He})/dt$ is its increase per year in [cc(STP)/(g·year)]. ρ_R and ρ_W are the rock and water densities, Λ is a release factor of helium from the rock which empirically is always 1, and n_{tot} and n_{eff} are the total and effective porosities valid for the groundwater flow. Uranium [U] and thorium [Th] concentrations in this formula are given as ppm. Typical uranium and thorium concentrations in aquifer rocks are in the range of fractions of a ppm to several ppm

resulting in typical production rates of $1 \cdot 10^{-13}$ to $5 \cdot 10^{-11}$ cc(STP)/(g·year). Values for the Hutton and Precipice Sandstones in the Surat basin range from 3–6 ppm and 3–8 ppm for U and Th respectively and together with estimates of porosity and rock density (APLNG 2014; Smith 2015) result in an in situ production rate of $1 \cdot 10^{-11}$ cc(STP)/(g·year). The concentration of ^{4}He in solubility equilibrium is ca. $5 \cdot 10^{-8}$ cc(STP)/g and can be determined with an accuracy of better than 10%. The in situ produced helium component would therefore be distinguishable from solubility equilibrium earliest after 500-1000 years and then increase linearly with time. This makes helium a dating tracer that has no theoretical upper limit of application.

As outlined in Torgersen and Stute (2013) this linear increase is hardly ever fulfilled and influx of helium from aquitards and underlying formations as well as diffusive losses of helium from the aquifer to surrounding formations dominate the concentration behaviour with time. Therefore any interpretation of helium has to be treated at least with as much caution as for ^{14}C and all tracers have to be combined with each other to derive estimates of flow rates and direction.

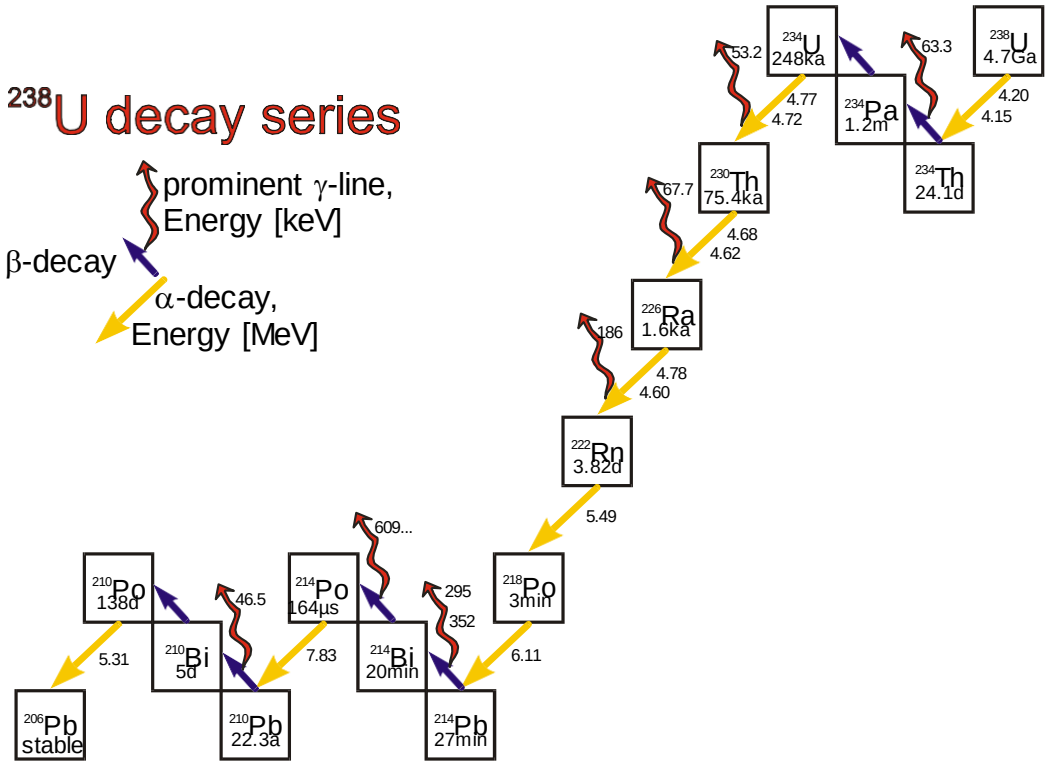

Figure A.4: Decay chain of ^{238}U (Suckow 2009), providing a total of 8 helium atoms per decaying ^{238}U (yellow arrows)

A.2 'Age' of groundwater is not a scalar but a distribution

Any groundwater sample contains not only one 'age', but many different ages (see Figure A.5 originating from (Torgersen *et al.* 2013)). The idea of an idealized age (as introduced in Section 2.6) is displayed in Figure A.5 A. Wider age distributions are caused by diffusion and dispersion along a single flow path (Figure A.5 B). More realistically, flow paths from different parts of the recharge area start in the recharge area and meet in the well, causing a wider distribution than expected from diffusion and dispersion alone (Figure A.5 C). Furthermore, exchange with the aquitard matrix can strongly influence the age distribution (Figure A.5 D), which is discussed in more detail in the next paragraph. These processes together can create large discrepancies between apparent ages calculated for different tracers. This is due to the fact that each tracer 'sees' only a small part of the whole age distribution. Any calculation according to formulas like Equation 3 therefore gives only an 'apparent age', and these apparent ages can differ easily by a factor of 2 or more for different tracers (Suckow 2013, 2014). The magnitude of the discrepancy between these apparent ages depends on the flow regime and on the sampling conditions.

However, all these processes A-D keep the age distribution in a uni-modal shape with only one maximum in the distribution. In reality this is even too simplistic an assumption. On long flow paths like several tens of kilometres, waters from different aquifers can mix, e.g. by the influence of faults or by windows in the aquitards separating the aquifers. This can cause bimodal or multimodal age distributions and render any apparent age meaningless (Figure A.5 E). Further downstream of such a confluence, hydrodynamic dispersion can then again spread out the difference between the single peaks and the age distribution can be uni-modal again, but much wider. This illustrates why the calculation of apparent ages in most cases is not a very useful approach (Suckow 2014) and is not followed in this report. Instead, different flow assumptions are tested against a multitude of tracers (Suckow 2013). Hereby it is necessary to always combine the tracers for 'old' groundwater (^{14}C, ^{4}He, ^{36}Cl) with those for young groundwater (CFCs, SF_6, ^{3}H) to de-convolute admixtures of young water in the sample (IAEA 2013).

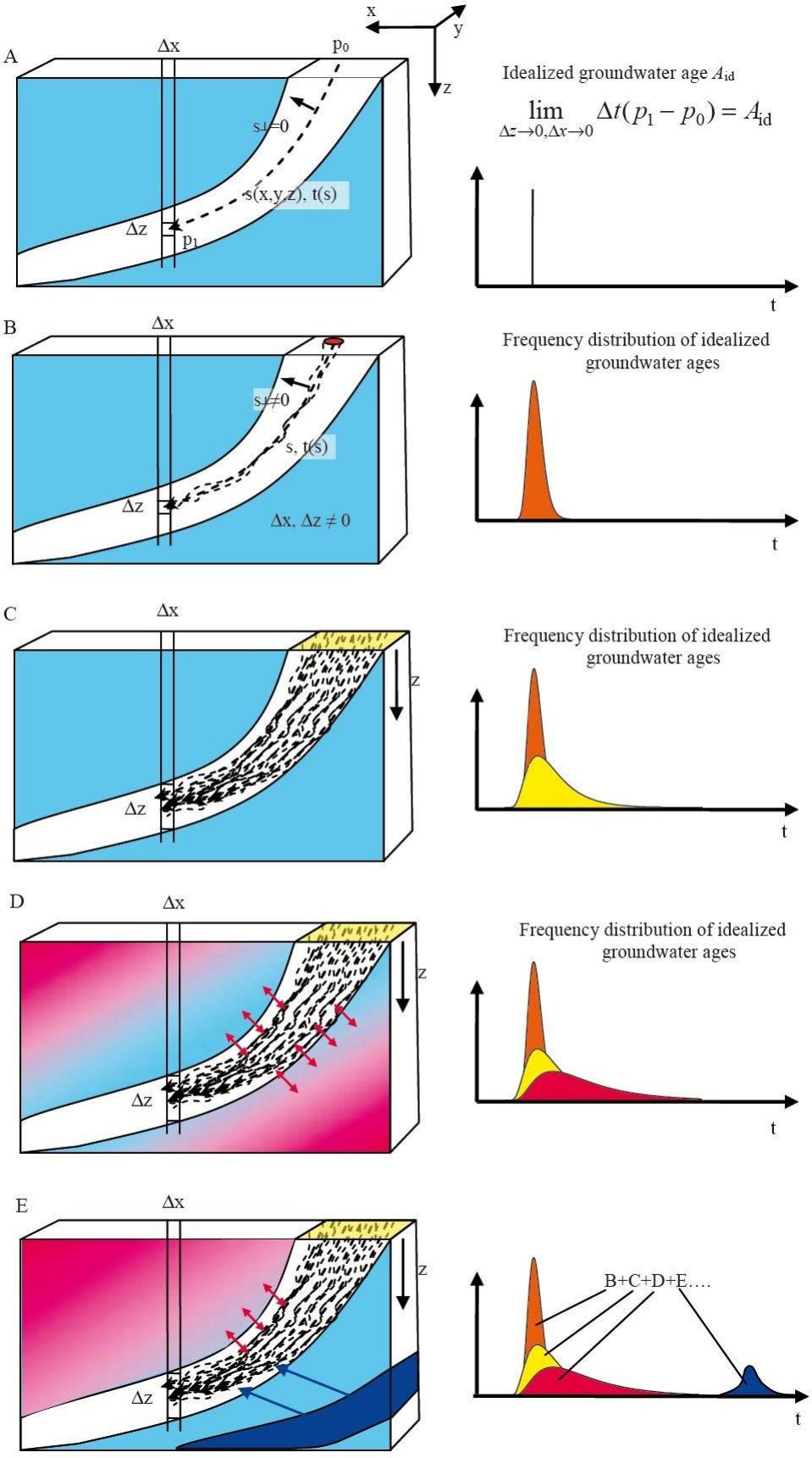

Figure A.5: Spreading of age distributions due to different processes relevant in groundwater (Torgersen et al. 2013)

A.3 Tracers in double porosity systems

Environmental tracers show special features in double porosity systems that may severely distort the derived flow velocity or apparent age. Double porosity here is defined as any situation in which the active flow system (the aquifer) can exchange any solutes (tracers) by diffusion with another stagnant part of the aquifer system. Such stagnant zones may exist in the aquifer itself (flow in fractures surrounding a stagnant matrix; preferential flow due to sedimentological differences), or these may be adjacent aquitards. In any case the flow in these zones is negligibly slow as compared to the aquifer. If the tracer concentration is lower in the stagnant zone as compared to the active flow zone, then the tracer is lost by diffusion into the stagnant zones. The length *L* is the distance how far the tracer can penetrate into the stagnant zone in a certain amount of time, and is only dependent on time *t* and the effective diffusion constant *D'* (Einstein 1905):

$$L(t) \cong \sqrt{D't} \qquad (7)$$

Variations of *D'* between different tracers in free water are up to a factor of 7 (e.g. at 10°C: $5.7 \cdot 10^{-9}$ m^2/s for ^{4}He (Jähne *et al.* 1987) and $0.8 \cdot 10^{-9}$ m^2/s for SF_6 (King and Saltzman 1995)). Diffusion rates decrease within the pore space of sediments due to tortuosity and this factor depends on details of the sediment properties but is normally also in the range of a factor of 10 or less. Furthermore, this tortuosity factor applies to all tracers the same way. Therefore the length *L(t)* is mainly a function of time, and the differences in diffusion coefficients between tracers are of minor importance. If one assumes an aquifer of thickness *a* separated by stagnant layers (aquitards) of thickness *b*, then Figure A.6 illustrates the principle of tracer diffusion into the pore space (Purtschert *et al.* 2013).

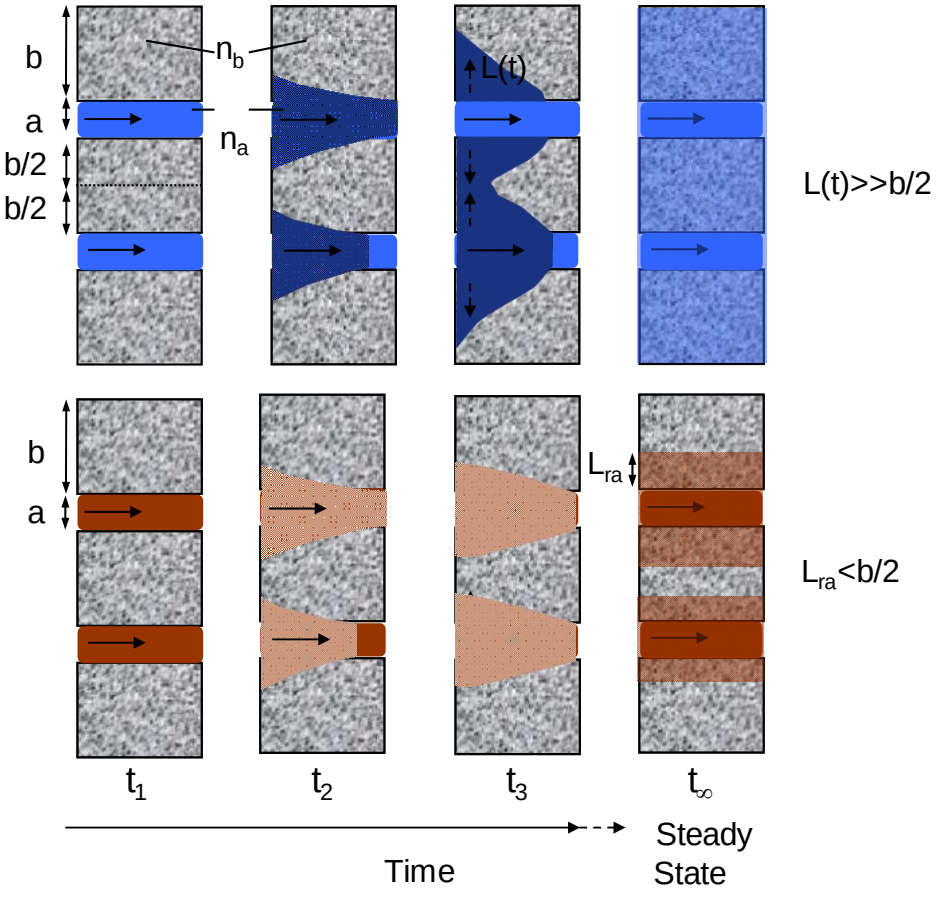

Figure A.6: Tracer retardation by matrix diffusive loss into stagnant zones (Purtschert *et al.* 2013)

Due to the diffusive loss into the aquitard, any environmental tracer that comes into the aquifer only with precipitation will result in a lower measured value if double porosity is important. This is true for ^{3}H, CFCs, SF_6, ^{14}C and ^{36}Cl and will result in a higher apparent age than the 'true' hydraulic age of the water. How much tracer is lost to the aquitard will depend on time (because *L(t)* depends on time, see Equation 7 and the left part of Figure A.6) and for long times on the ratio of water volume in the stagnant zone to water volume in the aquifer (right part of Figure A.6). Also for a tracer produced in the underground, like ^{4}He, the groundwater will 'see' the much larger production volume of aquifer plus thickness $2 \cdot L(t)$ of the aquitard of which ^{4}He produced from uranium and thorium decay is released to the flowing groundwater. Again this will result in a higher apparent age than the 'true' hydraulic age of the water.

For a simple one-dimensional system of one thin aquifer in an extended aquitard that observes no flow but only molecular diffusion, Sudicky and Frind (1981) gave an analytic solution for the relationship of steady-state tracer concentration in the aquifer with distance:

$$C(x) = C_0 \cdot \exp\left(x \cdot \left(\frac{v}{2D} - \sqrt{\left(\frac{v}{2D}\right)^2 + \frac{\lambda}{D} + \sqrt{\frac{\lambda D'}{D}}\,\frac{n_b}{a \cdot n_a}} \right) \right) \qquad (8)$$

Here c_0 is the initial tracer concentration at $x=0$, v is the flow velocity in the aquifer, λ the decay constant of the tracer, a the thickness of the aquifer and n_a and n_b are the porosities of aquifer and stagnant phases, respectively. D is the sum of hydrodynamic dispersion and diffusion in the aquifer, $D=\alpha_L \cdot v + D'$, where α_L is the dispersivity and D' the molecular diffusion of the tracer. The net effect of tracer loss by diffusion from the aquifer into the surrounding aquitard is that the radioactive tracer decreases (much) faster than according to radioactive decay. The effect can be easily a factor of ten or more, depending on aquifer thickness and travel distance. The resulting distribution of tracer versus distance is still exponential, as would be expected without the double-porosity effect. This makes it impossible to detect the importance of this effect from the tracer measurements alone if only *one* tracer is measured versus distance. Any apparent age as derived from a tracer like ^{14}C or ^{36}Cl would be larger than the flow time of water from the recharge to the sampling point.

This means, that the tracer loss manifests itself like a retardation factor R, in a similar manner as when chemical sorption occurs. This apparent retardation factor depends on the true hydraulic water age (represented as t), which in a steady state flow system is equivalent to flow distance x and on the ratio of available total volume to active flow volume (Maloszewski and Zuber 1985; Purtschert *et al.* 2013):

$$R(t) \cong \frac{a \cdot n_a + 2 \cdot L(t) \cdot n_b}{a \cdot n_a} \qquad (9)$$

Here n_a and n_b are the porosities of the aquifer and the stagnant zones respectively. Obviously this retardation factor is time dependent; for very short times it is negligible ($L(t)=0$ in Equation 7, so $R=1$ at $t=0$) and increases with the square root of time. For a stable tracer the loss into the stagnant zones – and therefore the retardation factor – can be very large, because it can penetrate also into very thick stagnant zones. A radioactive tracer, however, may not have enough time to penetrate a thick stagnant zone b, because it decays earlier (lower part of Figure A.6). Therefore for a radioactive tracer the maximum length L_{ra} to which it can penetrate a stagnant layer, is dependent on the decay constant λ:

$$L_{ra} \cong \sqrt{\frac{D'}{\lambda}} \qquad (10)$$

Obviously this maximum distance L_{ra} is the larger, the longer the half-life of the tracer is. Therefore in aquifer systems with very large stagnant layers like the Hutton Sandstone in the Surat Basin, also the *maximum* possible retardation factor increases with half live according to the following sequence:

$$R(t) \cong \frac{a \cdot n_a + 2 \cdot L_{ra} \cdot n_b}{a \cdot n_a}; \qquad R_{^3H} << R_{^{14}C} << R_{^{36}Cl} \tag{11}$$

One has to be aware that this sequence describes only the *maximum* retardation factor – after a flow distance *x* when the most short lived tracer (usually ^{3}H) reaches its L_{ra}, the retardation factors of the longer lived tracers (^{14}C and ^{36}Cl) will be nearly identical (distinguishable only due to the different diffusion constants in Equation 10), because for them *L(t)* is still much smaller than L_{ra}. As a further consequence, this retardation factor is only constant at one point along the flow path in a system in steady state towards flow and transport. In any transient or stationary system, the retardation factor will increase along the flow path until either L_{ra} is reached or until tracer diffusion created a homogeneous concentration in aquifer and pore space (right state in Figure A.6). After this point in time and space no further net tracer loss from the aquifer will occur for a stable tracer, but still for a radioactive tracer.

The Sudicky model of Equation 8 fitted with two tracers for the same flow velocity allows deriving the total amount of water flowing within a deeper aquifer formation. This can be understood when re-arranging Equation 8 to the following form:

$$C(x) = C_0 \cdot \exp\left(\frac{x \cdot v}{2D}\left(1 - \sqrt{1 + \frac{4D}{v} \cdot \left(\frac{\lambda}{v} + \sqrt{\frac{\lambda D'}{a \cdot v \cdot n_a}}\right)}\right)\right) \tag{12}$$

Here the terms in the exponential function have the following meaning: The term *xv/D* corresponds to the longitudinal Peclet number within the aquifer and describes how the tracer is spread within the aquifer in flow direction by dispersion. As mentioned earlier, dispersion is the product of dispersivity and flow velocity plus diffusion: $D=\alpha_L \cdot v + D'$. Since on the scales in discussion *x* is on the order of many 10,000 m and α_L is on the order of many meter, *D'* can be neglected and the term *xv/2D* decomposes to $x/2\alpha_L$. The same holds true for the term *4D/v* which decomposes to $4\alpha_L$. This allows for a Taylor development of the root in the exponential:

$$\sqrt{1+X} \approx 1 + \frac{1}{2}X - \frac{1}{8}X^2 \cdots \tag{13}$$

Which, together with the transformations of dispersion above allows us to transform the formula further:

$$C(x) \approx C_0 \cdot \exp\left(-x \cdot \frac{\lambda}{v} - x \cdot \sqrt{\lambda D' \cdot \frac{n_b}{a \cdot v \cdot n_a}}\right) \tag{14}$$

Note that this is independent of longitudinal dispersivity α_L, which explains the insensitivity of the Sudicky formula towards this parameter. As a result, in the case where the second porosity can be neglected (n_b=0) the whole exponential can be very well approximated by $\exp(-x\lambda/v)$ which corresponds to the transport of a radioactive tracer in a long tube. In cases where diffusion into the matrix is dominant for tracer loss, only the last term in the exponential becomes important. Here $\lambda D'$ is a measure of the length of matrix diffusion that is important for the tracer. This is largest for ^{36}Cl and is composed of physical constants and therefore not part of the fitting process and independent of the flow velocity or aquifer geometry. The term $n_b/(a \cdot v \cdot n_a)$ dominates the exponential decrease of tracer along the flow path and the fitting. The term $a \cdot v \cdot n_a$ is the amount of groundwater (in cubic meters per year) that is flowing through the aquifer in a vertical cross section per meter of aquifer length (thickness perpendicular to the cross section). Therefore, if diffusion into the matrix dominates the transport process, fitting of two independent tracer profiles like ^{14}C and ^{36}Cl to the Sudicky model gives an independent and comparably robust estimate of the amount of water flowing in the deeper parts of a thin confined aquifer.

CONTACT US

t 1300 363 400
+61 3 9545 2176
e enquiries@csiro.au
w www.csiro.au

YOUR CSIRO

Australia is founding its future on science and innovation. Its national science agency, CSIRO, is a powerhouse of ideas, technologies and skills for building prosperity, growth, health and sustainability. It serves governments, industries, business and communities across the nation.